AD-A127 073 FORCE METHOD OPTIMIZATION II VOLUME I THEORETICAL DEVELOPMENT(U) BELL AEROSPACE TEXTRON BUFFALO NY J R BATT ET AL. NOV 82 AFWAL-TR-82-3088-VOL-1 1/2

UNCLASSIFIED F33615-80-C-3214 F/G 12/1 • NL

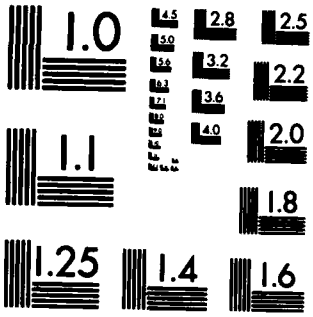

MICROCOPY RESOLUTION TEST CHART
NATIONAL BUREAU OF STANDARDS-1963-A

AD A127013

AFWAL-TR-82-3088
Volume I

FORCE METHOD OPTIMIZATION II
Volume I - Theoretical Development

J. R. Batt
S. Gellin
R. A. Gellatly

Bell Aerospace Textron
Buffalo, New York 14240

November 1982

Final Report for Period August 1980 to December 1982

Approved for Public Release; Distribution Unlimited

DTIC FILE COPY

FLIGHT DYNAMICS LABORATORY
AIR FORCE WRIGHT AERONAUTICAL LABORATORIES
AIR FORCE SYSTEMS COMMAND
WRIGHT-PATTERSON AIR FORCE BASE, OHIO 45433

A

83 04 21 067

NOTICE

When Government drawings, specifications, or other data are used for any purpose other than in connection with a definitely related Government procurement operation, the United States Government thereby incurs no responsibility nor any obligation whatsoever; and the fact that the government may have formulated, furnished, or in any way supplied the said drawings, specifications, or other data, is not to be regarded by implication or otherwise as in any manner licensing the holder or any other person or corporation, or conveying any rights or permission to manufacture, use, or sell any patented invention that may in any way be related thereto.

This report has been reviewed by the Office of Public Affairs (ASD/PA) and is releasable to the National Technical Information Service (NTIS). At NTIS, it will be available to the general public, including foreign nations.

This technical report has been reviewed and is approved for publication.

NARENDRA S. KHOT, Project Engineer
Design & Analysis Methods Group
Analysis & Optimization Branch

FREDERICK A. PICCHIONI, Lt. Col.
USAF, Ch. Analysis & Optimization Branch
Structures & Dynamics Division

For the Commander

RALPH L. KUSTER, JR., Col. USAF
Chief, Structures & Dynamics Div.

"If your address has changed, if you wish to be removed from our mailing list, or if the addressee is no longer employed by your organization please notify AFWAL/FIBRA, W-PAFB, OH 45433 to help us maintain a current mailing list".

Copies of this report should not be returend unless return is required by security considerations. contractual obligations, or notice on a specific document.

UNCLASSIFIED

SECURITY CLASSIFICATION OF THIS PAGE (When Data Entered)

REPORT DOCUMENTATION PAGE

READ INSTRUCTIONS BEFORE COMPLETING FORM

1. REPORT NUMBER
AFWAL-TR-82-3088, Volume I

2. GOVT ACCESSION NO.
AD-A127073

3. RECIPIENT'S CATALOG NUMBER

4. TITLE (and Subtitle)
FORCE OPTIMIZATION II,
Volume I - Theoretical Development

5. TYPE OF REPORT & PERIOD COVERED
Final Report
August 1980 - December 1982

6. PERFORMING ORG. REPORT NUMBER

7. AUTHOR(s)
J. R. Batt, S. Gellin,
R. A. Gellatly

8. CONTRACT OR GRANT NUMBER(s)
F33615-80-C3214

9. PERFORMING ORGANIZATION NAME AND ADDRESS
Bell Aerospace Textron
Buffalo, New York 14240

10. PROGRAM ELEMENT, PROJECT, TASK AREA & WORK UNIT NUMBERS
Project 2307
Task 2307N5
Work Unit 2307N518

11. CONTROLLING OFFICE NAME AND ADDRESS
Flight Dynamics Laboratory (FIBRA)
AF Wright Patterson Laboratories (AFSC)
Wright-Patterson Air Force Base, Ohio 45433

12. REPORT DATE
November 1982

13. NUMBER OF PAGES
120

14. MONITORING AGENCY NAME & ADDRESS(if different from Controlling Office)

15. SECURITY CLASS. (of this report)
UNCLASSIFIED

15a. DECLASSIFICATION/DOWNGRADING SCHEDULE

16. DISTRIBUTION STATEMENT (of this Report)

This document has been approved for public release and sale; its distribution is unlimited.

17. DISTRIBUTION STATEMENT (of the abstract entered in Block 20, if different from Report)

Approved for public release - distribution umlimited

18. SUPPLEMENTARY NOTES

19. KEY WORDS (Continue on reverse side if necessary and identify by block number)
Structural Optimization
Force Method of Finite Element Analysis
Minimum Weight Design
Rapid Reanalysis and Vulnerability Analysis

20. ABSTRACT (Continue on reverse side if necessary and identify by block number)

Investigates the utilization of the force method of finite element analysis for the automatic iterative design of aircraft structures with stress, displacements, maximum and minimum size and dynamic constraints. Develops a rapid reanalysis method based on the force method for damage assessment. Research has resulted in a computer code named OPTFORCE II an expansion of code OPTFORCE I documented in AFWAL-TR-80-3006. Multiple loading capabilities and four finite elements have been included. These are: membrane triangle,

DD FORM 1 JAN 73 1473 EDITION OF 1 NOV 65 IS OBSOLETE

UNCLASSIFIED

SECURITY CLASSIFICATION OF THIS PAGE (When Data Entered)

BLOCK 20

membrane quadrilateral, shear panel and bar (axial force). Examples of problems solved by the OPTFORCE II code are presented and compared to the optimization code OPTIM III for purposes of establishing the efficiency of the "force" method vs. the "displacement" method of analysis. A technical discussion of the research conducted is presented wherein conclusions and recommendations for future research topics are given.

FOREWORD

This report describes the work performed by Bell Aerospace Textron, a Division of Textron, Inc. Buffalo, New York. The work was sponsored by the Flight Dynamics Laboratory, Air Force Wright Aeronautical Laboratories, Wright-Patterson Air Force Base, Ohio, under Contract F33615-80-C3214.

The work was initiated under Project 2307, "Research in Flight Vehicle Dynamics" Task 2307N518, "Basic Research in Structures and Dynamics". The work was administered by Dr. N. S. Khot, Project Engineer of the Structures and Dynamics Division (FIBRA).

The contracted work was performed between August 1980 and December 1982.

The work was performed in the Structures and Vehicles Systems Directorate, Bell Aerospace Textron. Mr. James R. Batt was the Program Manager/Technical Director of the study.

DTIC COPY INSPECTED 2

Accession For
NTIS GRA&I
DTIC TAB
Unannounced
Justification
By
Distribution/
Availability Codes
Dist | Avail and/or Special
A

TABLE OF CONTENTS

SECTION		PAGE
	FOREWORD	
1.0	INTRODUCTION	1
2.0	THEORETICAL DEVELOPMENT	11
	2.1 Fundamentals of the Force Method	11
	2.2 Derivation of Finite Element Matrices	22
	2.3 Weight Optimization Methodology	40
	2.4 Rapid Reanalysis and Damage Assessment	59
3.0	OPTFORCE II PROGRAM	77
	3.1 Efficiency Studies	77
	3.2 Applications	103
4.0	CONCLUSIONS AND RECOMMENDATIONS	116
	REFERENCES	119

PRECEDING PAGE BLANK-NOT F

LIST OF ILLUSTRATIONS

FIGURE		PAGE
1	Truss (Rod) Element	22
2	Plane Stress Triangle	24
3	Edge Coordinate	26
4	Edge Segment Free Body Diagram	27
5	Plane Stress Quadrilateral	29
6	Symmetric Shear Panel	39
7	Three Bar Truss - Damage Assessment	72
8	Ten Bar Truss	73
9	Three Bar Truss - Residual Strength	76
10	Seventeen Bar Truss	79
11	OPTFORCE II Input Data - Seventeen Bar Truss, Case 2	81
12	Seventeen Bar Truss Results - Case 1	83
13	Seventeen Bar Truss Results - Case 2	86
14	Four Bar Pyramid	88
15	OPTFORCE II Input Data - Four Bar Pyramid, Case 1	90
16	Four Bar Pyramid Results - Case 1	93
17	Four Bar Pyramid Results - Case 2	94
18	Wingbox Configuration	97
19	OPTFORCE II Input Data - Wingbox	99
20	Wingbox Results	101
21	Swept Wingbox Configuration	104
22	OPTFORCE II Input Data - Case 1 Swept Wingbox	107
23	OPTFORCE II Input Data - Case 2 Swept Wingbox	109
24	Design Variable Distribution - Case 1 Swept Wingbox	111
25	Design Variable Distribution - Case 2 Swept Wingbox	115

LIST OF TABLES

TABLE		PAGE
1	Ten Bar Truss - Damage Assessment	74
2	Material Properties and Constraints - Seventeen Bar Truss	80
3	Seventeen Bar Truss Results - Case 1	82
4	Seventeen Bar Truss Results - Case 2	85
5	Material Properties & Constraints - Four Bar Pyramid	89
6	Four Bar Pyramid Results, Cases 1 & 2	91
7	Four Bar Pyramid Results, Cases 3-5	92
8	Material Properties and Constraints - Wingbox	98
9	Wingbox Results	100
10	Material Properties & Constraints - Case 1, Swept Wingbox	106
11	Material Properties & Constraints - Case 2, Swept Wingbox	108
12	Swept Wingbox Results - Case 1	110
13	Swept Wingbox Results - Case 2	113

1.0 INTRODUCTION

Modern technology of structural optimization is now nearly two decades old. During that period an intense amount of effort has been expended on studying the very many facets of the optimization problem. At a conservative estimate a bibliography of over 300 references to relevant work in this area could be compiled and, in fact, the search for the most efficient structure to perform a given task is much older than 20 years. The standard references to Michell, Ref. 1, and Clerk-Maxwell, Ref. 2, can be made to illustrate that the ideals and objectives of designing practical efficient structures are very fertile fields which have been studied in the extreme. Yet, in comparison with the erstwhile companion technology of finite element analysis, it must be recognized, regretfully, that structural optimization methodology has had little, if any, real impact on the design of modern structural systems. It has simply been not possible, in general, to translate the vast research into acceptable practical design tools. While a number of operational optimization programs have been developed - of various types - their use and acceptance has been very limited. There are exceptions, but there has been no general utilization of any optimization methods such as has occurred in the universal use of finite element technology.

The reasons for this are manifold. Firstly, optimization represents a degree of sophistication above pure analysis and hence is more costly. Secondly, the sophistication of mathematics may be suspect by designers and engineers who have no good reference for judging the validity of the concepts. Thirdly, the lack of a unified thrust on the part of researchers and developers to select an approach to the problem is strongly indicative of confidence in the value and validity of structural optimization and

fourthly, the nagging concern of designers about the "goodness" of an optimized structure. This final point is one which has long been the central point of a major controversy. The removal of concerns about the reliability of optimized structures should provide a major step forward in the widespread acceptance of optimization technology.

In this context, it is most relevant to consider the appropriate state-of-the-art in structural optimization and its applicability to the present study reported herein.

In spite of the very large effort of work expended by so many researchers, many of the most basic problems are still largely unsolved. Perhaps one of the most significant areas of progress has been in scoping our domain of ignorance. From the early days, when it was first proposed that some methods of operations research could be linked with iterative finite element analysis to the present day studies using Lagrangian formulations, there has been a much greater understanding of the true nature of the problems to be solved. The problems themselves have not necessarily been solved - they have just been identified more precisely.

In structural optimization, with the usual limitations of fixed geometry, etc., there is obviously a hierarchy of relevant constraints - member stresses, nodal deflections, local and overall stability, frequency response, flutter, etc. The precise order of higher order members in the hierarchy is more subjective and is influenced by the types of structures under consideration. The first two, strength and stiffness are, generally, prime requirements in virtually every structure.

Similarly, there are, theoretically, a number of potential candidate figures of merit by which the optimality of a structure can be measured - e.g., weight, cost, cost-effectiveness, reliability. While lip-service

has been paid frequently to some of the more esoteric merit criteria, the overwhelming majority of the work performed has fallen back on the use of weight for the objective function. Weight is usually important in most structures, especially aerospace applications, since it is simple to calculate and it is noncontrovertible. This is not to say that the use of the other criteria has not been investigated, but the enormity of the other aspects of the structural optimization problem has generally forced researchers to choose the simplest merit criterion initially (and finally) while justifying this situation, that other criteria may be usable within a general formulation - if they can be suitably quantified. The use of reliability as a criterion was addressed by Moses, Ref. 3, where concerns were being expressed that an optimized structure is more likely to fail catastrophically than a conventionally designed one. Regrettably, there appears to have been little follow-up work along the lines of that reference.

If, in spite of the expenditure of a large level of continuing effort, major fundamental problems still exist, what is the nature of such problems? Paradoxically, it appears that element stresses present greater problems than deflections.

Using a Lagrangian formulation, an exact solution may be determined for an optimum redundant structure subject to a single displacement constraint. For multiple displacement constraints, the same approach may be used, but the resulting equations become nonlinear. The solution of these equations has proved to be extremely difficult for anything but small-scale test problems. For stresses, attempts to use the Lagrangian formulation were not so successful. If a similar approach to that used for deflections is applied, the Lagrangian leads to fully stressed design. This is correct for determinate structures but is questionable for redundant

systems. To overcome this problem the effect of internal force distribution with variation in elastic properties must be introduced. This has been accomplished by using the force method of structural analysis, whereby the redundant structures are transformed to pseudo-determinate systems and the internal self-equilibrating force systems are treated as external loads.

The basic philosophy of the force method of structural analysis is well rooted in antiquity, definitely predating the much more popular displacement method. The concepts of "cutting" redundant structures, applying self-equilibrating forces and computing influence coefficients have been universally used to introduce novice structural engineers to the mysteries of analyzing complex structures. The fundamentals of the force method are addressed in many publications (see, for example, Refs. 4 and 5).

Although force method concepts are particularly simple and amenable to a ready physical comprehension by the neophyte, it is recognized that some computational complexity may occur in poorly formulated problems. While the displacement method may be more difficult to comprehend initially (the concept of a stiffness, per se, is not immediately obvious), the ability to automate the procedure coupled with a relative lack of conditioning problems, has led to its dominance in the field of structural analysis.

In the early work in structural optimization the use of the displacement method for the structural analysis stage was used, more or less automatically, because of the ready availability of developed finite element programs with extensive element libraries. Effort was concentrated on the development of rational redesign methods using various strategies.

Unfortunately, the most successful approach via the Lagrangian formulation, which handles displacement constraints in a very efficient manner, tends to break down when handling element stress constraints. The problem lies in the expression of the stress constraint in the form $\frac{S_i}{A_i \sigma_i} - 1$ where S_i is an element force, A_i its area or thickness, and σ_i the allowable stress. In the Lagrangian formulation, derivatives of the constraints with respect to the primary variables (A_i) must be formed. Since in a redundant structure the element force S_i is a function of every element area A_j, a term $\partial S_i/\partial A_j$ does exist. This term may be small, but its neglect is the reason the Lagrangian formulation leads directly to fully stressed design. In the displacement method no analytic expression for $\partial S_i/\partial A_j$ can be generated. The best that is possible lies in the use of finite difference approximations. Since the optimality criteria form a set of nonlinear equations which can only be solved using gradient methods (e.g., Newton-Raphson), the generation of second differentials using finite difference methods becomes computationally impractical. The solution lies in the use of the force method formulation. In this approach, the redundant structure is represented as a pseudo-determinate one in which S_i is not a direct function of all A_j. The true variation S_i is reflected by including the redundant forces X_j as variables. By this artifice, the missing term $\partial S_i/\partial A_j$ is incorporated through a variable redundant force term which shows up as a compatibility (displacement restraint) term in the basic Lagrangian. The additional terms are explicitly differentiable and permit the generation of nonlinear equations in an analytic form. These equations are then amenable to solution using a combination of linear-programming and Newton-Raphson techniques.

Based upon this force method approach a pilot program, OPTFORCE I

was developed at Bell Aerospace Textron and is presented in Reference 4. Typical of pilot programs, OPTFORCE I was limited in a number of important respects. It was one of the principal objectives of the research reported herein to expand OPTFORCE I into a usable computer code by eliminating or reducing its deficiencies; the new code is aptly named OPTFORCE II.

Two principal options were available to accomplish this: Expand the existing OPTFORCE I analysis program through the development of new elements and other sophistications or acquire an existing developed program and integrate it into the optimization stage of OPTFORCE I. One of the concerns in acquiring developed programs is the capability and efficiency of the available programs. Their capacities, as measured in terms of element numbers or degrees of freedom are generally adequate. The major deficiency discovered resided in the area of frequency constraints expressed in the force method of formulation. Thus, frequency constraint formulations were developed and are reported in this text as well as additional finite element formulations.

The typical form of a frequency constraint is that the basic structural frequency (undamped) shall be greater than a given value. In some instances a less than constraint may be specified, although this is less likely. Higher order harmonics are generally left unconstrained. While a frequency is a generalized structural response, like a deflection, its incorporation into an optimization program will introduce additional problems. Their exclusion from standard optimization programs may be indicative of both their difficult nature and of their lack of wide-spread usefulness.

Optimization involving frequency constraints of various types has been explored (Refs. 5 & 6) with some success. Generally, they have been used alone rather than in combination with the more usual stress, deflection and

fabrication constraints. The expanded version of OPTFORCE I provides an integration of frequency constraints with the other types mentioned. A full integration of the frequency constraints into an optimization program is theoretically similar to the rigorous treatment of any other types of multiple constraints, i.e., the problem becomes extremely nonlinear, but solvable through the use of some form of Newton-Raphson technique.

The optimized structure may be more sensitive to damage. Hence, it is essential to make provisions for the service reliability or vulnerability of optimized structures. To assess the service reliability of the structures, the concept of partial degradation was introduced. This may simulate battle damage or any other type of partial failure which may occur as a result of extensive service operation. To assess the suitability/reliability of the initial structure, the behavior of the degenerate (damaged) structure is analyzed. If the primary structure is still largely capable of carrying out its prescribed mission even when damaged then its reliability is acceptable. The above evaluations of reliability are clearly only qualitative in nature. Another objective of the study program was to establish a quantitative means for the assessment of a damaged structure.

To determine the effect of damage on the optimized structure, repeated re-analysis of degenerate forms of the original highly efficient structure are required. Re-analysis methods have been under development since the work reported in 1969 by R. J. Melosh, Ref. 7, and more recently with increased intensity by other researchers such as V. Venkayya and N. Khot, Refs. 8 & 9. The search for more efficient re-analysis methods is paramount to the solution of aerospace structural optimization and damage assessment problems. These methods are vital to the determination of the vulnerability of a damaged structure. At the present time re-analysis

methods can be broadly classified into two groups; namely, direct and iterative. The former eliminates problems associated with convergence but could be burdened more with problems of efficiency than the latter. Considerations of efficiency are of utmost importance if new design tools such as produced herein are to become practical. Examination of the re-analysis methods developed to date showed that viable methods do exist and some are applicable to large scale structural analyses and design of air-frame components. These, however, were not cast within the framework of the force method. Thus a new method of rapid re-analysis of damaged structures was developed including vulnerability assessment. Vulnerability methodology must account for the interaction of optimization-reanalysis programs in order to provide sufficient details of the damaged structure such that, for example, residual strength can be determined. Another item of vulnerability is the change in the vibration characteristics of the damaged structure. Perhaps what is of most importance is the ability to define the level of vulnerability or in other words the ability to determine the operational capability of a damaged structure. This facet of vulnerability was investigated and is provided.

As a result of the efforts previously described a set of analytical tools capable of designing lighter and less costly structural components is available to the designer. It was appropriate then that efforts were expended to analyze representative structures in order to demonstrate the utility of the computer codes developed. This was accomplished on structures varying from relatively simple trusses to a swept wingbox aircraft structure. Details of the analyses conducted are presented.

The analytical tools developed and based on the force method of finite analysis increases the versatiblity and scope of analyses which can

be performed using the force method of approach provided in OPTFORCE I, Ref. 4. However, two fundamental questions remain: Does the force method offer an improvement in efficiency resulting in lower computer costs compared with the displacement method of finite element analysis? And which of the two methods is the most accurate, i.e., which one provides the "correct" minimum weight solution?

As noted in the optimization literature when the iteration algorithm is based on the displacement method of finite element analysis, a complete re-analysis of the structure must be conducted whenever large changes are made in the design variables. Thus, substantial computational effort is devoted to the analysis of the structure. In the force method, the basic framework of computational effort is not increased with changes in the design variables after the basic and redundant load system is selected. This should mean that there is an improvement in efficiency and a speedup in the iterative analysis for the force method algorithm. Hence, a comparison of computer cpu time expended by the OPTFORCE II program solving classical problems with known solutions, versus an existing displacement method optimization program OPTIM III, Ref. 10, solving the same problems was conducted. This provided the needed comparison data to answer the fundamental "dollars and cents" question. More importantly, these comparison studies also provided a means to assess the relative accuracy of the two optimization codes. These items formed the basis for recommending future development of a general purpose optimization program.

Thorough discussions of the technical areas discussed above are given in Sections 2.0 and 3.0. Section 2.0 presents the theoretical background of the OPTFORCE II code and emphasizes the expansion of the

pilot program OPTFORCE I. The discussion commences with a review of the fundamentals of the force method in Section 2.1. Derivation of finite element matrices for bar (axial force), membrane triangle, membrane quadrilateral and shear panel elements within the context of the force method are presented next. Weight optimization methodology is given in Section 2.3 including provisions for handling variable stress, multiple displacement, maximum and minimum size, multiple loading and natural frequency constraints. Rapid re-analysis and damage assessment technology is presented and illustrated in Section 2.4. The newly developed OPTFORCE II code is amply exercised in Section 3.0. Efficiency studies and applications of the code to a swept wingbox structure are described. Program results are profusely given to enable the reader to fully understand its capabilities. It is noted here that Volume 2 (Ref. 11) of this report presents details of the program and the input/output format of OPTFORCE II. A technical discussion of the research conducted is presented in Section 4.0 wherein conclusions and recommendations are given.

2.0 THEORETICAL DEVELOPMENT

2.1 Fundamentals of the Force Method

The force method of analysis was used to model structural behavior and determine minimum weight under static loading. An additional requirement above the static constraints of minimum size, stress and displacement was to constrain the structure from having certain of its fundamental vibration frequencies falling within a specified range. In order to accomplish the task of stating these frequency constraints in a particular mathematical form compatible with the weight optimization method as set forth in Section 2.3, below, it was necessary to formulate a force method dynamic analysis that would yield frequencies and modes when the structure was in a state of free vibration. What follows is a discussion of the theoretical basis for both static and dynamic analyses.

2.1.1 Basic Static Analysis

A force method formulation is based on minimizing the complimentary energy functional with respect to parameters used to describe a chosen approximation to the stress field. The requirements for the approximate stress field are that it satisfies equilibrium throughout the body, that the stress boundary conditions are satisfied, and that the choice admits non-trivial solutions, at least a priori. The principle of minimum complimentary energy may be written as

$$\delta U^* + \delta V^* = 0 \ . \tag{1}$$

U^* is the complimentary strain energy and V^*, for a finite element idealization of a body, is usually

$$V^* = - \{P\}^T \{\Delta\} \tag{2}$$

where $\{P\}$ and $\{\Delta\}$ are the finite element nodal forces and displacements, respectively.

The stress field for each element in the structure is given by the following expression,

$$\vec{\sigma}_i = [N_i] \{S_i\} \tag{3}$$

where the $[N_i]$ are functions of the spatial coordinates defined for the element and $\{S_i\}$ are the undetermined parameters for the stress field, which serve as coefficients for linear combinations of the $[N_i]$. The $[N_i]$ must satisfy the homogeneous equations of equilibrium, and must admit a non-trivial solution for each stress field in $\vec{\sigma}_i$. The number of parameters $\{S_i\}$ must be at least the number of degrees of freedom for the element minus the minimum number of support forces needed to suppress rigid body motion of the element. With the constitutive law written as

$$\vec{\varepsilon}_i = [E_i]^{-1} \vec{\sigma}_i \tag{4}$$

the complimentary strain energy for the ith element is

$$U_i^* = \frac{1}{2} \{S_i\}^T [f_i] \{S_i\} \tag{5}$$

where the element flexibility matrix is

$$[f_i] = \int_V [N_i]^T [E_i]^{-1} [N_i] \, dV. \tag{6}$$

The total complementary strain energy of the structure is the sum of the individual strain energies of the elements. If $\{S\}$ is the collection of all the $\{S_i\}$ and $[f]$ is a matrix formed by placing the $[f_i]$ along the main "diagonal" of an otherwise trivial $[f]$, then this sum may be written as

$$U^* = \frac{1}{2} \{S\}^T [f] \{S\}. \tag{7}$$

A relation between $\{S\}$ and $\{P\}$ must be found in order to use (1) find a solution. The derivation of such a relation presents the greatest difficulty in the force method formulation particularly when the $\{S\}$ are devoid of physical meaning. One approach is to relate the $\{S_i\}$ of an element with $\{F_i\}$, the element nodal forces. The criterion selected for this relation is that $\{F_i\}$ be chosen such that the work done by the traction field, as calculated from the stress field evaluated on the element's boundary, is the same as the work done by $\{F_i\}$ through the nodal displacements. To accomplish this, it becomes necessary to choose a boundary displacement field $\vec{u}_i$ in terms of the nodal displacements $\{\Delta_i\}$; thus,

$$\vec{u}_i = [Y_i] \{\Delta_i\}. \tag{8}$$

The work-equivalency criterion is expressed as

$$\{\Delta_i\}^T \left(\oint_S [Y_i]^T [L_i] \, dS\right) \{S_i\} = \{\Delta_i\}^T \{F_i\} \tag{9}$$

where $[L_i]$ is $[N_i]$ evaluated on S. Equation (9) yields the relation

$$\{F_i\} = [B_i] \{S_i\} \tag{10}$$

where

$$[B_i] = \oint_S [Y_i]^T [L_i] \, dS. \tag{11}$$

The introduction of $[Y_i]$ into the formulation gives it a hybrid character (Ref. 12). While the choice of $\vec{u}_i$ appears arbitrary, an interelement continuous shape would be best to choose.

The collection of equations (10) may be written as

$$\{F\} = [B] \{S\}. \tag{12}$$

It is also convenient to include in both $\{F\}$ and $\{S\}$ the set of reactions $\{R\}$. Equilibrium equations are now written for each degree of freedom as

$$\{P\} = [C] \{F\} \tag{13}$$

where $[C]$ is a Boolean matrix. Substituting (12) into (13) yields

$$\{P\} = [A] \{S\}. \tag{14}$$

If the structure is statically determinate, then $[A]$ is square and invertible, and (14) is solved directly for $\{S\}$, and thence the stress field. In order to find the nodal displacements $\{\Delta\}$, equation (14) is substituted in (1) and variations are taken with respect to $\{P\}$, yielding the relation

$$((\{A\}^{-1})^T [f] [A]^{-1}) \{P\} = \{\Delta\}. \tag{15}$$

The matrix product pre-multiplying $\{P\}$ in (15) is the global flexibility matrix of the structure.

If the structure is statically indeterminate, the number of columns of $[A]$ will exceed the number of rows; thus, partition (14) into

$$\{P\} = [A_o \vdots A_1] \begin{bmatrix} S_o \\ \hline X \end{bmatrix} \tag{16}$$

where $[A_o]$ is square and invertible. The subset $\{X\}$ of $\{S\}$ are known as the "redundants". Solving (16) for $\{S_o\}$ yields

$$\{S_o\} = -[A_o]^{-1}[A_1]\{X\} + [A_o]^{-1}\{P\} . \tag{17}$$

Combining (17) with identity relations for $\{X\}$ gives

$$\{S\} = [b_1]\{X\} + [D]\{P\} \tag{18}$$

where

$$[b_1] = \begin{bmatrix} -[A_o]^{-1}[A_1] \\ [I] \end{bmatrix} ; \quad [D] = \begin{bmatrix} [A_o]^{-1} \\ [0] \end{bmatrix} . \tag{19}$$

Equations (18) are used in (17), and then substituted into (1), with variations taken with respect to both $\{X\}$ and $\{P\}$. The two sets of equations formed are

$$[\phi]\{X\} + [\psi]\{P\} = \{0\} \tag{20a}$$

$$[\psi]^T\{X\} + [\Omega]\{P\} = \{\Delta\} \tag{20b}$$

$$[\phi] = [b_1]^T[f][b_1]; \; [\psi] = [b_1]^T[f][D]; \; [\Omega] = [D]^T[f][D]. \tag{21}$$

Equations (20a) are solved for $\{X\}$, and may be used in (18) to subsequently determine the stress field throughout the structure. Substituting (20a) for $\{X\}$ in (20b) yields the global flexibility relations

$$[\mathfrak{F}]\{P\} = \{\Delta\} \tag{22}$$

where the global flexibility matrix is

$$[\mathfrak{F}] = [\Omega] - [\psi]^T[\phi]^{-1}[\psi]. \tag{23}$$

Note that since $\{P\}$ is known and $\{\Delta\}$ is unknown that (15) or (22) need

not be inverted; on the other hand, the inversion of $[A_o]$ requires the same amount of effort as the inversion of a global stiffness matrix.

In order to facilitate incorporation of the above formulation into the weight optimization method, several special properties of the force method need to be recognized. First, the finite elements used have volumes which can be written in the form

$$V_i = A_i R_i \tag{24}$$

where R_i is a one or two-dimensional element domain and A_i is the corresponding two or one-dimensional element size. For a given structural layout and discretization, R_i will be fixed for an element with A_i to be determined. Furthermore, the bounding surface of the element can be written as

$$S_i = A_i C_i \tag{25}$$

where C_i is a one or zero dimensional "curve" surrounding R_i.

Suppose that the parameters for the stress field $\{S_i\}$ are dimensionally given in units of force. This seems logical if the set of reactions are to be incorporated with $\{S\}$; furthermore, matrices $[B_i]$ and thus $[A]$ become strictly non-dimensional under this assumption. If shape functions $[\bar{N}_i]$ are defined as

$$[\bar{N}_i] = A_i [N_i] \tag{26}$$

then use of (26) and (24) in (6) yields

$$[f_i] = \int_{R_i} \left(\frac{1}{A_i} [\bar{N}_i]^T\right) [E]^{-1} \left(\frac{1}{A_i} [\bar{N}_i]\right) A_i \, dR_i = \frac{1}{A_i} [\bar{f}_i] \tag{27}$$

where $[\bar{f}_i]$ is independent of A_i. In addition, (26) and (25) are used in (11) to form

$$[B_i] = \oint_{C_i} [Y_i]^T \left(\frac{1}{A_i} [\bar{L}_i]\right) A_i \, dC_i \tag{28}$$

where $[\bar{L}_i]$ is $[\bar{N}_i]$ evaluated on C_i, thus rendering $[B_i]$ independent of A_i. The result is that $[A]$, and thus $[b_1]$ and $[D]$ are independent of the element sizes and strictly a function of the geometric layout and discretization of the structure. This eliminates repetitive computations as element sizes are changed during the weight optimization analysis.

The second special property of the formulation becomes apparent when equations (18) are partitioned by elements; thus,

$$\{S_i\} = [b_{1_i}] \{X\} + [D_i] \{P\} . \tag{29}$$

In addition, the reactions are calculated as

$$\{R\} = [b_{1_R}] \{X\} + [D_R] \{P\} . \tag{30}$$

The diagonal nature of $[f]$, combined with the partition (29) and (27) yields for the expressions (21)

$$[\phi] = \sum_{i=1}^{N_E} \frac{1}{A_i} [\bar{\phi}_i], [\psi] = \sum_{i=1}^{N_E} \frac{1}{A_i} [\bar{\psi}_i], \quad [\Omega] = \sum_{i=1}^{N_E} \frac{1}{A_i} [\bar{\Omega}_i] \tag{31}$$

where N_E is the number of elements and

$$[\bar{\phi}_i] = [b_i]^T [\bar{f}_i][b_i]; [\bar{\psi}_i] = [b_i]^T [\bar{f}_i][D_i]; [\bar{\Omega}_i] = [D_i]^T [\bar{f}_i][D_i] . \tag{32}$$

Note that $[\bar{\phi}_i]$, $[\bar{\psi}_i]$ and $[\bar{\Omega}_i]$ are independent of A_i, and that the A_i dependence of the basic static equations (20) may be explicitly written.

2.1.2 Basic Dynamic Analysis

As stated above, a force method approach to solutions of structural problems requires that equilibrium be satisfied throughout the body. In order to extend the force method to problems of structural dynamics, it is required that the appropriate forms of Newton's second law be satisfied throughout the body. It will be convenient to use D'Alembert's principle and introduce "inertial loads" into the equations of "dynamic equilibrium".

When analyzing a structural dynamics problem using a finite element lumped mass approach, the structure is assumed to be composed of particles at the node points containing mass, connected by massless elements. Since the elements will have no inertial loading as a result of this idealization, the equations of dynamic equilibrium reduce to those of static equilibrium. Thus, the static shape functions $[N_i]$ may still be used to describe the stress field within the element. The formulation proceeds exactly as in the statics case from equations (3) - (12).

Equations (13) must be modified to include the inertial loading $\{P_I\}$ as part of the overall "external load". With $\{P\}$ designating the actual applied loading only, (13) is changed to

$$\{P\} + \{P_I\} = [C]\{F\} \quad . \tag{33}$$

The formulation proceeds much like the statics case, except $\{P\} + \{P_I\}$ is substituted for $\{P\}$ in the equations where it appears. In particular (22) (or 15) becomes

$$[\mathfrak{F}]\,(\{P\} + \{P_I\}) = \{\Delta\}. \tag{34}$$

The inertial loads are related to the displacements by

$$\{P_I\} = -[M_\ell]\{\ddot{\Delta}\} \tag{35}$$

where $[M_\ell]$ is the diagonal lumped mass matrix and a dot indicates a time derivative. Integrating (2.35) with respect to time from 0 to t gives

$$\{\dot{\Delta}(t)\} = \{\dot{\Delta}_0\} - [M_\ell]^{-1} {}_0\int^t \{P_I(\tau)\}\, d\tau \tag{36}$$

where $\{\dot{\Delta}_0\}$ are the initial nodal velocities. Integrating again yields

$$\{\Delta(t)\} = \{\Delta_0\} + \{\dot{\Delta}_0\}t - [M_\ell]^{-1} {}_0\int^t (t-\tau)\, \{P_I(\tau)\}\, d\tau^* \tag{37}$$

where $\{\Delta_0\}$ are the initial nodal displacements. Substituting (36) into (34) and rearranging terms yields

$$[\mathfrak{F}]\, \{P_I\} + [M_\ell]^{-1} {}_0\int^t (t-\tau)\, \{P_I(\tau)\}\, d\tau = \{\Delta_0\} + \{\dot{\Delta}_0\} - \{\Delta_{stat}(t)\} \tag{38}$$

where

$$\{\Delta_{stat}(t)\} = [\mathfrak{F}]\, \{P(t)\} \quad . \tag{39}$$

The basic equations (38) are integral relations with $\{P_I\}$ as the basic variable. Differential equations with $\{\Delta\}$ as the basic variable could be derived, but that type of formulation would not be in the spirit of the force method, where forces are the basic unknowns. Furthermore, the form of (38) is directly analagous to a stiffness formulation.

Fundamental modes and frequencies for the structure may be found by formulating the free vibration problem. Assume that $\{P_I\}$ may be written as

$$\{P_I\} = \{P_{Ic}\} \cos \omega t + \{P_{Is}\} \sin \omega t \ . \tag{40}$$

$$*\ {}_0\int^t [{}_0\int^{t'} \{P_I(\tau)\} d\tau] dt' = t' {}_0\int^{t'} \{P_I(\tau)\} d\tau \Big|_0^t - {}_0\int^t t' \{P_I(t')\} dt'$$

$$= t\, {}_0\int^t \{P_I(\tau)\} d\tau - {}_0\int^t \tau \{P_I(\tau)\} d\tau$$

$$= {}_0\int^t (t-\tau)\, \{P_I(\tau)\}\, d\tau$$

Using (40) in (38), and remembering that for free vibration $\{P(t)\} = \{0\}$, gives

$$([\mathfrak{F}] - \frac{1}{\omega^2}[M_\ell]^{-1})\{P_I\} + (\frac{1}{\omega^2}[M_\ell]^{-1}\{P_{Ic}\} - \{\Delta_0\})$$

$$+ (\frac{1}{\omega}[M_\ell]^{-1}\{P_{Is}\} - \{\dot{\Delta}_0\})t = \{0\} . \tag{41}$$

With $\{\dot{\Delta}_0\}$ and $\{\Delta_0\}$ arbitrary, $\{P_{Ic}\}$ and $\{P_{Is}\}$ may be chosen such that (41) reduces to

$$([\mathfrak{F}] - \frac{1}{\omega^2}[M_\ell]^{-1})\{P_I\} = \{0\} . \tag{42}$$

In order for non-trivial $\{P_I\}$ to exist, the determinant of $[\mathfrak{F}] - \frac{1}{\omega^2}[M_\ell]^{-1}$ must be zero. The resulting equation yields the fundamental frequencies. In order to facilitate the numerical calculation of modes and frequencies by using standard matrix operation subroutine packages, it is desirable to make the substitution

$$\{P_I\} = [M_\ell]^{\frac{1}{2}}\{q\} \tag{43}$$

in (42). Note that $[M_\ell]^{\frac{1}{2}}$ is easy to calculate, considering the diagonal nature of $[M_\ell]$. Pre-multiplying (42) by $[M_\ell]^{\frac{1}{2}}$ gives

$$([Q] - \frac{1}{\omega^2}[I])\{q\} = \{0\} \tag{44}$$

where

$$[Q] = [M_\ell]^{\frac{1}{2}}[\mathfrak{F}][M_\ell]^{\frac{1}{2}} . \tag{45}$$

Thus, the fundamental frequencies are the inverse square roots of the eigenvalues of $[Q]$.

The eigenvalues of [Q] are found simultaneously. Suppose the kth eigenvector, i.e., the one corresponding to frequency ω_k, is denoted as $\{q_k\}$; then, the kth inertial load mode $\{P_I^k\}$ is found from (43) ; the kth redundant "force" mode from (20a) the kth parametric mode from (18) ; and the kth stress mode from (3) . The kth displacement mode is found most easily by comparing (42) with (34) to yield

$$\{\Delta_k\} = \frac{1}{\omega^2} [M_\ell]^{-1} \{P_I^k\} . \tag{46}$$

Mode normalization may take place on either $\{P_I^k\}$ or $\{\Delta_k\}$.

The diagonal mass matrix $[M_\ell]$ may be found as a function of the element sizes. Introducing the mass per unit volume, ρ_i, the mass of the ith element is written as

$$m_i = \rho_i V_i = \rho_i A_i R_i = A_i \bar{m}_i \tag{47}$$

where use has been made of (24) ; thus, $\bar{m}_i$ is known from input data. This mass is equally divided and assumed lumped at the node points of the element. The number β_{gi} is the fraction of the mass of element i located at node g. Note that β_{gi} can be defined as zero for those nodes that are not part of element i. Arbitrary criteria for assignment of β_{gi} to the various nodes may be made. In the present study, $\beta_{gi} = 1/N_{N_i}$, where N_{N_i} is the number of nodes associated with element i, was chosen. If g′ is a degree of freedom associated with node g, then

$$M_{\ell g'} = \sum_{i=1}^{N_E} \beta_{gi} \bar{m}_i A_i . \tag{48}$$

Problems of forced vibration, as well as a consistent mass formulation, may be derived, but were not utilized in the present study. The interested reader is referred to Reference 13.

2.2 Derivation of Element Matrices

Material and geometric information combined with an admissible choice for a stress field will produce matrices for a given element. In fact, only two matrices are of importance (at the element level): $[f_i]$ and $[B_i]$. Both of these are defined relative to local coordinates. The $[B_i]$ matrix must be transformed to global coordinates before incorporating it into $[B]$ for use in equation (2.12).

2.2.1 Truss (Rod) Element

Figure 1 shows a typical truss element. The x axis indicated is a local coordinate axis. The element's domain consists of the points $0<x<L$, while the "bounding surface" is simply the node points. A single parameter S is used to describe the stress field:

$$\sigma_x = \frac{1}{A} S \tag{49}$$

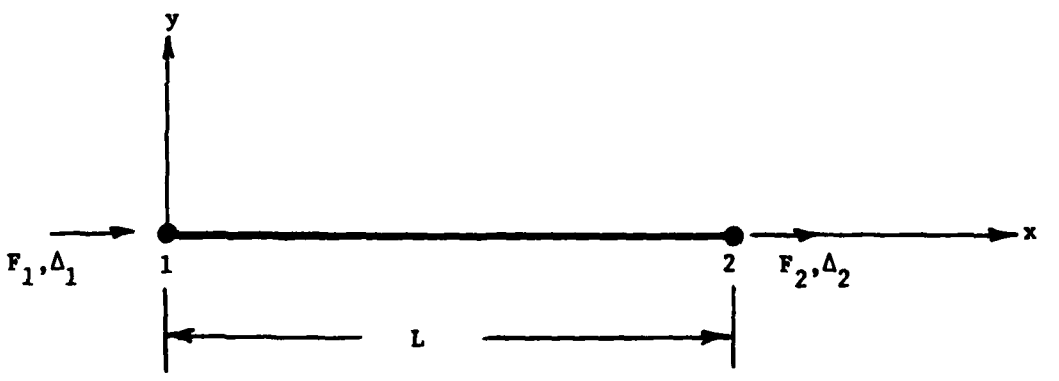

Figure 1 Truss (Rod) Element

where A is the cross sectional area of the truss element, and serves as the element size. Thus

$$[\bar{N}] = 1 \tag{50}$$

with

$$[E]^{-1} = \frac{1}{E} . \tag{51}$$

For this element,

$$[\bar{f}] = \int_0^L \frac{1}{E}\, dx = L/E . \tag{52}$$

In order to find $[B_i]$, it is important to realize that C_i may be made up of n natural subdivisions C_i^j, $j = 1, \cdots, n$. Thus

$$[B_i] = \sum_{j=1}^{n} \int_{C_i^j} [Y_i^j]^T [\bar{L}_i^j]\, dC_{ij}^j . \tag{53}$$

For the truss element, C_i^1 is node 1 and C_i^2 is node 2. Thus,

$$[Y_i^1] = \begin{bmatrix} 1 \\ 0 \end{bmatrix}, \; [Y_i^2] = \begin{bmatrix} 0 \\ 1 \end{bmatrix}, \; [\bar{L}_i^1] = [-1] \;\&\; [L_i^2] = [1] . \tag{54}$$

Substituting (54) into (53) yields

$$[B_i] = \begin{bmatrix} -1 \\ 1 \end{bmatrix} . \tag{55}$$

2.2.2 Plane Stress Triangle

Shown in Figure 2 is a typical, triangular shaped plane stress element. The x and y axes shown are the element's local coordinate axes. The element domain consists of the triangular region enclosed by the boundary edges. Three parameters are used to describe the stress field

$$\vec{\sigma} = \begin{bmatrix} \sigma_x \\ \sigma_y \\ \tau_{xy} \end{bmatrix} = \frac{1}{t\sqrt{A}} \begin{bmatrix} 1 & 0 & 0 \\ 0 & 1 & 0 \\ 0 & 0 & 1 \end{bmatrix} \begin{bmatrix} S_1 \\ S_2 \\ S_3 \end{bmatrix} \tag{56}$$

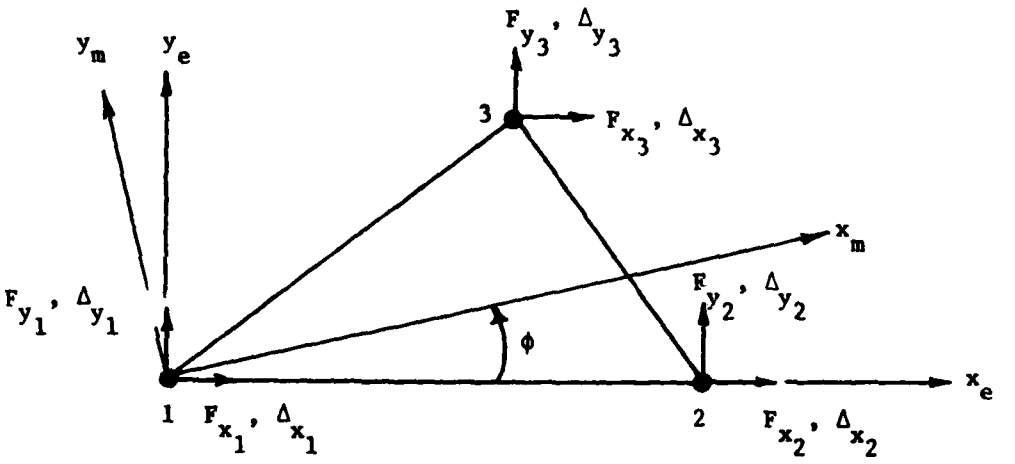

Figure 2 Plane Stress Triangle

where t is the cross-sectional thickness of the element, and serves as the element size. A is the triangular surface area, whose square root serves as a linear scaling factor. The $[\bar{N}]$ matrix is simply

$$[\bar{N}] = \frac{1}{\sqrt{A}} [I] \ . \tag{57}$$

Orthotropic material behavior will be assumed. When the material axis, x_m, is aligned with the x_e axis, the 3 x 3 compliance matrix is written in the form

$$[E_m]^{-1} = \begin{bmatrix} \frac{1}{E_x} & -\frac{\nu_{xy}}{E_x} & 0 \\ -\frac{\nu_{yx}}{E_y} & \frac{1}{E_y} & 0 \\ 0 & 0 & \frac{1}{G_{xy}} \end{bmatrix} \tag{58}$$

where the m subscript refers to the material axes. For a general set of axes, where ϕ is the counter-clockwise rotation from the element's x axis to the corresponding material axis, the elements of $[E]^{-1}$ may be written as follows:

$$(E^{-1})_{11} = \frac{1}{E_x} \cos^4 \phi + (\frac{1}{G_{xy}} - 2\beta) \sin^2 \phi \cos^2 \phi + \frac{1}{E_y} \sin^4 \phi$$

$$(E^{-1})_{22} = \frac{1}{E_x} \sin^4 \phi + (\frac{1}{G_{xy}} - 2\beta) \sin^2 \phi \cos^2 \phi + \frac{1}{E_y} \cos^4 \phi$$

$$(E^{-1})_{33} = 4 \sin^2 \phi \cos^2 \phi \, (\frac{1}{E_x} + \frac{1}{E_y} + 2\beta) + \frac{1}{G_{xy}} (\cos^2 \phi - \sin^2 \phi)^2$$

$$(E^{-1})_{12} = (E^{-1})_{21} = - \{\beta(\cos^4 \phi + \sin^4 \phi) + [\frac{1}{G_{xy}} - \frac{1}{E_x} - \frac{1}{E_y}] \sin^2 \phi \cos^2 \phi\}$$

$$(E^{-1})_{13} = (E^{-1})_{31} = \sin \phi \cos \phi \, \{\frac{2}{E_x} \cos^2 \phi - \frac{2}{E_y} \sin^2 \phi - (\frac{1}{G_{xy}} - 2\beta) (\cos^2 \phi - \sin^2 \phi)\}$$

$$(E^{-1})_{23} = (E^{-1})_{32} = \sin \phi \cos \phi \, \{\frac{2}{E_x} \sin^2 \phi - \frac{2}{E_y} \cos^2 \phi + (\frac{1}{G_{xy}} - 2\beta) (\cos^2 \phi - \sin^2 \phi)\} \tag{59}$$

where

$$\beta = \frac{\nu_{xy}}{E_x} = \frac{\nu_{yx}}{E_y} . \tag{60}$$

Use of (59) and (57) in the calculation of $[\bar{f}]$ yields

$$[\bar{f}] = [E]^{-1}. \tag{61}$$

The calculation of $[B_i]$ is performed by summing the contribution from each edge of the element. Figure 3 represents a typical edge of a triangular (or any general polygonal) element with nodes (i,j) at the end of the edge. The displacement fields $\vec{u}_{i-j}$ are defined to be linear in the edge coordinate x', thus

$$u_{i-j} = \begin{bmatrix} u_{i-j}\ (x') \\ V_{i-j}\ (x') \end{bmatrix} = \begin{bmatrix} 0 & 0\cdots\cdot 1 - \frac{x'}{\ell} & 0 & \frac{x'}{\ell'} & 0\cdots\cdot 0 & 0 \\ 0 & 0\cdots\cdot 0 & 1 - \frac{x'}{\ell'} & 0 & \frac{x'}{\ell'}\cdots 0 & 0 \end{bmatrix} \{\Delta\}^T \tag{62}$$

where

$$\{\Delta\}^T = [\Delta_{x_1}, \Delta_{y_1} \cdots \Delta_{x_i}, \Delta_{y_i} \cdots \Delta_{x_j}, \Delta_{y_j} \cdots \Delta_{x_N}, \Delta_{y_N}] .$$

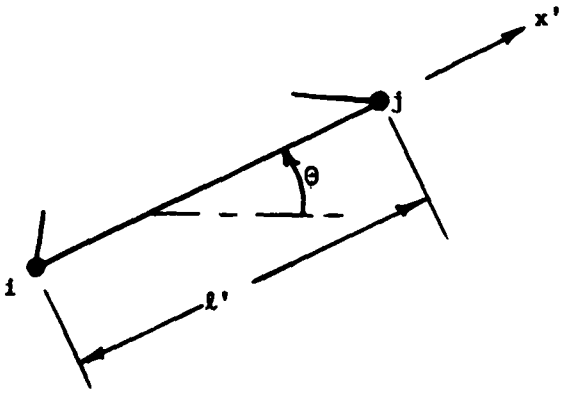

Figure 3 Edge Coordinate

N is the number of nodes for the polygon element. Note that $[Y_i]$ is a (2 x 2N) matrix, and thus for the triangular element it would be of order (2 x 6).

To determine the traction field for an edge, equilibrium must be satisfied for an edge segment. Noting Figure 4 , the traction field is determined as

$$\vec{T} = \begin{bmatrix} T_x\ (x') \\ T_y\ (x') \end{bmatrix} = \begin{bmatrix} \sin\theta & 0 & -\cos\theta \\ 0 & -\cos\theta & \sin\theta \end{bmatrix} \begin{bmatrix} \sigma_x \\ \sigma_y \\ \tau_{xy} \end{bmatrix} \tag{63}$$

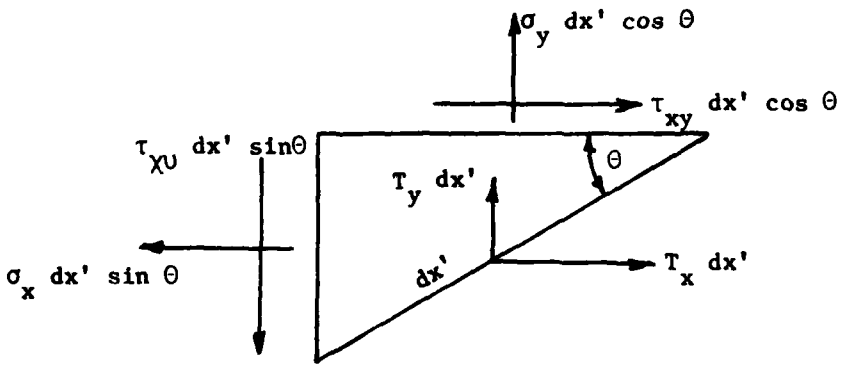

Figure 4 Edge Segment Free Body Diagram

where the stresses are evaluated on edge i-j. For the constant stress triangle, the relation is (2.56); thus,

$$[\bar{L}] = \frac{1}{\sqrt{A}} \begin{bmatrix} \sin\theta & 0 & -\cos\theta \\ 0 & -\cos\theta & \sin\theta \end{bmatrix} . \tag{64}$$

Using (64) and (62) in one term of (53) , say, edge 1-2, gives

$$[B_{1-2}] = \int_0^{\ell'} \begin{bmatrix} 1-x'/\ell' & 0 \\ 0 & 1-x'/\ell' \\ x'/\ell' & 0 \\ 0 & x'/\ell' \\ 0 & 0 \\ 0 & 0 \end{bmatrix} \frac{1}{\sqrt{A}} \begin{bmatrix} \sin\theta & 0 & -\cos\theta \\ 0 & -\cos\theta & \sin\theta \end{bmatrix} dx'$$

$$[B_{1-2}] = \frac{1}{2\sqrt{A}} \begin{bmatrix} y_2-y_1 & 0 & -(x_2-x_1) \\ 0 & -(x_2-x_1) & y_2-y_1 \\ y_2-y_1 & 0 & -(x_2-x_1) \\ 0 & -(x_2-x_1) & y_2-y_1 \\ 0 & 0 & 0 \\ 0 & 0 & 0 \end{bmatrix} \tag{65a}$$

where the subscripts pertain to the local coordinates of the elements grid points.

Similarly,

$$[B_{2-3}] = \frac{1}{2\sqrt{A}} \begin{bmatrix} 0 & 0 & 0 \\ 0 & 0 & 0 \\ y_3-y_2 & 0 & -(x_3-x_2) \\ 0 & -(x_3-x_2) & y_3-y_2 \\ y_3-y_2 & 0 & -(x_3-x_2) \\ 0 & -(x_3-x_2) & y_3-y_2 \end{bmatrix} \tag{65b}$$

$$[B_{3-1}] = \frac{1}{2\sqrt{A}} \begin{bmatrix} y_1-y_3 & 0 & -(x_1-x_3) \\ 0 & -(x_1-x_3) & y_1-y_3 \\ 0 & 0 & 0 \\ 0 & 0 & 0 \\ y_1-y_3 & 0 & -(x_1-x_3) \\ 0 & -(x_1-x_3) & y_1-y_3 \end{bmatrix} \tag{65c}$$

Adding (65a-c) to form $[B_i]$ gives

$$[B_i] = \frac{1}{2\sqrt{A}} \begin{bmatrix} y_2-y_3 & 0 & x_3-x_2 \\ 0 & x_3-x_2 & y_2-y_3 \\ y_3-y_1 & 0 & x_1-x_3 \\ 0 & x_1-x_3 & y_3-y_1 \\ y_1-y_2 & 0 & x_2-x_1 \\ 0 & x_2-x_1 & y_1-y_2 \end{bmatrix} \tag{66}$$

2.2.3 Plane Stress Quadrilateral

Figure 5 shows a typical quadrilateral shaped plane stress element. The x and y axes shown are considered to be the elements local axes. A minimum of five parameters are necessary to describe the stress

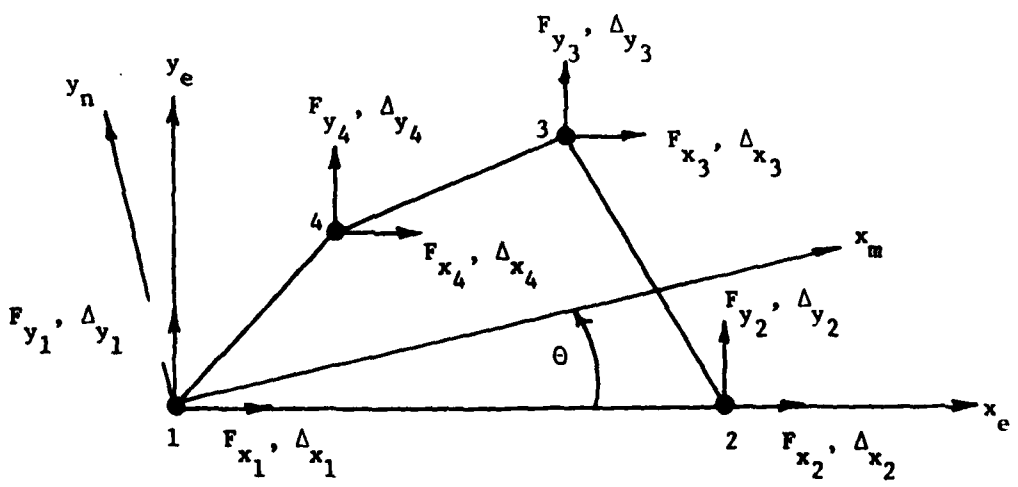

Figure 5 Plane Stress Quadrilateral

field. The admissible functions chosen were

$$\vec{\sigma} = \begin{bmatrix} \sigma_x \\ \sigma_y \\ \tau_{xy} \end{bmatrix} = \frac{1}{t} \begin{bmatrix} \frac{1}{\sqrt{A}} & \frac{y}{A} & 0 & 0 & 0 \\ 0 & 0 & \frac{1}{\sqrt{A}} & \frac{x}{A} & 0 \\ 0 & 0 & 0 & 0 & \frac{1}{\sqrt{A}} \end{bmatrix} \{S\} \tag{67}$$

where $\{S\}^T = [S_1, S_2, S_3, S_4, S_5]$ and $[\tilde{N}]$ is the (3 x 5) matrix on the right-hand side of (67). The compliance matrix $[E]^{-1}$ is the same as that given for the plane stress triangle element. Performing the calculation for $[\bar{f}]$ yields

$$[\bar{f}] = \begin{bmatrix} (E^{-1})_{11} & & & & \\ \frac{y_c}{\sqrt{A}}(E^{-1})_{11} & \frac{I_{xx}}{A^2} & \text{— symmetric —} & & \\ (E^{-1})_{21} & \frac{y_c}{\sqrt{A}}(E^{-1})_{21} & (E^{-1})_{22} & & \\ \frac{x_c}{\sqrt{A}}(E^{-1})_{21} & \frac{I_{xy}}{A^2}(E^{-1})_{21} & \frac{x_c}{\sqrt{A}}(E^{-1})_{22} & \frac{I_{yy}}{A^2}(E^{-1})_{22} & \\ (E^{-1})_{31} & \frac{y_c}{\sqrt{A}}(E^{-1})_{31} & (E^{-1})_{32} & \frac{x_c}{\sqrt{A}}(E^{-1})_{32} & (E^{-1})_{33} \end{bmatrix} \tag{68}$$

where A is the surface area of the quadrilateral; x_c and y_c are the coordinates of the centroidal position; and I_{xx}, I_{yy} and I_{xy} are second moments of area.

As with the plane stress triangle, the edge displacements are assumed linear. In addition, the relation (63) holds, but now the evaluation of the stresses are more complex due to the coordinate dependence as specified in (67). In order to express, for example, the stresses on edge 1-2 due to x' dependence, it is worth noting that the relation between x or y and x' is linear and thus can be specified much like the displacement along the edge:

$$x = x_1 \left[1 - \frac{x'}{\ell'}\right] + x_2 \frac{x'}{\ell'}$$

$$y = y_1 \left[1 - \frac{x'}{\ell'}\right] + y_2 \frac{x'}{\ell'} \tag{69}$$

Thus for edge 1-2

$$[\bar{L}_{1-2}] = \begin{bmatrix} \sin\theta & 0 & -\cos\theta \\ 0 & -\cos\theta & \sin\theta \end{bmatrix} \begin{bmatrix} \frac{1}{\sqrt{A}} & \frac{1}{A}\left[y_1\left(1-\frac{x'}{\ell'}\right)+y_2\frac{x'}{\ell'}\right] & 0 & 0 & 0 \\ 0 & 0 & \frac{1}{\sqrt{A}} & \frac{1}{A}\left[x_1\left(1-\frac{x'}{\ell'}\right)+x_2\frac{x'}{\ell'}\right] & 0 \\ 0 & 0 & 0 & 0 & \frac{1}{\sqrt{A}} \end{bmatrix}$$

$$= \begin{bmatrix} \frac{1}{\sqrt{A}}\sin\theta & \frac{1}{A}\sin\theta\left[y_1\left(1-\frac{x'}{\ell'}\right)+y_2\frac{x'}{\ell'}\right] & 0 & 0 & -\frac{1}{\sqrt{A}}\cos\theta \\ 0 & 0 & -\frac{1}{\sqrt{A}}\cos\theta - \frac{1}{A}\cos\theta\left[x_1\left(1-\frac{x'}{\ell'}\right)+x_2\frac{x'}{\ell'}\right] & \frac{1}{\sqrt{A}}\sin\theta \end{bmatrix} \tag{70}$$

With

$$[Y_{1-2}] = \begin{bmatrix} 1-\frac{x'}{\ell'} & 0 & \frac{x'}{\ell'} & 0 & 0 & 0 & 0 \\ 0 & 1-\frac{x'}{\ell'} & 0 & \frac{x'}{\ell'} & 0 & 0 & 0 & 0 \end{bmatrix}$$

$$[B_{1-2}] = \int_0^{\ell'} dx' \begin{bmatrix} \frac{1}{\sqrt{A}}(1-\frac{x'}{\ell'})\sin\theta & \frac{1}{A}(1-\frac{x'}{\ell'})\sin\theta[y(x')] & 0 & 0 & -\frac{1}{\sqrt{A}}(1-\frac{x'}{\ell'})\cos\theta \\ 0 & 0 & -\frac{1}{\sqrt{A}}(1-\frac{x'}{\ell'})\cos\theta & -\frac{1}{A}(1-\frac{x'}{\ell'})[\frac{x'}{\ell'}] & \frac{1}{\sqrt{A}}(1-\frac{x'}{\ell'})\sin\theta \\ \frac{1}{\sqrt{A}}\frac{x'}{\ell'}\sin\theta & \frac{1}{A}\frac{x'}{\ell'}\sin\theta[y(x')] & 0 & 0 & \frac{1}{\sqrt{A}}\frac{x'}{\ell'}\cos\theta \\ 0 & 0 & -\frac{1}{\sqrt{A}}\frac{x'}{\ell'}\cos\theta & -\frac{1}{A}\frac{x'}{\ell'}[x(x')] & \frac{1}{\sqrt{A}}\frac{x'}{\ell'}\sin\theta \\ 0 & 0 & 0 & 0 & 0 \\ 0 & 0 & 0 & 0 & 0 \\ 0 & 0 & 0 & 0 & 0 \\ 0 & 0 & 0 & 0 & 0 \end{bmatrix} \quad (71)$$

$$[B_{1-2}] = \frac{1}{2}\begin{bmatrix} \frac{y_2-y_1}{\sqrt{A}} & \frac{(y_2-y_1)(2y_1+y_2)}{3A} & 0 & 0 & \frac{-(x_2-x_1)}{\sqrt{A}} \\ 0 & 0 & \frac{-(x_2-x_1)}{\sqrt{A}} & \frac{-(x_2-x_1)(2x_1+x_2)}{3A} & \frac{y_2-y_1}{\sqrt{A}} \\ \frac{y_2-y_1}{\sqrt{A}} & \frac{(y_2-y_1)(y_1+2y_2)}{3A} & 0 & 0 & \frac{-(x_2-x_1)}{\sqrt{A}} \\ 0 & 0 & \frac{-(x_2-x_1)}{\sqrt{A}} & \frac{-(x_2-x_1)(x_1+2x_2)}{3A} & \frac{y_2-y_1}{\sqrt{A}} \\ 0 & 0 & 0 & 0 & 0 \\ 0 & 0 & 0 & 0 & 0 \\ 0 & 0 & 0 & 0 & 0 \\ 0 & 0 & 0 & 0 & 0 \end{bmatrix} \tag{72a}$$

Similarly,

$$[B_{2-3}] = \frac{1}{2}\begin{bmatrix} 0 & 0 & 0 & 0 & 0 \\ 0 & 0 & 0 & 0 & 0 \\ \frac{y_3-y_2}{\sqrt{A}} & \frac{(y_3-y_2)(2y_2+y_3)}{3A} & 0 & 0 & \frac{-(x_3-x_2)}{\sqrt{A}} \\ 0 & 0 & \frac{-(x_3-x_2)}{\sqrt{A}} & \frac{-(x_3-x_2)(2x_2+x_3)}{3A} & \frac{y_3-y_2}{\sqrt{A}} \\ \frac{y_3-y_2}{\sqrt{A}} & \frac{(y_3-y_2)(y_2+2y_3)}{3A} & 0 & 0 & \frac{-(x_3-x_2)}{\sqrt{A}} \\ 0 & 0 & \frac{-(x_3-x_2)}{\sqrt{A}} & \frac{-(x_3-x_2)(x_2+2x_3)}{3A} & \frac{y_3-y_2}{\sqrt{A}} \\ 0 & 0 & 0 & 0 & 0 \\ 0 & 0 & 0 & 0 & 0 \end{bmatrix} . \tag{72b}$$

$$[B_{3-4}] = \frac{1}{2}\begin{bmatrix} 0 & 0 & 0 & 0 & 0 \\ 0 & 0 & 0 & 0 & 0 \\ 0 & 0 & 0 & 0 & 0 \\ 0 & 0 & 0 & 0 & 0 \\ \frac{y_4-y_3}{\sqrt{A}} & \frac{(y_4-y_3)(2y_3+y_4)}{3A} & 0 & 0 & \frac{-(x_4-x_3)}{\sqrt{A}} \\ 0 & 0 & \frac{-(x_4-x_3)}{\sqrt{A}} & \frac{-(x_4-x_3)(2x_3+x_4)}{3A} & \frac{y_4-y_3}{\sqrt{A}} \\ \frac{y_4-y_3}{\sqrt{A}} & \frac{(y_4-y_3)(y_3+2y_4)}{3A} & 0 & 0 & \frac{-(x_4-x_3)}{\sqrt{A}} \\ 0 & 0 & \frac{-(x_4-x_3)}{\sqrt{A}} & \frac{-(x_4-x_3)(x_3+2x_4)}{3A} & \frac{y_4-y_3}{\sqrt{A}} \end{bmatrix} \tag{72c}$$

$$[B_{4-1}] = \frac{1}{2}\begin{bmatrix} \frac{y_1-y_4}{\sqrt{A}} & \frac{(y_1-y_4)(y_4+2y_1)}{3A} & 0 & 0 & \frac{-(x_1-x_4)}{\sqrt{A}} \\ 0 & 0 & \frac{-(x_1-x_4)}{\sqrt{A}} & \frac{-(x_1-x_4)(x_4+2x_1)}{3A} & \frac{y_1-y_4}{\sqrt{A}} \\ 0 & 0 & 0 & 0 & 0 \\ 0 & 0 & 0 & 0 & 0 \\ 0 & 0 & 0 & 0 & 0 \\ 0 & 0 & 0 & 0 & 0 \\ \frac{y_1-y_4}{\sqrt{A}} & \frac{(y_1-y_4)(2y_4+y_1)}{3A} & 0 & 0 & \frac{-(x_1-x_4)}{\sqrt{A}} \\ 0 & 0 & \frac{-(x_1-x_4)}{\sqrt{A}} & \frac{-(x_1-x_4)(2x_4+x_1)}{3A} & \frac{y_1-y_4}{\sqrt{A}} \end{bmatrix} \tag{72d}$$

Adding (72 a-d) together yields

$$[B_1] = \frac{1}{2}\begin{bmatrix} \frac{y_2-y_4}{\sqrt{A}} & \frac{(y_2-y_4)(y_4+y_1+y_2)}{3A} & 0 & 0 & \frac{-(x_2-x_4)}{\sqrt{A}} \\ 0 & 0 & \frac{-(x_2-x_4)}{\sqrt{A}} & \frac{-(x_2-x_4)(x_4+x_1+x_2)}{3A} & \frac{y_2-y_4}{\sqrt{A}} \\ \frac{y_3-y_1}{\sqrt{A}} & \frac{(y_3-y_1)(y_1+y_2+y_3)}{3A} & 0 & 0 & \frac{-(x_3-x_1)}{\sqrt{A}} \\ 0 & 0 & \frac{-(x_3-x_1)}{\sqrt{A}} & \frac{-(x_3-x_1)(x_1+x_2+x_3)}{3A} & \frac{y_3-y_1}{\sqrt{A}} \\ \frac{y_4-y_2}{\sqrt{A}} & \frac{(y_4-y_2)(y_2+y_3+y_4)}{3A} & 0 & 0 & \frac{-(x_4-x_2)}{\sqrt{A}} \\ 0 & 0 & \frac{-(x_4-x_2)}{\sqrt{A}} & \frac{-(x_4-x_2)(x_2+x_3+x_4)}{3A} & \frac{y_4-y_2}{\sqrt{A}} \\ \frac{y_1-y_3}{\sqrt{A}} & \frac{(y_1-y_3)(y_3+y_4+y_1)}{3A} & 0 & 0 & \frac{-(x_1-x_3)}{\sqrt{A}} \\ 0 & 0 & \frac{-(x_1-x_3)}{\sqrt{A}} & \frac{-(x_1-x_3)(x_3+x_4+x_1)}{3A} & \frac{y_1-y_3}{A} \end{bmatrix} \quad (73)$$

2.2.4 Symmetric Shear Panel

The thoretical formulation for a shear panel may be approached in various ways. One way would be to consider it to be a special case of a plane stress quadrilateral with normal stresses identically zero. Thus, for a general quadrilateral shear panel

$$\tau_{xy} = \frac{1}{t\sqrt{A}} S \tag{74a}$$

$$[\bar{f}] = (E^{-1})_{33} \tag{74b}$$

$$[B_i] = \frac{1}{2\sqrt{A}} \begin{bmatrix} -(x_2 - x_4) \\ y_2 - y_4 \\ -(x_3 - x_1) \\ y_3 - y_1 \\ -(x_4 - x_2) \\ y_4 - y_2 \\ -(x_1 - x_3) \\ y_1 - y_3 \end{bmatrix} \tag{74c}$$

Equations (74 a-c) are taken from (67), (68), and (73) where S_5 (here identified as S) is the only non-zero parameter. The element apparently has eight degrees of freedom, but only four are independent; or, shifting the argument to a force method point of view, the loads on the panel must be such that the constraints implied by (74c) are satisfied; that is, a panel that is supported against rigid body motion, may not be loaded in an arbitrary manner at the free nodes and still

maintain its identity as a shear panel. It is quite possible that a structure assumed to be composed of quadrilateral shear panels would yield equations (14) with dependent or contradictory equations.

Since the primary application of quadrilateral shear panels is modeling spar webs in wing structures, the most obvious solution to the problem described above is the creation of a symmetric web element, Figure 6. In this form, only half an element is used in the analysis, and thus only two nodes remain. When rigid body modes are restrained, only one degree of freedom will remain. Note that some support condition on nodes 1 or 2 implies some loading on the lower, non-analyzed

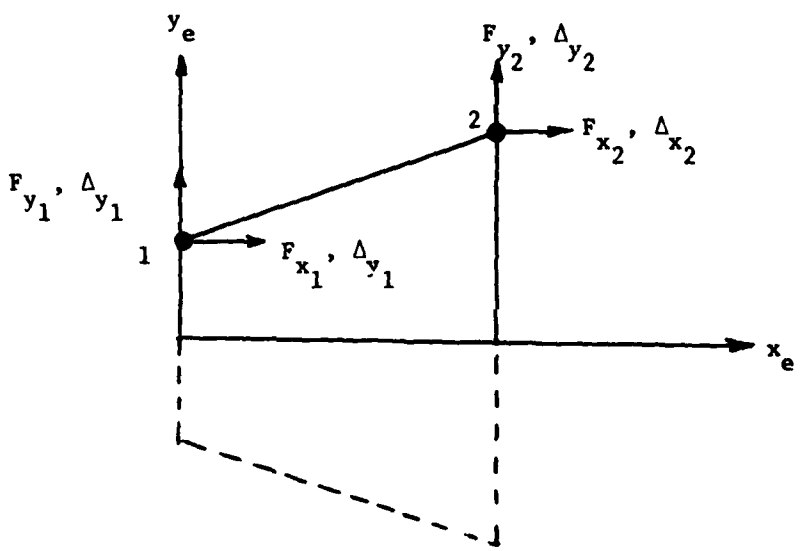

Figure 6 Symmetric Shear Panel

half of the web. The element matrices may now be written for the (upper half of the) symmetric shear web as

$$\tau_{xy} = \frac{S}{[(x_2-x_1)(y_1+y_2)]^{\frac{1}{2}}} \tag{75a}$$

$$[\bar{f}] = \frac{1}{G_{xy}} \tag{75b}$$

$$[B_i] = \frac{1}{2} \begin{bmatrix} [(x_2-x_1/(y_1+y_2)]^{\frac{1}{2}} \\ -[(y_1+y_2)/(x_2-x_1)]^{\frac{1}{2}} \\ [(x_2-x_1)/(y_1+y_2)]^{\frac{1}{2}} \\ [(y_1+y_2)/(x_2-x_1)]^{\frac{1}{2}} \end{bmatrix} \tag{75c}$$

where, in (75b) the x axis is chosen as the material axis.

2.3 Weight Optimization Method

In this section, the optimization method developed is described. What is desired is to obtain the minimum weight of a structure of given geometric layout, material properties and loading that satisfies a set of size and structural constraints. The basic unknowns of the optimization procedure are the element sizes, A_i, $i=1, \ldots, N_E$, where N_E is the number of elements.

2.3.1 Theoretical Basis

The theoretical basis for the generation of the proper equations for the optimization procedure are the Kuhn-Tucker optimality criteria (Reference 14). These criteria are formulated by extending the standard "Lagrange multiplier" method of optimizing a quantity subject to constraints to cases of inequality constraints. An informal review of the theory is now presented.

For the basic Lagrange scheme, a function $Z=f(x_1, x_2, \ldots, x_n)$ subject to equality constraints $g_i(x_1, x_2, \ldots, x_m) = 0$, $i=1, 2, \ldots, m<n$, is to be optimized. A quantity known as the Lagrangian is formed as

$$L = f(x_j) + \sum_{i=1}^{m} \lambda_i \, g_i(x_j) \tag{76}$$

Derivatives are taken with respect to each x_j and λ_i and set to zero to obtain the system of equations:

$$\frac{\partial L}{\partial x_j} = \frac{\partial f}{\partial x_j} + \sum_{i=1}^{m} \lambda_i \frac{\partial g_i}{\partial x_j} = 0 \qquad j=1,2,\ldots,n \tag{77a}$$

$$\frac{\partial L}{\partial \lambda_i} = g_i = 0. \qquad i=1,2,\ldots,m \tag{77b}$$

Equations (77b) are just a reiteration of the constraint equations. The system (77) contains (m+n) equations for (m+n) unknowns. Note that there are no restrictions on the signs of either the x's or the λ's.

Suppose the optimization problem contained inequality constraints, say, less than or equal to constraints, and the function Z is to be minimized subject to those constraints. Then a set of variables G_i may be introduced to make the inequality constraints equality constraints by

$$g_i + G_i^{\,2} = 0 \qquad i = 1,2,\ldots,m. \tag{78}$$

Now the Lagrangian is

$$L = f + \sum_{i=1}^{m} \lambda_i \, (g_i + G_i^{\,2}). \tag{79}$$

Taking derivatives with respect to x_j's, λ_i's and G_i's gives

$$\frac{\partial L}{\partial x_j} = \frac{\partial f}{\partial x_j} + \sum_{i=1}^{m} \lambda_i \frac{\partial g_i}{\partial x_j} = 0 \tag{80a}$$

$$\frac{\partial L}{\partial \lambda_i} = g_i + G_i^{\,2} = 0 \tag{80b}$$

$$\frac{\partial L}{\partial G_i} = 2\lambda_i G_i = 0 \ . \tag{80c}$$

Equation (80c) implies that either λ_i or G_i equals zero. If $G_i = 0$, then $g_i = 0$, that is, the constraint is satisfied at equality, or, as it will be described later, the constraint is "on". If $\lambda_i = 0$, then G_i would not necessarily be zero and the corresponding constraint is $g_i \leq 0$, or satisfied in the inequality sense, or "off".

Since a minimization is required here, the pure second derivatives of L must be non-negative; in particular, from (80c).

$$\frac{\partial^2 L}{\partial G_i^2} = 2\ \lambda_i \geqslant 0 \tag{81}$$

or, that the Lagrange multipliers must be non-negative. The discussion above allows for the elimination of G_i from the analysis by writing for (80b, c):

$$\begin{aligned} &\text{If } \lambda_i = 0, \text{ then } g_i \leq 0; \\ &\text{If } \lambda_i > 0, \text{ then } g_i = 0; \\ &\quad \lambda_i \text{ non-negative.} \end{aligned} \tag{82}$$

Greater-than-or-equal-to constraints may be multiplied by -1 to convert to less-than constraints, or their corresponding multipliers must be non-positive. Since a strict equality constraint can be thought of as simultaneously a less-than and greater-than constraint, the Lagrange multiplier will be unrestricted in sign, as seen above in (77).

It is necessary for the generalized problem, then, to satisfy equations (80a) and conditions (82) at the optimal condition. There may be other extremum where these conditions are satisfied as well. Only when certain conditions of convexity are satisfied are these conditions sufficient for an optimum; furthermore, the equations themselves give no clue on how to solve them.

2.3.2 Problem Formulation

The solution method for a system of equations such as (80a) and (82) can only be determined after the specific form of the system is known. The weight optimization problem is thus formulated. The total weight of the structure must be minimized; hence, the function Z is

$$W = \sum_{i=1}^{N_E} \bar{W}_i A_i \tag{83}$$

where $\bar{W}_i$ is the weight per unit element size, and may be calculated as

$$\bar{W}_i = \bar{m}_i g \tag{84}$$

where $\bar{m}_i$ is defined in (47) and g is the acceleration due to gravity. In addition the structure is subject to the following constraints:

a) Minimum size constraints: The element sizes (thickness, cross-sectional area) must exceed a certain minimum (positive) value due to constraints arising from manufacturing capabilities. If the minimum value for the ith element is A_i^*, then

$$A_i > A_i^* \quad i=1, 2, \ldots, N_E. \tag{85}$$

b) Maximum Stress Constraints: Suppose the yield (or some other failure) stress for the ith element is σ_i^*. Then a stress constraint must

be in the form

$$\sigma_{e_i} < \sigma_i^* \qquad i = 1, 2, \ldots, N_E \tag{86}$$

where σ_{e_i} is an effective stress measure. Not only does σ_{e_i} depend on the element sizes, but it also depends on the state of loading.

c) Displacement Constraints: A typical displacement constraint is in the form

$$\Delta_j \lesseqgtr \Delta_j^* \qquad j = 1, 2, \ldots, N_{DC} \tag{87}$$

where Δ_j^* is the limiting value on the jth displacement that is desired to be constrained. The number of such constrained displacements is N_{DC}.

d) Frequency Range Constraints: In general, these constraints may be written as

$$\omega_{k_\ell} \gtreqless \omega_\ell^* \qquad \ell = 1, 2, \ldots, N_\omega \tag{88}$$

where ω_k is the k_ℓ'th fundamental frequency to be constrained to the ℓth extreme value ω_ℓ^* for the ℓth constraint in the set of N_ω frequency constraints.

While the mathematical forms of the constraints are rather simple to write, the actual calculation of the left-hand sides in terms of the element sizes are not simple for either force or displacement method formulations. The form of (80a) demands that an explicit differentiation of the constraint equations (when stated in a specified form) with respect to the element sizes be performed. In Section 2.1 of this volume, the dependence of many of the basic matrices on the element sizes is explicitly given. The state of the applied loading, of course, is also given; however, the set of redundants, $\{X\}$, which acts as a conduit of

information to find the displacements and stresses, cannot be written in a direct, explicit manner as a function of the element sizes. It may be advantageous to extend the set of basic variables to include $\{X\}$; and, if done, the relation between $\{X\}$ and element sizes must be explicitly written. This relation is nothing more than (20a), and will serve as another set of constraints. Note that the explicit element size dependence in (20a) is one which is a sum of terms each containing an element size in the inverse first power. The displacements are calculated from (20b), where this condition also exists, as well as (3) used to calculate the stress field. It thus seems likely that constraints (86) and (87) will also be in this form. Equations (85) can be converted into this form as well. Excluding (88) for now, the constraint equations may be rewritten in one of two forms:

$$\sum_{j=1}^{N_E} \frac{C_{ij}^{1}}{A_j} - 1 \leq 0 \tag{89a}$$

or

$$\sum_{j=1}^{N_E} \frac{C_{ij}^{2}}{A_j} \leq 0 \, . \tag{89b}$$

Substituting (89) and (83) into (76) yields

$$L = \sum_{i=1}^{N_E} \bar{W}_i A_i + \sum_{i=1}^{m_1} \lambda_i^1 \left(\sum_{j=1}^{N_E} \frac{C_{ij}^{1}}{A_j} - 1 \right) + \sum_{i=1}^{m_2} \lambda_i^2 \left(\sum_{j=1}^{N_E} \frac{C_{ij}^{2}}{A_j} \right) \tag{90}$$

where m_1 and m_2 are the number of constraints of the type of (89a) and (89b), respectively. Differentiate (90) with respect to A_K to yield

$$\frac{\partial L}{\partial A_k} = \bar{W}_k - \frac{1}{A_k^2} \sum_{i=1}^{1} \lambda_i^2 C_{ik}^{1} - \frac{1}{A_k^2} \sum_{i=1}^{2} \lambda_i^2 C_{ik}^{2} \, . \tag{91}$$

Now form

$$L + \sum_{k=1}^{N_E} A_k \frac{\partial L}{\partial A_k} = \sum_{i=1}^{N_E} \bar{W}_i A_i + \sum_{i=1}^{m_1} \lambda_i^1 \left(\sum_{j=1}^{N_E} \frac{C_{ij}^1}{A_j} - 1 \right) + \sum_{i=1}^{m_2} \lambda_i^2 \sum_{j=1}^{N_E} \frac{C_{ij}^2}{A_j}$$

$$+ \sum_{k=1}^{N_E} \bar{W}_k A_k - \sum_{k=1}^{N_E} \frac{1}{A_k} \sum_{i=1}^{m_1} \lambda^2 C_i^1 - \sum_{k=1}^{N_E} \frac{1}{A_k} \sum_{i=1}^{m_2} \lambda_i^2 C_{ik}^2 = 2W - \sum_{i=1}^{m_1} \lambda_i^2 . \tag{92}$$

Evaluating (92) at the optimum condition will imply

$$L = W^* \; ; \; \frac{\partial L}{\partial A_k} = 0, \; k=1, \ldots, N_E \tag{93}$$

where W^* is the optimum weight; thus, substituting (93) into (92) gives

$$\sum_{i=1}^{m_1} \lambda_i^1 = W^* \tag{94}$$

at the optimum design. <u>Thus, the sum of the Lagrange multipliers for the constraints written in the form (89a) equals the minimum weight of the structure for the optimum design</u>. This circumstance will play a prominent role in the solution algorithm.

The constraint equations are now rewritten to be in one of the forms shown by (89).

a) <u>Minimum Size Constraints</u> - Equations (85) are rearranged to form

$$g_{A_i} = \frac{A_i^*}{A_i} - 1 \leq 0 \qquad L = 1, 2, \ldots, N_E . \tag{95}$$

b) Maximum Stress Constraints - The effective stress measure is dependent on the physical assumptions used for a given element as well as the mathematical form of the stress field in terms of the chosen stress parameters. In general, a Mises-Henchy criteria, $(\sigma_x^2+\sigma_y^2-\sigma_x\sigma_y+3\tau_{xy}^2)^{\frac{1}{2}}$, will be used for all the elements.

i) Truss Element

$$\sigma_{e_i} = (\sigma_x^2)^{\frac{1}{2}} = \frac{1}{A_i}(S_i^2)^{\frac{1}{2}} = \frac{1}{A_i}\left|S_i\right| . \tag{96}$$

ii) Plane Stress Triangle

$$\sigma_{e_i} = (\sigma_x^2 + \sigma_y^2 - \sigma_x\sigma_y + 3\tau_{xy}^2)^{\frac{1}{2}}$$

$$= \frac{1}{t_i\sqrt{A}}(S_1^2+S_2^2-S_1S_2+3S_3^2)^{\frac{1}{2}} \tag{97}$$

iii) Plane Stress Quadrilateral

$$\sigma_{e_i} = (\sigma_x^2 + \sigma_y^2 - \sigma_x\sigma_y + 3\tau_{xy}^2)^{\frac{1}{2}}$$

$$= \frac{1}{t_i\sqrt{A}}\left[(S_1+S_2\frac{y_c}{\sqrt{A}})^2 + (S_3+S_4\frac{x_c}{\sqrt{A}})^2 - (S_1+S_2\frac{y_c}{\sqrt{A}})(S_3+S_4\frac{x_c}{\sqrt{A}})+3S_5^2\right]^{\frac{1}{2}} \tag{98}$$

Note that for this element, the stress is evaluated arbitrarily at the centroid of the quadrilateral.

iv) Shear Panel

$$\sigma_{e_i} = [3\,\tau_{xy}^2]^{\frac{1}{2}} = \frac{1}{t_i}\sqrt{\frac{3}{A}}\;|S| \tag{99}$$

It is noted that in each case, (96) - (99) , the form of the equivalent stress is

$$\sigma_{e_i} = \frac{Y_i\,(\{S_i\})}{A_i} \tag{100}$$

where A_i represents the element's design variables, t or A. Substituting into (86) and rearranging yields

$$g_{\sigma_i} = \frac{Y_i\,(\{S_i\})}{A_i\,\sigma_i^*} - 1 \leq 0 \qquad i = 1, 2, \ldots, N_E\,. \tag{101}$$

c) Displacement Constraints - The displacement constraints are derived from (20b) using (31). For the jth displacement:

$$\sum_{i=1}^{N_E}\sum_{k=1}^{N_x}\frac{1}{A_i}\,\bar{\psi}_{ij}^{i}\,x_k + \sum_{i=1}^{N_E}\sum_{\ell=1}^{N_{DN}}\frac{1}{A_i}\,\bar{\Omega}_{j\ell}^{i}\,P_\ell = \Delta_j \tag{102}$$

where N_x is the number of redundants in $\{x\}$ and N_{DN} is the number of non-supported degrees of freedom. Comparing (102) with (87), and allowing for multiplication by -1 to express all constraints in a "less-than-or-equal-to" form, gives

$$g_\Delta^j = \frac{1}{\Delta_j^*}\sum_{i=1}^{N_E}\frac{C_{ij}}{A_i} - 1 \leq 0 \tag{103}$$

where

$$C_{ij} = \pm \left(\sum_{k=1}^{N_x} \psi_{ij}^{-i} x_k + \sum_{\ell=1}^{N_{DN}} \bar{\Omega}_{j\ell}^{i} P_\ell \right. . \tag{104}$$

d) Frequency Range Constraints - In order to formulate these constraints correctly, it is necessary to rewrite equations (20) for free vibration. The kth fundamental mode and frequency satisfies

$$[\phi] \{x_k\} + [\psi] \{P_k\} = \{0\}$$

$$[\psi]^T \{x_k\} + ([\Omega] - \frac{1}{\omega_k^2} [M_\ell]^{-1}) \{P_k\} = \{0\} . \tag{105}$$

Premultiplying the first equation by $\{x_k\}^T$, the second equation by $\{P_k\}^T$, and adding, yields

$$\{x_k\}^T [\phi] \{x_k\} + 2 \{x_k\}^T [\psi] \{P_k\} + \{P_k\}^T [\Omega] \{P_k\}$$

$$- \frac{1}{\omega_k^2} \{P_k\}^T [M_\ell]^{-1} \{P_k\} = 0 . \tag{106}$$

The first three terms of (106) are grouped together as a quantity f_k. Specifically,

$$f_k = \sum_{j=1}^{N_x} \sum_{\ell=1}^{N_x} \phi_{j\ell} (x_k)_j (x_k)_\ell + \sum_{j=1}^{N_x} \sum_{\ell=1}^{N_{DN}} \psi_{j\ell} (x_k)_j (P_k)_\ell$$

$$+ \sum_{j=1}^{N_{DN}} \sum_{\ell=1}^{N_{DN}} \Omega_{j\ell} (P_k)_j (P_k) . \tag{107}$$

Substituting (31) into (107) yields

$$f_k = \sum_{i=1}^{N_E} \frac{f_{ik}}{A_i} \tag{108}$$

where

$$f_{ik} = \sum_{j=1}^{N_x} \sum_{\ell=1}^{N_x} \bar{\phi}^i_{j\ell} (X_k)_j (X_k)_\ell + \sum_{j=1}^{N_x} \sum_{\ell=1}^{N_{DN}} \bar{\psi}^i_{j\ell} (X_k)_j (P_k)_\ell$$

$$+ \sum_{j=1}^{N_{DN}} \sum_{\ell=1}^{N_{DN}} \bar{\Omega}^i_{j\ell} (P_k)_j (P_k)_\ell . \tag{109}$$

The term multiplying the frequency is denoted as $\frac{1}{m_k}$. Specifically,

$$\frac{1}{m_k} = \sum_{\ell=1}^{N_{DN}} \{(P_k)_\ell^2 \,/\, [\sum_{i=1}^{N_E} \frac{1}{\beta_{\ell i}\, \bar{m}_i\, A_i}]\} . \tag{110}$$

Although the denominator of (110) is not exactly in the form of (89), it will be shown that it causes no problems in the formulation.

The quantity m_k is certainly non-negative. Suppose the constraint (88) is in a "less than" form, multiplying both sides by m_k after squaring (88) yields

$$m_k \omega_{k_\ell}^2 \leq m_k (\omega_\ell^*)^2 . \tag{111}$$

A negative inverse operation preserves the inequality, thus

$$-\frac{1}{m_k\, \omega_{k_\ell}^2} \leq -\frac{1}{m_k (\omega_\ell^*)^2} . \tag{112}$$

Adding f_k to both sides of (112) and employing (106) yields

$$0 \leq f_{k_\ell} - \frac{1}{m_{k_\ell} (\omega_\ell^*)^2} \tag{113}$$

or

$$g_{\omega}^{\ell} = \frac{1}{m_k(\omega_{\ell}^{*})^2} - f_k \leq 0 \tag{114}$$

A "greater-than" constraint form would have the left-hand side of (114) multiplied through by -1.

e) Constraints Relating {X} with Element Sizes - These constraints are equations (20a). Substituting (31) into (20a) yields

$$g_x^j = \sum_{i=1}^{N_E} \frac{D_{ij}}{A_i} = 0 \qquad j=1, 2, \ldots, N_x \tag{115}$$

where

$$D_{ij} = \sum_{k=1}^{N_x} \bar{\phi}_{jk}^{i} X_k + \sum_{i=1}^{N_{DN}} \bar{\Psi}_{j\ell}^{i} P_{\ell} \tag{116}$$

Note that equations (115) are strict equalities.

It is quite possible that the structure may be subject to more than one set of static loads. The design must satisfy the various constraints for each of the load conditions. Additional constraints are formed for each load condition, i.e., for each constraint dependent on {P}. Thus, additional sets of stress, displacement and equilibrium constraints must be included for each additional load case.

The Lagrangian may now be rewritten by combining (83), (95), (101), (103), (114), and (115) and introducing Lagrange multipliers μ. Thus

$$L = W + \sum_{i=1}^{N_E} \mu_A^i g_A^i + \sum_{i=1}^{N_E} \sum_{j=1}^{N_L} \mu_\sigma^{i,j} g_\sigma^{i,j} + \sum_{i=1}^{N_{DC}} \sum_{j=1}^{N_L} \mu_\Delta^{i,j} g_\Delta^{i,j} + \sum_{i=1}^{N_\omega} \mu_\omega^i g_\omega^i$$

$$+ \sum_{i=1}^{N_X} \sum_{j=1}^{N_L} \mu_x^{i,j} g_x^{i,j} \tag{117}$$

where N_L refers to the number of load cases. For simplicity, the formulation will continue with $N_L = 1$, thus avoiding double subscripting. From (117), the Kuhn-Tucker optimality conditions are derived. (It is to be remembered that L is a function of {X} as well.) Application of these conditions yields

$$\frac{\partial L}{\partial A_i} = 0 \qquad i=1, 2, \ldots, N_E \tag{118a}$$

$$\frac{\partial L}{\partial X_j} = 0 \qquad j = 1, 2, \ldots, N_x \tag{118b}$$

If $\mu_A^i \geq 0$, then $g_A^i = 0$ <u>or</u>

If $\mu_A^i = 0$, then $g_A^i \leq 0$ $\qquad i=1, 2, \ldots, N_E$ (118c)

If $\mu_\sigma^i \geq 0$, then $g_\sigma^i = 0$ <u>or</u>

If $\mu_\sigma^i = 0$, then $g_\sigma^i \leq 0$ $\qquad i=1, 2, \ldots, N_E$ (118d)

If $\mu_\Delta^i \geq 0$, then $g_\Delta^i = 0$ <u>or</u>

If $\mu_\Delta^i = 0$, then $g_\Delta^i \leq 0$ $\qquad i=1, 2, \ldots, N_{DC}$ (118e)

If $\mu_\omega^i \geq 0$, then $g_\omega^i = 0$ <u>or</u>

If $\mu_\omega^i = 0$, then $g_\omega^i \leq 0$ $\qquad i=1, 2, \ldots, N_\omega$ (118f)

$$g_x^i = 0 \qquad i=1, 2, \ldots, N_X \tag{118g}$$

The left-hand side of equations (118a, b) involve first derivatives of the constraint equations. The dependence in the element sizes for the

constraint equations is that of (89), except for the $\frac{1}{m_k}$ term in the frequency constraints, and thus the first derivatives are fairly straightforward. For the frequency constraint,

$$\frac{\partial g_\omega^k}{\partial A_i} = \frac{1}{(\omega_k^*)^2} \frac{\partial}{\partial A_i} \left(\frac{1}{m_i}\right) - \frac{\partial f_k}{\partial A_i}$$

$$= \frac{-1}{(\omega_k^*)^2} \sum_{\ell=1}^{N_{DN}} \frac{(P_k)_\ell^2 \beta \ell j \bar{m}_i}{\left[\sum_{j=1}^{N_E} \beta \ell j \bar{m}_j A_j\right]^2} + \frac{f_{ik}}{A_i^2} \tag{119}$$

where use has been made of (108) and (110). Note that

$$g_\omega^k + \sum_{i=1}^{N_E} A_i \frac{\partial g_\omega^k}{\partial A_i} = 0 \tag{120}$$

thus preserving the form (94).

The first derivatives of the constraints with respect to the redundants must be calculated for use in (118b). Size and frequency constraints are independent of the loading, and thus independent of the set of redundants. (For the frequency constraints, it is important to note the difference between $\{X\}$, the set of redundants as calculated from the static loads, and X_k, the kth "redundant mode" of the structure when it is in a state of free vibration.) The first derivatives of the other constraints are calculated as follows:

a) <u>Stress Constraints</u> - With g_{σ_i}, (101), expressed as a function of the stress parameters, the derivative with respect to X_j is calculated by the chain rule as

$$\frac{\partial g_{\sigma_i}}{\partial X_j} = \frac{1}{A_i \sigma_i^*} \sum_{k=1}^{N_{P_i}} \frac{\partial Y_i}{\partial S_{i,k}} \frac{\partial S_{i,k}}{\partial X_j} \tag{121}$$

where N_{P_i} is the number of stress parameters for the ith element. The form of $\partial Y_i / \partial S_{i,k}$ is determined for each element. (See (96) - (99)0. The second set of terms in the summation is calculated from (29). Thus,

$$\frac{\partial S_{i,k}}{\partial X_j} = b^i_{1,kj} \; . \tag{122}$$

b) <u>Displacement Constraints</u> - Noting (103) and (104),

$$\frac{\partial g^i_\Delta}{\partial X_j} = \frac{1}{\Delta_i^*} \sum_{k=1}^{N_E} \frac{\bar{\psi}^k_{ji}}{A_k} \; . \tag{123}$$

c) <u>Equilibrium Constraints</u> - Noting (115) and (116),

$$\frac{\partial g^i_x}{\partial x_j} = \sum_{k=1}^{N_E} \frac{\bar{\phi}^k_{ij}}{A_k} \; . \tag{124}$$

The optimization problem is now specified explicitly in terms of the unknown element sizes and redundants, and quantities determined from the loading, discretization, and choice of material properties of the elements.

2.3.3 Description of the Algorithm

Much of the algorithm to be described herein is a modification of the one developed in Reference 4 the initial force method optimization study program.

The guiding principle to be applied is expressed in (94) and that equation's implications.

Suppose a set of element sizes are chosen such that the set of constraints (118 c-g) are satisfied. Now, such a set may be quite difficult to find. With {X} determined by (118g),, top priority may then be given to (118c) and (118d). The values for the sizes and the redundants are used in (118a) and (118b) to generate linear equations in the Lagrange multipliers μ. With the sum of the Lagrange multipliers of the type in (89a) as the objective function, and (118 a,b) as the constraints, a linear programming problem for the Lagrange multipliers is formulated. The linear programming process results in a full vertex solution, i.e., for the $N_E + N_X$ equality constraints (118 a,b) there will be precisely $N_E + N_X$ non-zero valued μ's in the solution. It is anticipated that the N_X non-constrained (in sign) μ_x's will be in this basis, thus leaving a total of N_E from among the μ_A's, μ_σ's, μ_Δ's and μ_ω's. The non-zero μ's correspond to particular constraints being "on", i.e., satisfied at equality. These constraints form a system of $N_E + N_X$ equations for the N_E sizes and N_X redundants for a new design as specified by the set of non-zero multipliers.

This linear programming phase may be initialized in one of several ways. Firstly, initial sizes may be read from data cards; secondly, they may be set to minimum sizes A_i^* by default; thirdly, the stress ratio method may be employed either a finite number of iterations, or until convergence is reached. This solution is known as a fully-stressed design (FSD) and is mathematically a full vertex solution when only size and stress constraints are considered.

The new design as indicated by the set of non-zero μ's is solved from a system of nonlinear equations. If some of the equations are minimum

size constraint equations, a reduction of the system may be accomplished by setting the corresponding sizes to the minimum directly, and eliminating these constraints. The remaining system is satisfied by employing a Newton-Raphson procedure. If this procedure should not converge after a specified number of iterations, the results from the last iteration are used in (118a, b) and the linear programming process is repeated. The entire cycle is repeated a maximum of three times.

If the linear programming process does not converge after three iterations, an FSD design is generated. This design, or the one generated by linear programming if that procedure converged, is used in (118a, b) to determine values for the corresponding μ's to check for their non-negativity, and to check the remaining constraints (118c-f) for violations. If all the μ's are positive and no constraint is violated, the solution is found. If a constraint is violated, a standard "fix-up" procedure is performed which is dependent upon the particular constraint in question. For instance, suppose a g_A constraint is "on" for a given element and the resulting size and set of redundants yields a stress in the element violating its g_σ constraint. The size is raised adequately to turn the g_σ "on" and the g_A "off". The reverse situation is handled in a similar manner. If a g_Δ constraint is violated, all the areas are multiplied by a common factor in order to satisfy it. This operation, however, turns "off" the g_A and g_σ constraints. An algorithm to "fix up" g_ω constraints can be derived by considering inverse mass to flexibility relationships, to find which elements can have their sizes increased to increase the frequency without an excessive weight penalty.

If a particular μ is negative, then the corresponding constraints is turned "off" and the multiplier is set to zero.

The current design at this point has no more than $N_E + N_X$ constraint equations "on". These equations, plus (118a, b) form a system for the element sizes, the redundants, and the non-zero Lagrange multipliers associated with the constraints. A Newton-Raphson procedure is used to solve this system. This procedure will require the calculation of second derivatives of the constraints which are expressed explicitly as follows:

a) Minimum Size Constraints: From (95),

$$\frac{\partial^2 g_A^i}{\partial A_j \partial A_k} = 2\,\frac{A_i^*}{A_i^3} \quad \text{if } i=j=k; \quad = 0 \text{ otherwise.} \tag{125}$$

The derivatives with respect to the redundants are identically zero.

b) Maximum Stress Constraints: From (101) it is seen that

$$\frac{\partial^2 g_\sigma^i}{\partial A_j \partial A_k} = \frac{2}{A_i^3}\,\frac{Y_i}{\sigma_i^*} \quad \text{if } i=j=k; \quad = 0 \text{ otherwise.} \tag{126}$$

The other derivatives are calculated from (121) and (122). Thus,

$$\frac{\partial^2 g_\sigma^i}{\partial X_j\, A_\ell} = \frac{1}{A_i^2 \sigma_i^*} \sum_{k=1}^{N_{P_i}} \frac{\partial Y_i}{\partial S_{i,k}}\, b_1{}^i{}_{,\,k_j} \quad \text{if } i=1; \quad = 0 \text{ otherwise} \tag{127}$$

$$\frac{\partial^2 g_\sigma^i}{\partial X_j \partial X_\ell} = \frac{1}{A_i \sigma_i^*} \sum_{k=1}^{N_{P_i}} - \sum_{m=1}^{N_{P_i}} \frac{\partial^2 Y_i}{\partial S_{i,k} \partial S_{i,m}}\, b_1{}^i{}_{,kj}\, b_1{}^i{}_{,m\ell}\,. \tag{128}$$

c) Displacement Constraints - From (103),

$$\frac{\partial^2 g_\Delta^i}{\partial A_j \partial A_k} = \frac{2}{A_j{}^3}\,\frac{C_{ij}}{\Delta_i^*} \quad \text{if } j=k; \quad = 0 \text{ otherwise} \tag{129}$$

with C_{ij} is defined in (104); from (123),

$$\frac{\partial^2 g_\Delta{}^i}{\partial X_j \partial A_k} = -\frac{1}{\Delta_i{}^*} \frac{\bar{\psi}_{jk}^{\ i}}{A_k{}^2} \tag{130}$$

and the second derivatives with respect to the redundants are zero.

d) <u>Frequency Constraints</u> - From (119),

$$\frac{\partial^2 g_\omega{}^i}{\partial A_j \partial A_k} = \frac{2}{(\omega_i^*)^2} \sum_{\ell=1}^{N_{DN}} \frac{(P_i)^2 \beta_{\ell j} \bar{m}_j \beta_{\ell k} \bar{m}_k}{\left[\sum_{m=1}^{N_E} \beta_{\ell m} \bar{m}_m A_m \right]^3} - \frac{2 f_{ji}}{A_j{}^3} \tag{131}$$

where the second term is included only if j=k. Since $g_\omega{}^i$ is independent of the loading, all derivatives with respect to the redundants are zero.

e) Equilibrium Constraints - From (115),

$$\frac{\partial^2 g_x{}^i}{\partial A_j \ A_k} = \frac{2\ D_{ji}}{A_j{}^3} \quad \text{if} \quad j=k; \ = 0 \text{ otherwise} \tag{132}$$

where D_{ji} is defined in (116); from (124).

$$\frac{\partial^2 g_x{}^i}{\partial X_j \partial A_k} = \bar{\phi}_{ij}^{\ k} \ . \tag{133}$$

The second derivatives with respect to redundants are zero.

Assuming a given set of equations form a system that will converge in a Newton-Raphson procedure, the new design is checked for feasibility. The violated constraints are "fixed-up" in the manner prescribed previously, and those constraints with corresponding negative multipliers are turned off. The procedure of adding and subtracting constraints from the system

to form a new set of equations for the Newton-Raphson procedure leads eventually to a solution.

2.4 Rapid Reanalysis

The purpose of a rapid reanalysis procedure is to analyze a damaged structure using, as much as possible, quantities calculated in the analysis of the original structure. Various means to accomplish this task have been investigated by numerous researchers References 15 to 20. . This work, for the most part, has been based on the matrix displacement method and iterative schemes. Past investigators have defined damage models by removing structural finite elements entirely or reducing values of the design parameters which effect the structures flexibility and mass. J. S. Arora, in Reference 15 for example, defines the damage condition as follows: "A damage condition for the structure is defined to consist of complete or partial removal of selected members or parts of a structure. Some joints of the structure may be removed as a result of damage." These authors applied this definition to a helicopter boom design made of truss members which was subsequently damaged due to munition blast loads occurring inside or near the boom. Another study illustrates a different approach to the damage question. D. S. Scott, et.al., Refere ce 16 , were concerned with lifting surface drag due to holes in the surfaces caused by ballistic penetrations. Their main concern was the derivation of aerodynamic loads on surfaces containing holes and the consequent effect on aeroelastic behavior.

The work of F. G. Hemming, et. al., References 17 and 18, considered battle damage or initial flaw propagation by removal of entire finite elements or by reducing the properties of the damaged elements.

Property reduction could correspond to loss of strength due to crack propagation for instance. In either case only a few finite elements were used to describe the damage condition. Additional work by V. B. Venkayya, References 19 & 20, considered "severe damage" to a three spar - five rib delta wing by removing two top and two bottom membrane elements and one shear panel in the midspar. The work being accomplished by the University of Dayton Research Institute, Dayton, Ohio, Reference 21 , also encompasses the type of damage models described. It was concluded from these and Bell's studies that for the contractual requirements two damage models can be defined; namely, Types A and B. Type A damage consists of complete removal of finite elements due to ballistic damage for instance. Type B damage considers the reduction of finite element properties such that flexibility is increased. This type of damage could represent increased flexibility due to fatigue cracks or small holes caused by ballistic impacts.

The rapid reanalysis method developed for these two types of damage is described below. A few introductory comments follow. Note that previously defined force method matrices are used throughout the development.

Damage will be measured on an element by element basis, and will consist of two separate measurements: d_K^i, the "stiffness damage" to the ith element, and d_M^i, the "mass damage". The numbers d_K^i and d_M^i lie between 0 and 1 inclusive, and represent a fractional decrease in load carrying capacity and mass, respectively. Generally, $d_M^i = 0$ except in cases of physical removal of the element, in which case $d_M^i = 1$. It is conceivable that in cases of phase change at high temperatures that d_M^i may lie strictly between 0 and 1, but, as will be seen, the value of

d_M^i will not effect the method of analysis. The value of d_K^i may have any value in the range.

The following section describes the procedure to be used when $d_K^i < 1$. When $d_K^i = 1$, a special method must be used, and it is described in Section 2.4.2. Finally, the residual elastic strength of the structure is defined and discussed.

2.4.1 Small Scale Damage

Small scale damage is defined as less-than-total stiffness damage, i.e., when $d_K^i < 1$. The effect upon element flexibility is thus

$$[f_i]_d = [f_i]/(1 - d_K^i) \tag{134}$$

where the d refers to values in the damaged state. Note that the flexibility <u>increases</u> with <u>increasing</u> damage. The difference between the new and old states is

$$[\Delta f_i] = [f_i]_d - [f_i] \tag{135}$$

for each of the N_D damaged elements.

Since the geometric layout of the elements and, for the statics case, the loading is assumed not to change, the values of $[b_i]$, $[D]$ and $\{P\}$ remain the same. Thus, if the definitions

$$[\phi]_d = [\phi]+[\Delta\phi];[\psi]_d = [\psi]+[\Delta\psi];[\Omega]_d = [\Omega]+[\Delta\Omega] \tag{136}$$

are made, then

$$[\Delta\phi] = \sum_{i=1}^{N_E} [b_1{}^i]^T[\Delta f_i][b_1{}^i];[\Delta\psi] = \sum_{i=1}^{N_E} [b_1{}^i]^T[\Delta f_i][D_i];[\Delta\Omega] = \sum_{i=1}^{N_E} [D_i]^T[\Delta f_i][D_i]. \tag{137}$$

In the actual numerical procedure the summation is carried out only over the damaged elements.

The equations of statics for the damaged case are those of (2.20), where d subscripts would be added to all quantities used in those equations, except for $\{P\}$. If it is noted that

$$\{X\}_d = \{X\} + \{\Delta X\} \; ; \; \{\Delta\}_d = \{\Delta\} + \{\Delta\Delta\} \tag{138}$$

then, after subtracting (20a) for the undamaged case from (20a) of the damaged case, $\{\Delta X\}$ may be obtained as

$$\{\Delta X\} = -[\phi]_d^{-1} \left([\Delta\phi]\{X\} + [\Delta\psi]\{P\}\right). \tag{139}$$

The inverse of $[\phi]_d$ may pose a problem. Noting (136) and formulating the expansion

$$[\phi]_d^{-1} = [\phi]^{-1} - [\phi]^{-1}[\Delta\phi][\phi]^{-1} + [\phi]^{-1}[\Delta\phi][\phi]^{-1}[\Delta\phi][\phi]^{-1} \cdots \tag{140}$$

will avoid the costly inverse operation, since $[\phi]^{-1}$ is probably obtained in the basic analysis. The rate of convergence of (140) will likely depend on individual d_k values, as well as the proportion of elements affected by damage. In order to assure convergence for values of d_k above some cutoff, say, .4, a scheme is derived whereby the damage is "compounded" at a particular rate for a finite number of times until the total, desired damage level is achieved. If $c_k^{\,i}$ is this compounding rate, then

$$c_k^{\,i} = 1-(1-d_k^{\,i})^{\frac{1}{N}} \tag{141}$$

where N is an integral number of steps. A criteria for choosing N would be the minimum number of compounding steps to achieve d_k^{max}, the maximum damage level from among all the damaged elements, with a compounding rate of less than .4. Manipulating (141) with $d_k^{i} = .4$ yields,

$$N = \log (1-d_k^{max}) / \log .6 \quad . \tag{142}$$

The value N is then raised to the nearest integer and used in (141) to determine individual compounding rates.

Let j-1 iterations in the scheme be complete. The jth iteration consists of deriving the new flexibilities

$$[f_i]_d^{(j)} = [f_i]_d^{(j-1)} / (1-c_k^{i}) \tag{143}$$

from which

$$[\Delta f_i]^{(j)} = [f_i]_d^{(j)} - [f_i]_d^{(j-1)} \tag{144}$$

is defined. As in (137) , $[\Delta\phi]^{(j)}$ is defined as

$$[\Delta\phi]^{(j)} = \sum_{i=1}^{N_E} [b_1^{i}]^T [\Delta f_i]^{(j)} [b_1^{i}] \tag{145}$$

and thus

$$[\phi]_d^{(j)} = [\phi]_d^{(j-1)} + [\Delta\phi]^{(j)} \quad . \tag{146}$$

Using (146) in (140) yields

$$\left([\phi]_d^{(j)}\right)^{-1} = \left([\phi]_d^{(j-1)}\right)^{-1} - \left([\phi]_d^{(j-1)}\right)^{-1} [\Delta\phi]^{(j)} \left(\left([\phi]_d^{(j-1)}\right)^{-1} + \ldots \right. \tag{147}$$

Equations (143) - (147) are repeated for j=1, 2, ..., N. Note that the zeroth state is the undamaged state and the Nth state is the total damaged state.

Returning to the basic re-analysis procedure, equations (20b) for the undamaged state are subtracted from the corresponding equations of the damaged state to yield

$$([\psi] + [\Delta\psi])^T\{\Delta X\} + [\Delta\psi]^T\{X\} + [\Delta\Omega]\{P\} = \{\Delta \Delta\} \tag{148}$$

thus solving the re-analysis problem completely. Another approach is to find

$$[\mathfrak{F}]_d = [\Omega]_d - [\psi]_d^T[\phi]_d^{-1}[\psi]_d \tag{149}$$

and obtain

$$[\mathfrak{F}]_d\{P\} = \{\Delta\}_d. \tag{150}$$

The global flexibility matrix is required when a dynamic re-analysis is needed. For this case, the mass damage must also be specified. Its effect is

$$(m_i)_d = m_i\ (1-d_m{}^i) \tag{151}$$

thus

$$\Delta m_i = -\ d_m{}^i\ m_i. \tag{152}$$

Using (152) in (48) yields

$$\Delta M_{\ell_g} = \sum_{i=1}^{N_E} \beta_{gi}\ \Delta m_i \tag{153}$$

and thus

$$[M_\ell]_d = [M_\ell] + [\Delta M_\ell] \tag{154}$$

where $[\Delta M_\ell]$ is the proper collection of terms (153). The matrix $[Q]_d$ is now formed as in (45) with use of (154) and (149) and eigenvalues and eigenvectors are now calculated. If they are found using some iterative technique, such as the power method, the eigenvectors of the original analysis are used as initial guesses.

2.4.2 Large Scale Damage

Large scale damage is defined as the state when at least one $d_k = 1$. This would lead to an infinite flexibility according to (134). The resulting computational hazards would then make the entire small scale damage algorithm useless. Note that this is unlike the displacement method whereby the damaged element's stiffness is simply "removed" from the global system.

An approach is developed whereby "total loss of load carrying capacity" is translated into "carrying no load". That is, for the ith damaged element

$$\{S_i\}_d = \{0\} \cdot \tag{155}$$

For the collection of the totally damaged elements,

$$\{S_d\}_d = 0 \tag{156}$$

where the d within the brackets denotes those stress parameters which are to be constrained to zero. Noting that

$$\{S_d\} = [b_1{}^d]\{X\} + [D_d]\{P\} \tag{157}$$

equations (1) can be extended by use of Lagrange multipliers $\{\lambda\}$ as

$$\delta U^* + \delta V^* + \delta(\{\lambda\}^T\{S_d\}_d) = 0. \tag{158}$$

It should be noted that not only is the geometric layout the same, and thus $[b_1]$ and $[D]$, but that the flexibilities of the damaged elements are not affected, and thus $[\phi]$, $[\psi]$ and $[\Omega]$ remain the same. Taking variations with respect to $\{X\}$ and $\{P\}$ in (158) yields

$$[\phi]\ \{X\}_d + [\psi]\{P\} + [b_1{}^d]^T\ \{\lambda\} = \{0\} \tag{159a}$$

$$[\psi]^T\ \{X\}_d + [\Omega]\{P\} + [D_d]^T\{\lambda\} = \{\Delta\}. \tag{159b}$$

Variations with respect to the multipliers return the constraints (156) expressed as

$$[b_i{}^d]\ \{X\}_d + [D_d]\{P\} = \{0\}. \tag{160}$$

For the statics case, the solution method for (159) - (160) proceeds by introducing $\{\Delta X\}$ and $\{\Delta\Delta\}$ as in the small scale damage case. Subtracting (20a) from (159a) yields

$$[\phi]\ \{\Delta X\} + [b_1{}^d]^T\ \{\lambda\} = \{0\}\ . \tag{161}$$

The vector $\{\Delta X\}$ is solved in terms of $\{\lambda\}$, and used in (160) to obtain

$$[b_1{}^d]\{X\} - [b_1{}^d][\phi]^{-1}[b_1{}^d]^T\{\lambda\} + [D_d]\{P\} = \{0\}. \tag{162}$$

Noting (157) , the multipliers are

$$\{\lambda\} = ([b_1{}^d][\phi]^{-1}[b_1{}^d]^T)^{-1}\ \{S_d\}. \tag{163}$$

Subtracting (20b) from (159b) yields

$$[\psi]^T\{\Delta X\} + [D_d]^T\{\lambda\} = \{\Delta\Delta\} \tag{164}$$

An alternative approach is to find $[\mathfrak{F}_d]$. This will lend itself readily to adoption for dynamics. Solve (159a) for $\{X_d\}$, substitute into (160) to solve for $\{\lambda\}$ and back substitute into (159b) to give the form

$$[\mathfrak{F}]_d \{P\} = \{\Delta\} \tag{165}$$

where

$$[\mathfrak{F}_d] = [\mathfrak{F}] + ([D_d] - [b_1{}^d][\phi]^{-1}[\psi])^T([b_1{}^d][\phi]^{-1}[b_1{}^d]^T)^{-1}([D_d]-[b_1{}^d][\phi]^{-1}[\psi]). \tag{166}$$

The procedure for determining $[M_\ell]_d$ is the same as before, as well as the procedure for determining new modes and frequencies.

This method for large scale damage is straight forward in approach and calculation. One difficulty that may exist involves the inverse of the matrix product $[b_1{}^d]\,[\phi]^{-1}[b_1{}^d]^T$. If the number of parameters in $\{S_d\}$ exceeds the number of redundants, then this matrix is singular. The physical interpretation can be either the lack of rigid body motion constraints (as in a rectangular truss frame) or by what will be termed "node removal". For instance, if a rectangular plate is divided into triangular elements, and the corner of the plate, represented by one triangle, is removed, the corner node is no longer physically there. The two equilibrium equations at that node are identically satisfied (assuming no loads originally applied there) and should be removed from the analysis. A generalized method to overcome this and similar difficulties is now presented.

Equations (14) are partitioned as

$$\{P\} = [A_u \mid A_d] \begin{bmatrix} S_u \\ \hline S_d \end{bmatrix} \tag{167}$$

where the u subscript refers to the undamaged portion of the structure. Perform a Gauss-Jordan elimination scheme on $[A_u]$ with column as well as row pivoting. It is quite possible (and definite, if the number of rows of $[A_u]$ exceeds the number of columns) that this procedure yields the form

$$\begin{bmatrix} P_u' \\ \hline P_d \end{bmatrix} = \left[\begin{array}{c|c} A_{uu}' & A_{ud}' \\ \hline 0 & A_{dd}' \end{array}\right] \begin{bmatrix} S_u' \\ \hline S_d \end{bmatrix} \tag{168}$$

where the prime indicates that the values are transformed from the original values. The lower partition of (168) are relations strictly among the $\{S_d\}$. Note further that unless $\{P_d'\} = \{0\}$, a contradiction exists and the re-analysis may not continue. Physically, this would imply that a non-damaged truss member, say, would be required to support a transverse applied load. This would cause a basic remodeling of the damaged structure for analysis, and thus a rapid re-analysis cannot be done. Thus, for a properly posed large scale damage problem, the bottom partition is

$$[A_{dd}'] \{S_d\} = \{0\} . \tag{169}$$

A Gauss-Jordan elimination procedure with column pivoting is performed on $[A_{dd}']$, which should have at least as many columns as rows. This yields the form

$$[I \mid A_{dd}^*] \begin{bmatrix} S_d^I \\ \hline S_d^* \end{bmatrix} = \{0\} \tag{170}$$

The form of (170) reveals that if $\{S_d^*\} = \{0\}$, then $\{S_d^I\} = \{0\}$, and thus $\{S_d\} = \{0\}$ simply by equilibrium. Thus, in general, only the elements of $\{S_d^*\}$ need be explicitly set to zero as in (156) in order to obtain the results for the desired damage case. Furthermore, if <u>every</u> element was removed, then $[A_{dd}'] = [A]$, and thus $[A_{dd}^*]$ has a number of column equal to the number of redundants, and thus $[b_1^d][\phi]^{-1}[b_1^d]^T$ is the same size as $[\phi]$.

Finally, it should be noted that if some elements have $d_k^i < 1$ and others have $d_k^i = 1$, that a small scale analysis can be done first with the less than totally damaged elements, and then that solution be used as the undamaged structure for the large scale damage.

2.4.3 Residual Elastic Strength

The previous discussion has centered on the results of methods derived for the rapid reanalysis of damaged structures. Output of these methods are such that the vulnerability of the structure can be determined, this being defined as the ability of the structure to withstand damage as measured by residual elastic strength. This parameter will identify critical damage areas and attendant structural loads which can cause complete failure of the structure. The damage in a structure may, for example, be in the form of a crack in a stringer extending into an adjacent sheet. For analysis purposes the damaged portion of the structure (such as the cracked plates and portions of the cracked stringer in our example) will be removed from the finite element idealization and an elastic reanalysis performed. In

general, if the structure had been optimized and the yield stress criterion was invoked in the design, then obviously the structure is weaker when damaged and for the applied loads for which the structure was optimized there will be no residual strength up to the yield stress values. However, for loads less than those used in the optimization process there may be some residual strength remaining after damage which is proportional to the difference between the allowable yield stress and the applied stresses.

The strength of the damaged structure will depend on the type of damage as related to the failure mode. Thus, for statically determinant structures damage by removal of a structural element can result in a catastrophic failure. However, for a redundant structure a damaged structural element will cause a load shift to other elements and failure will be governed by the strength of remaining elements. It should be noted that in a highly redundant structure maximum residual strength may depend on the failure of more than one structural element.

In the light of the above complexities and in an effort to estimate the remaining strength of a damaged structure, residual elastic strength will be taken to occur at loads which produce gross elastic stresses which are equal to:

a) The yield stress of the material

b) Allowable stress used in the optimization cycle

c) The critical gross (nominal) catastrophic fracture stress based on fracture mechanics concepts.

As part of the optimization process, allowable stresses of the material are used as failure criteria in the optimum design of the structure. Using

these already identified allowable stresses, the residual strength of the structure corresponding to modes of failure can be obtained.

2.4.4 Computer Code & Illustrative Examples

The rapid reanalysis methodology described above was programmed into a remote terminal interactive, (VSPC) computer code which is aptly described and illustrated in Appendix B of Volume II - User's Manual. The reader is referred to this volume for particular program details.

The use of this computer program is illustrated here to assess the damage and residual elastic strength of three and ten bar truss structures. Program input consists of the characteristics of the optimized structure and its loading. The damage level is then expressed in terms of the previously defined parameters d_k^i and d_m^i.

Results for a three bar truss are shown on Figure 7 for four damage levels. (Note that element one sustains the damage.) The tabular data shows the increased stress levels each bar experiences as damage levels increase. It is observed that the first element will yield under the loads used in the optimization cycle as the damage level nears 20%. This denotes the vulnerability of this particular structure to the imposed damage conditions.

Figure 8 depicts a ten bar truss which was examined under a variety of damage cases: Types A and B damage were evaluated in this instance. This truss has been the subject of study by many investigators of weight optimization methods but vulnerability studies have only been conducted by Messrs. Venkaya and Khot in Reference 20. Thus, it provides a good basis of comparison between the Force and Displacement methods of structural analysis. Results of analyses conducted are given in Table 1. Each damage case is given and appropriate results for that case are tabulated. Removal of the

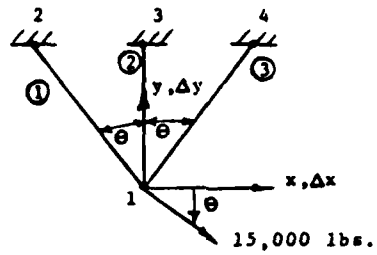

d_k^1	0	.2	.4	.6
El. No.	CROSS SECTIONAL AREA			
1	.625	.500	.391	.250
2	.010	.010	.010	.010
3	.175	.175	.175	.175
El. No.	ELEMENT STRESS (PSI)			
1	25000	31200	39749	61800
2	0	4700	12500	27970
3	-25000	-25166	-25446	-26000
Δx	.52	.59	.70	.92
Δy	0	-.05	-.13	-.28

OPTIMIZATION CONSTRAINTS: A_{min} = .010in^2; all bars

σ= ±25,000psi; all bars

No displacement constraints

W_{min} = 10.1 lbs.

TRUSS CHARACTERISTICS: ρ= .100 lb/in^3

E = 1.0 x 10^7 PSI

θ = 36.87°

$L_{①} = L_{③}$ = 125.0"

$L_{②}$ = 100.0"

Figure 7 Three Bar Truss - Damage Assessment

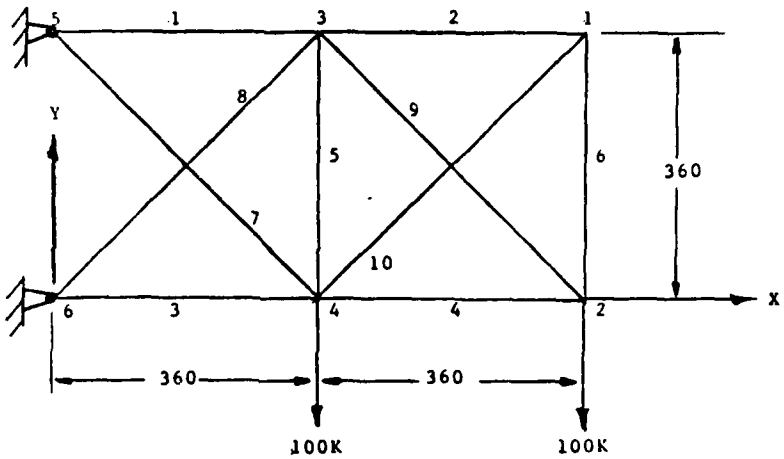

OPTIMIZATION CONSTRAINTS: $A_{min} = .10 in^2$,
$\sigma = \pm 25{,}000$ psi,
$\Delta_{max} = 2.0$ in.

TRUSS CHARACTERISTICS: $\rho = .10$ lbs/in^3
$E = 1.0 \times 10^7$ psi

RESULTS OF OPTIMIZATION: $W_{min} = 5062$ lbs.

EL. NO.	AREA	EL. NO.	AREA
1	30.10	6	.57
2	.10	7	7.51
3	22.73	8	21.33
4	15.45	9	21.70
5	.10	10	.10

Figure 8 Ten Bar Truss

TABLE 1 TEN BAR TRUSS - DAMAGE ASSESSMENT

DAMAGE CASE	d_k^i	σ_i	σ_{max_j}	Δmax	COMMENT
1,i=9	0	6525	σ_5=24970	-2.0	Not Critical
	.5	13014	σ_5=25149	-2.5	Not Critical
	.1	63040	σ_9=63040	-6.1	Structure Collapse
	1.0	-	σ_{10}>1.0E6	-146.4	Structure Collapse
2,i=10	1.0	-	σ_5=25050	-1.99	Not Critical
3,i=7	1.0	-	σ_5=800,000	-30.0	Structure Collapse
4,i=6	1.0	-	σ_5=25050	-1.63	Not Critical

i = Damaged Bar Element Number

σ in pounds per square inch

Δ in inches

Δmax = Displacement of Structure

σ_{max_j} = Max. Stress Occurs in jth Element

ninth element, indicated by i=9, produces a condition of complete collapse of the structure as evidenced by a maximum displacement of 146.4 in. and stress levels exceeding one million pounds per square inch. It must be noted that this result is in agreement with Reference 20 and unlike the reanalysis method used in that reference no iteration procedure is used. The additional conditions tabulated illustrate the vulnerability of the truss to damage and demonstrates the importance of finding those members which cause the entire structure to fail. Conditions such as these permit definition of residual strength levels.

Figure 9 displays the approach to determining the elastic residual strength of the three bar truss through use of the method discussed above. The stresses in each element of the optimized truss were limited to ±25,000 psi. Assuming that a 60% damage level (d_k^1=.6) will be sustained by the first element then the maximum load that the damaged truss can accommodate is P_d=.40P_o, where P_o is the loading that the optimized structure was designed to. In this instance the residual elastic strength level is 40%.

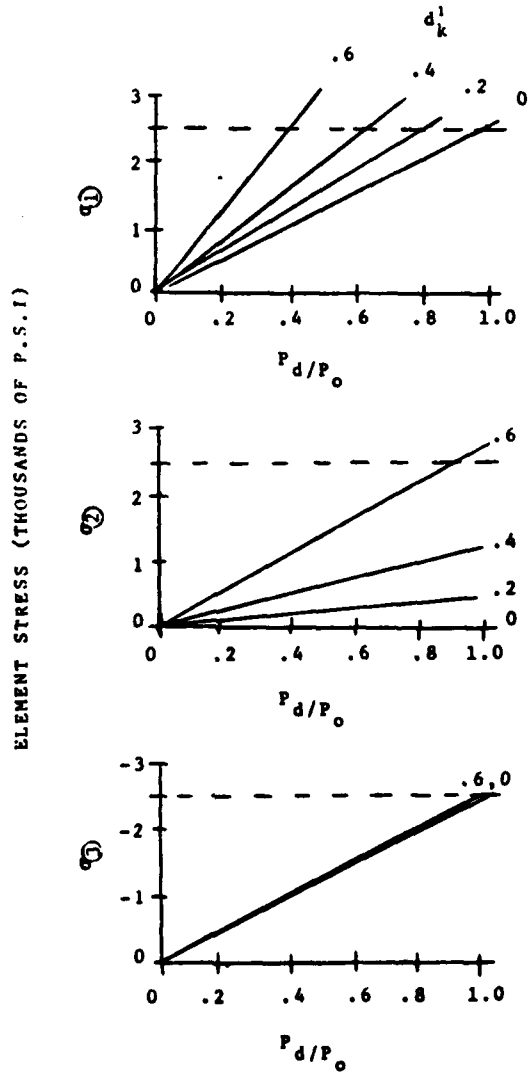

Figure 9 Three Bar Truss - Residual Strength

3.0 OPTFORCE II PROGRAM

3.1 Efficiency Studies

Task VI of the work effort required that the efficiency of the force method optimization program, ØPTFØRCE II, be compared with an existing displacement method optimization program OPTIM III (Ref. 10). Much of the optimization literature in which solution methods are compared report the number of analyses required, apparently using this as a measure of efficiency of the method being discussed. This may be a valid measure of efficiency, but it appears to be dependent on specific machine capability. For example, if only a few analyses are required but each analysis is rather complex, requiring somewhat more computer time, this method would appear to be more efficient on the basis of number of analyses required than a method requiring many analyses, each of very short duration. On the other hand, using computer time (seconds) as a measure of efficiency requires that the problems to be used for comparison be exercised on the same computer system to avoid faster or slower machine influences. The efficiency studies discussed herein were based on computer time but due note was taken of the number iteration cycles as well. Each of the problems were solved either on Bell's IBM 3031 or IBM 3033 computer and the time recorded is the cpu computer time, in seconds, to optimize the structure.

It became very evident, as the study progressed and structural optimization problems were solved, that different design variable populations were obtained for the same minimum weight value using both of the above computer codes and other reference material. Thus, the "efficiency" studies were expanded to include program accuracy as well. The "accuracy" of a particular optimization code was gauged by how well it predicts the

true minimum weight solution. The measure used to accomplish this task was the agreement obtained between different codes and known analytical solutions. The ensuing discussion considers each of the above elements to assess the efficiency of the OPTFORCE II code. Three structures were optimized and are discussed below in turn.

3.1.1 Seventeen Bar Truss

The configuration of the seventeen bar truss is given in Figure 10 with two external loading cases; each load is applied simultaneously, they are not considered as multiple load cases. Material properties and constraints for each loading case are given in Table 2. Only stress and minimum size constraints were considered. The OPTFORCE II NASTRAN compatible input data for this structure is displayed in Figure 11 for Case 2. The OPTIM III input data file is essentially identical to those data shown in Figure 11.

Case 1 results using *OPTFORCE II and OPTIM III optimization programs* are displayed in Table 3 and Figure 12. Data from Drs. Khot and Berke's research, Reference 22, are also included for comparative purposes. Their solution procedures are based on the use of two algorithms. The first algorithm is a recurrence relation based on the fully stressed design (FSD) criterion and the second algorithm uses a recurrence relationship based on equivalent displacement constraints. Examination of the results shows the excellent agreement obtained among the methods used. Note that OPTIM III and Khot and Berke's methods are "displacement" based whereas OPTFORCE II is "force" based. Of particular interest is the initial weight value, W_i, and number of iterations, I, comparisons. This particular application of OPTFORCE II used the stress ratio option to arrive at an initial guess for the design variable vector. This procedure yielded

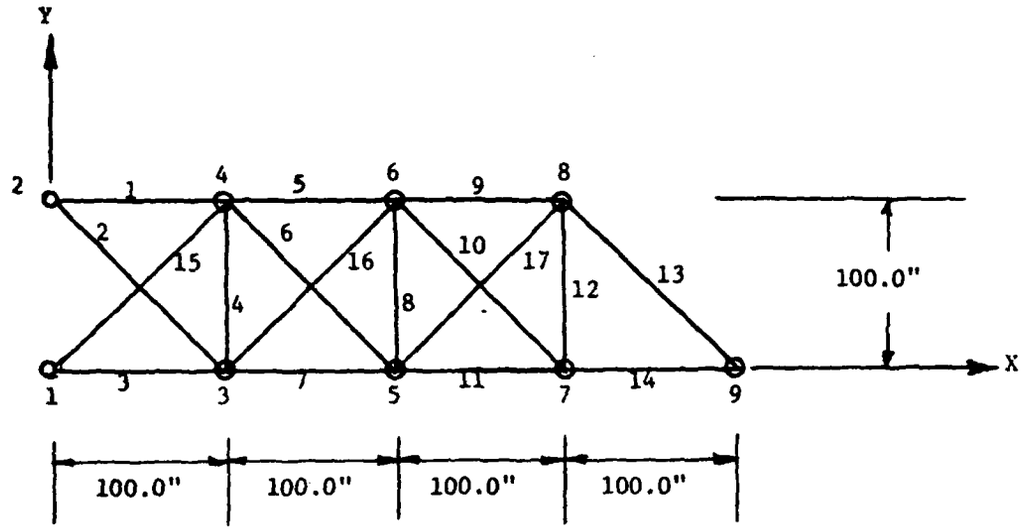

Case	Grid Point	Axis	Load
1	9	+Y	-100000.0 lbs.
2	3,5,7,9	+Y	-100000.0 lbs.

Figure 10 Seventeen Bar Truss

TABLE 2 MATERIAL PROPERTIES & CONSTRAINTS - SEVENTEEN BAR TRUSS

(1) Material Properties

Aluminum:

$E = 30 \times 10^6$ psi

$\rho = .268$ lbs. per cubic inch

$\nu = .30$

(2) Minimum size (size constraints)

Bar element area = .10 in^2

(3) Allowable stress (stress constraints)

Case 1:

$\sigma_l = -50000.0$ psi, $\sigma_u = 50000.0$ psi all elements

Case 2:

$\sigma_l = -50000.0$ psi, $\sigma_u = 50000.0$ psi all elements except No. 2, 6, 10

$\sigma_l = -125{,}000.0$ psi, $\sigma_u = 125{,}000.0$ psi elements No. 2, 6, 10

```
 10 TITLE
 11   SEVENTEEN BAR TRUSS-FOUR LOADS
 20 GRID    1                0.0     0.0     0.0             123
 30 GRID    2                0.0     100.0   0.0             123
 40 GRID    3                100.0   0.0     0.0             3
 50 GRID    4                100.0   100.0   0.0             3
 60 GRID    5                200.0   0.0     0.0             3
 70 GRID    6                200.0   100.0   0.0             3
 80 GRID    7                300.0   0.0     0.0             3
 90 GRID    8                300.0   100.0   0.0             3
100 GRID    9                400.0   0.0     0.0             3
110 OPLOADS 1                        1
150 OPTIM   YES     NO       YES                                     OPT
160 FORCE   1       3                1.0+5   0.0     -1.0    0.0
170 FORCE   1       5                1.0+5   0.0     -1.0    0.0
180 FORCE   1       7                1.0+5   0.0     -1.0    0.0
190 FORCE   1       9                1.0+5   0.0     -1.0    0.0
200 CONROD  1       2        4       1       0.10    0       0       0
210 CONROD  2       2        3       2       0.10    0       0       0
220 CONROD  3       1        3       1       0.10    0       0       0
230 CONROD  4       3        4       1       0.10    0       0       0
240 CONROD  5       4        6       1       0.10    0       0       0
250 CONROD  6       4        5       3       0.10    0       0       0
260 CONROD  7       3        5       1       0.10    0       0       0
270 CONROD  8       5        6       1       0.10    0       0       0
280 CONROD  9       6        8       1       0.10    0       0       0
290 CONROD  10      6        7       4       0.10    0       0       0
300 CONROD  11      5        7       1       0.10    0       0       0
310 CONROD  12      7        8       1       0.10    0       0       0
320 CONROD  13      8        9       1       0.10    0       0       0
330 CONROD  14      7        9       1       0.10    0       0       0
340 CONROD  15      1        4       1       0.10    0       0       0
350 CONROD  16      3        6       1       0.10    0       0       0
360 CONROD  17      5        8       1       0.10    0       0       0
370 MAT1    1       30.+6            0.3     0.268                           +MATA
380 +MATA   -5.0+4  +5.0+4
390 MAT1    2       30.+6            0.3     0.268                           +MATB
400 +MATB   -12.5+4 +12.5+4
410 MAT1    3       30.+6            0.3     0.268                           +MATC
420 +MATC   -12.5+4 +12.5+4
430 MAT1    4       30.+6            0.3     0.268                           +MATD
440 +MATD   -12.5+4 +12.5+4
450 ENDDATA
```

Fiugre 11 Optforce II Input Data - Seventeen Bar Truss, Case 2

TABLE 3 SEVENTEEN BAR TRUSS RESULTS - CASE 1

El. No.	OPTFORCE II Area(in^2)	OPTFORCE II Stress(psi)	OPTIM III Area(in^2)	OPTIM III Stress(psi)	Khot & Berke (Ref 22) Area(in^2)	Khot & Berke (Ref 22) Stress(psi)
1	7.93	50000.0	7.93	50000.0	7.93	(not given)
2	.10	49380.0	.10	49380.0	.10	
3	6.07	-50000.0	6.07	-50000.0	6.07	
4	.10	-1242.0	.10	-1242.0	.10	
5	4.07	50000.0	4.07	50000.0	4.07	
6	2.73	50000.0	2.73	50000.0	2.73	
7	5.93	-50000.0	5.93	-50000.0	5.93	
8	.10	5989.0	.10	5992.0	.10	
9	3.95	50000.0	3.94	50000.0	3.95	
10	.10	39154.0	.10	39151.0	.10	
11	2.06	-50000.0	2.06	-50000.0	2.06	
12	.10	-27688.0	.10	-27688.0	.10	
13	2.83	50000.0	2.83	50000.0	2.83	
14	2.00	-50000.0	2.00	-50000.0	2.00	
15	2.73	-50000.0	2.73	-50000.0	2.73	
16	.10	-47625.0	.10	-47623.0	.10	
17	2.75	-50000.0	2.75	-50000.0	2.75	
W_i	1315.75 lbs.		3733.56 lbs.		3733.80 lbs.	
W_m	1295.49 lbs.		1295.56 lbs.		1295.49 lbs.	
Y_9	-4.00 in.		-4.00 in.		-4.00 in.	
CPU	18.39 sec.		11.84 sec.		-	
I	1		36		30	

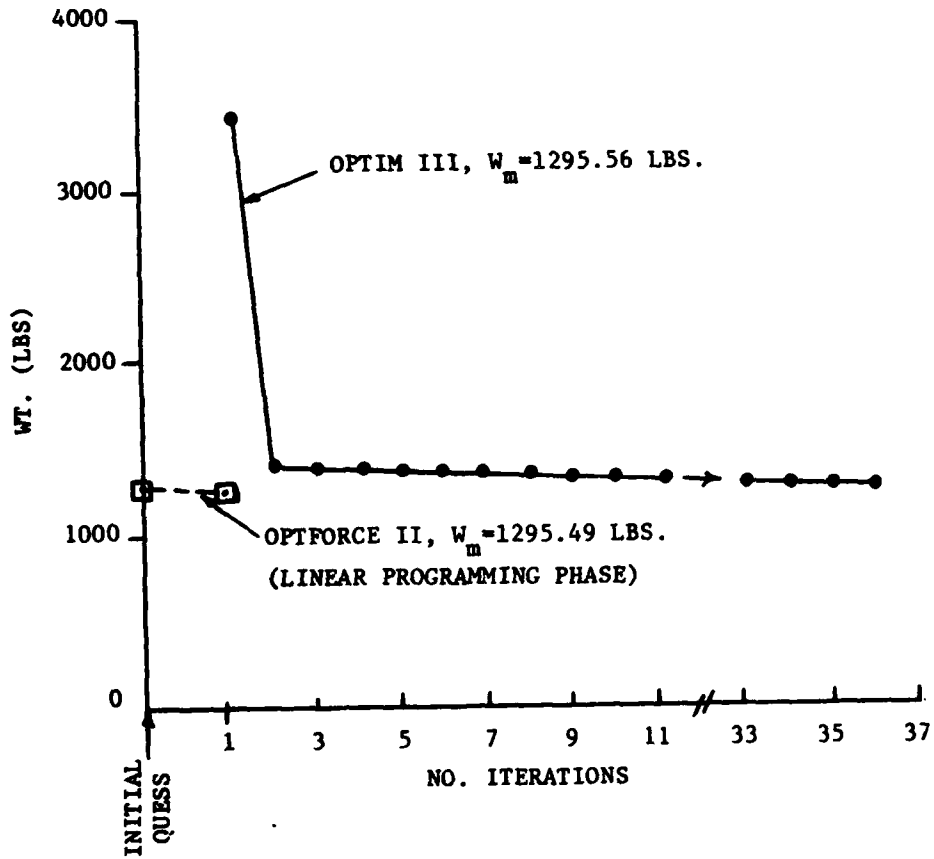

OPTFORCE II SOLUTION

- INITIAL QUESS - STRESS RATIO METHOD USING MIN. SIZES, W=1315.7 LBS.
  ↓
- ENTER LINEAR PROGRAMMING, ITER #1. SOLUTION NOT FEASIBLE - USE FULLY STRESSED DESIGN
  ↓
- LAGRANGE MULTIPLIER CHECK: ALL λ'S POSITIVE, USE F.S.D.

Figure 12 Seventeen Bar Truss Results - Case 1 A_{min}=.10in^2

W_i = 1315.75 lbs, a value very near the minimum weight value of W=1295.49 lbs. Observe that this is not the case for the other computer codes shown. The OPTIM III code does not have this capability and uses the minimum values of the design variables as the initial guess. The OPTFORCE II code yielded the optimum weight solution in one iteration (Linear Programming Phase) whereas the other methods required 30 to 36 iterations. Computer time recorded shows that the OPTFORCE II code requires 6.55 more cpu seconds then the OPTIM III code. The inset on Figure 12 indicates that a solution is not feasible in the Linear Programming phase. A non-feasible solution violates at least one of the constraints. For a given problem, it is possible that no feasible solutions exist. Conversely, a feasible solution is any solution of the constraint equations.

Case 2 results are shown in Table 4 and Figure 13. No agreement is obtained between the OPTFORCE II and OPTIM III codes, however, agreement occurs between OPTFORCE II and Reference 22 solutions. It is discussed in that reference that the FSD algorithm yielded a "minimum weight" design of 3081.62 lbs. which is the same design obtained using the OPTIM III code. As discussed in Reference 22 this solution is a non-optimum design and is not the correct one. It was further shown in Reference 22 that the equivalent displacement algorithm yielded the optimum design, it being of weight equal to 2460.24 lbs. Thus as seen the correct distribution of areas and weight for the optimum design were obtained by the OPTFORCE II code and not the OPTIM III code. Note that the stress distribution for all three methods shown are identical which illustrates that there can be more than one design with the same stress distribution but different weights. This, of course, was also observed and quoted in Reference 22. Computer time

TABLE 4 SEVENTEEN BAR TRUSS RESULTS - CASE 2

El. No.	OPTFORCE II Area(in^2)	OPTFORCE II Stress(psi)	OPTIM III Area(in^2)	OPTIM III Stress(psi)	Khot & Berke(Ref 22) Area(in^2)	Khot & Berke(Ref 22) Stress(psi)
1	16.10	50000.0	19.89	50000.0	16.10	50000.0
2	3.67	75000.0	.10	75000.0	3.67	75000.0
3	15.90	-50000.0	12.10	-50000.0	15.90	-50000.0
4	.10	50000.0	7.75	50000.0	.10	50000.0
5	8.00	50000.0	11.86	50000.0	8.00	50000.0
6	2.83	100000.0	.10	100000.0	2.83	100000.0
7	10.00	-50000.0	6.14	-50000.0	10.00	-50000.0
8	.10	50000.0	5.72	50000.0	.10	50000.0
9	4.10	50000.0	5.86	50000.0	4.10	50000.0
10	1.34	100000.0	.10	100000.0	1.34	100000.0
11	3.90	-50000.0	2.14	-50000.0	3.90	-50000.0
12	.10	50000.0	1.86	50000.0	.10	50000.0
13	2.83	50000.0	2.83	50000.0	2.83	50000.0
14	2.00	-50000.0	2.00	-50000.0	2.00	-50000.0
15	5.80	-50000.0	11.17	-50000.0	5.80	-50000.0
16	2.83	-50000.0	8.29	-50000.0	2.83	-50000.0
17	2.97	-50000.0	5.46	-50000.0	2.97	-50000.0
W_i	2420.17 lbs.		8582.27 lbs.		8582.88 lbs.	
W_m	2460.24 lbs.		3081.62 lbs.		2460.24 lbs.	
Y_9	-4.33 in.		-4.33 in.		Not given	
CPU	14.16 sec.		8.78 sec.		Not given	
I	4		24		30	

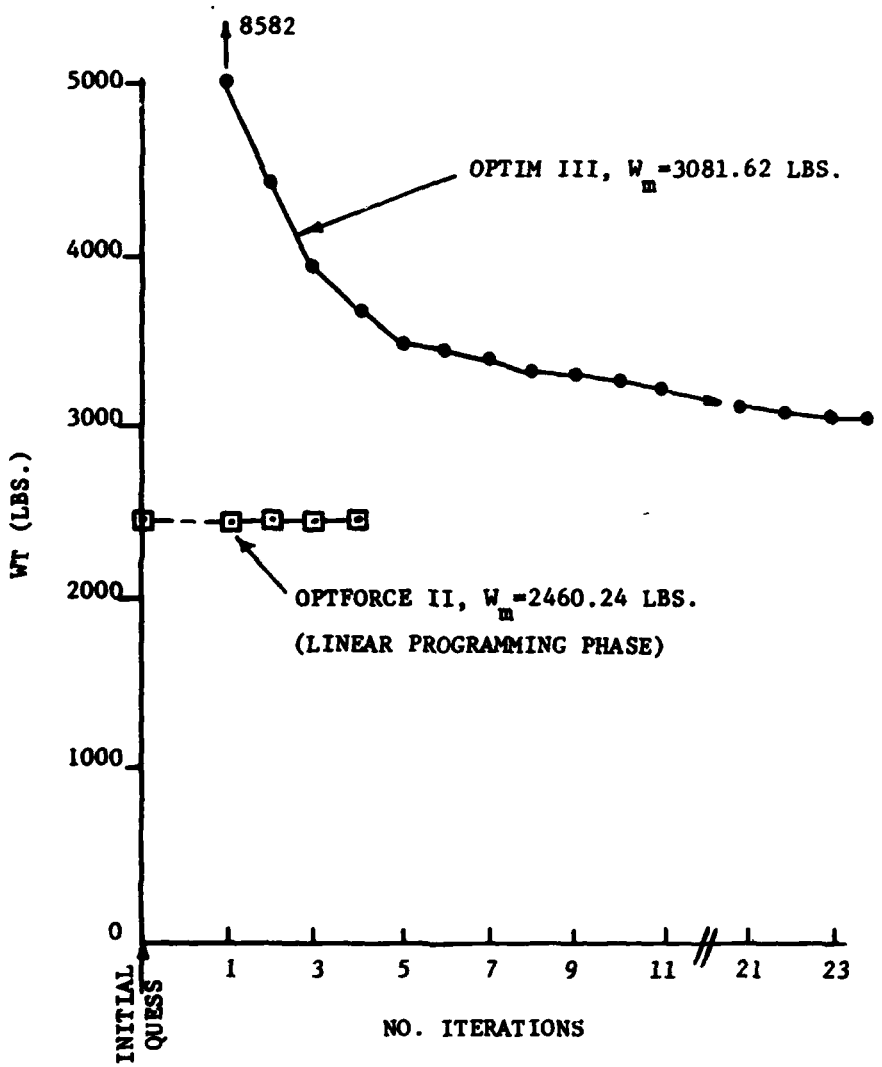

OPTFORCE II SOLUTION

- INITIAL QUESS - STRESS RATIO METHOD USING MIN. SIZES, W=2420.17 LBS.
  ↓
- ENTER LINEAR PROGRAMMING, ITER. #1 SOLUTION FEASIBLE. DESIGN CONVERGED IN PARTIAL NEWTON-RAPHSON.
  ↓
- LAGRANGE MULTIPLIER CHECK: ALL λ'S POSITIVE, USE SOLUTION FROM LINEAR PROGRAMMING.

Figure 13 Seventeen Bar Truss - Case 2 A_{min}.10in^2

displayed in Table 4 again shows that the force method incurs additional solution time but requires one-sixth the number of iterations.

3.1.2 Four Bar Pyramid

Figure 14 displays the geometrical configuration of the four bar pyramid. The external loading applied to this structure is also shown. This loading system is not considered as a multiple load case; rather each of the loads are applied to the structure simultaneously. Material properties and constraints are listed in Table 5. Only stress and minimum size constraints were considered. OPTFORCE II input data is displayed in Figure 15; OPTIM III data is essentially identical to that shown in that figure. Analyses results are given in Tables 6 and 7 and Figures 16 and 17.

Three cases were considered differing only in the value of the minimum size constraints. The minimum weight for these cases was calculated to be 65.76 lbs.; the value accepted as the optimum by various investigators. Displacement and stress values obtained were identical for all cases displayed, however distinctly different designs are evident as shown by the values of the areas obtained. Case 1, OPTFORCE II analysis, starts with an initial guess vector for the design variables based on the stress ratio method which yielded the area vector (.43, 1.76, 1.26, .55). This vector was subsequently revised through use of the Linear Programming subroutine to that shown in Table 6 and Figure 16. Identical results were obtained to those shown when the stress ratio option was not exercised. Note, however, the additional computer time and iterations needed. Figure 16 aptly portrays these results. OPTIM III code computations converged to the area vector (.43, 1.76, 1.26, .55) a result obtained by Gellatly, (Reference 23), and Venkayya (Reference 24) using $A_{min.} = 0.0$ in^2. Reduction

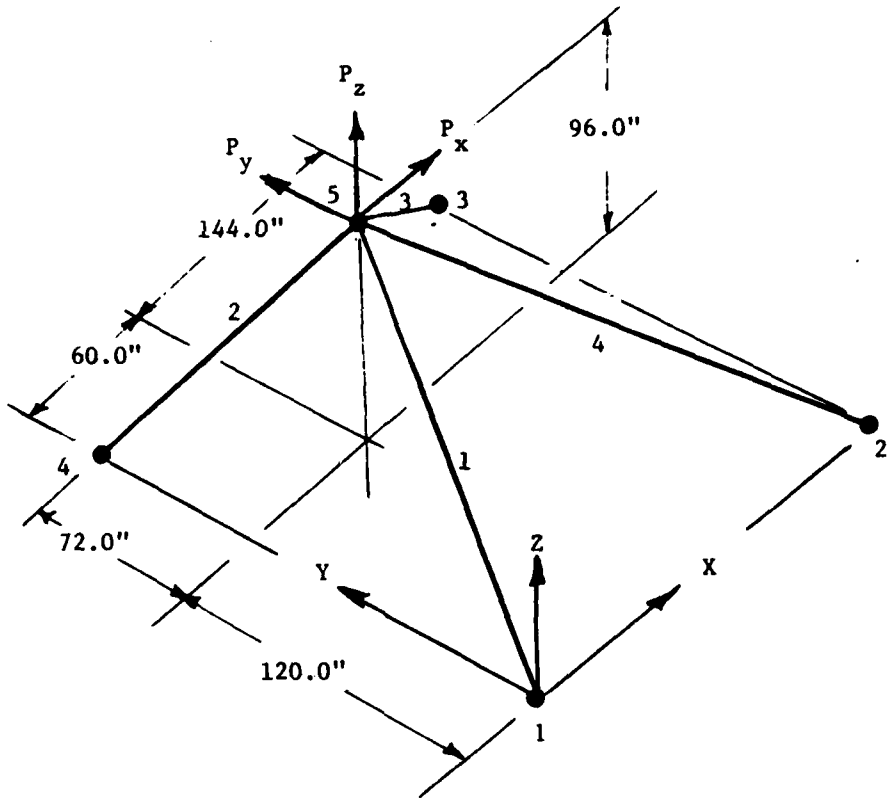

LOADING (lbs.):

P_x = 10000.0

P_y = 20000.0

P_z = -60000.0

Figure 14 Four Bar Pyramid

AD-A127 073 FORCE METHOD OPTIMIZATION II VOLUME I THEORETICAL DEVELOPMENT(U) BELL AEROSPACE TEXTRON BUFFALO NY J R BATT ET AL. NOV 82 AFWAL-TR-82-3088-VOL-1 2/2

UNCLASSIFIED F33615-80-C-3214 F/G 12/1 • NL

END
DATE
FILMED
5 83
DTIC

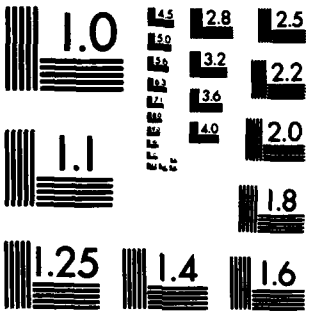

MICROCOPY RESOLUTION TEST CHART
NATIONAL BUREAU OF STANDARDS-1963-A

TABLE 5 MATERIAL PROPERTIES & CONSTRAINTS - FOUR BAR PYRAMID

(1) Material Properties

Aluminum:

$E = 10.0 \times 10^6$ psi

$\rho = .10$ lbs. per cubic inch

$\nu = .30$

(2) Minimum size (size constraint)

Rod element area:

Case 1, $A = .20$ in^2
Case 2, $A = .10$ in^2
Case 3, $A = .00010$ in^2

(3) Allowable stress (stress constraints)

σ_{lower} -25000.0 psi; $\sigma_{upper} = 25000.0$ psi

```
 10 TITLE
 20    FOUR BAR PRYAMID
 30 GRID    1                0.0      0.0      0.0
 40 GRID    2                204.0    0.0      0.0
 50 GRID    3                204.0    192.0    0.0
 60 GRID    4                0.0      192.0    0.0
 70 GRID    5                60.0     120.0    96.0
 80 SPC1    1        123     1        2        3        4
 90 OPTIM   NO       NO      YES      0                                  OPT
100 OPLOADS 1                         1
110 FORCE   1        5                10000.0  1.0      2.0      -6.0
143 CONROD  1        1       5        1        .20      0        0        0
150 CONROD  2        4       5        1        .20      0        0        0
160 CONROD  3        3       5        1        .20      0        0        0
170 CONROD  4        2       5        1        .20      0        0        0
180 MAT1    1        10.0+6           .30       .10                                    MAT
190 +MAT    -25000.025000.0
200 ENDDATA
```

Figure 15 Optforce II Input Data - Four Bar Pyramid, Case 1

TABLE 6 FOUR BAR PYRAMID - CASES 1 & 2

Case 1 A_{min} = .20 in^2				
El. No.	OPTFORCE II Area(in^2)	OPTFORCE II Stress(psi)	OPTIM III Area(in^2)	OPTIM III Stress(psi)
1	.70	-25000.0	.43	-25000.0
2	1.53	-25000.0	1.76	-25000.0
3	1.57	-25000.0	1.26	-25000.0
4	.20	-25000.0	.55	-25000.0
W_i	65.76/13.94* lbs.		122.35 lbs.	
W_m	65.76 lbs.		65.76 lbs.	
X_5	.21 in.		.21 in.	
Y_5	-.12 in.		-.12 in.	
Z_5	-.69 in.		-.69 in.	
CPU	6.30/23.54* sec.		2.46 sec.	
I	4/25*		3	

* Stress ratio option not used for initial quess.

Case 2 A_{min} = .10 in^2				
El. No.	OPTFORCE II Area(in^2)	OPTFORCE II Stress(psi)	OPTIM III Area(in^2)	OPTIM III Stress(psi)
1	.78	-25000.0	.43	-25000.0
2	1.47	-25000.0	1.75	-25000.0
3	1.66	-25000.0	1.26	-25000.0
4	.10	-25000.0	.55	-25000.0
W_i	65.76 lbs.		122.35 lbs.	
W_m	65.76 lbs.		65.76 lbs.	
X_5	.21 in.		.21 in.	
Y_5	-.12 in.		-.12 in.	
Z_5	-.69 in.		-.69 in.	
CPU	6.71 sec.		2.40 sec.	
I	5		3	

TABLE 7 FOUR BAR PYRAMID - CASES 3-5

Case 3 A_{min} = .0001 in^2			
OPTFORCE II		OPTIM III	
Area(in^2)	Stress(psi)	Area(in^2)	Stress(psi)
.86	-25000.0	.43	-25000.0
1.41	-25000.0	1.76	-25000.0
1.75	-25000.0	1.26	-25000.0
.0001	-25000.0	.55	-25000.0
W_i	65.76 lbs.	122.35 lbs.	
W_m	65.76 lbs.	65.76 lbs.	
X_5	.21 in.	.21 in.	
Y_5	-.12 in.	-.12 in.	
Z_5	-.69 in.	-.69 in.	
CPU	9.72 sec.	3.29 sec.	
I	5	4	

	Case 4, A_{min} = 0.0 in^2	Case 5, A_{min} = .0001 in^2
El. No.	Gellatly (Ref. 23) Venkayya (Ref. 24)	Harless (Ref. 25)
1	.43 in^2	.0316 in^2
2	1.76	2.0790
3	1.26	.8055
4	.55	1.0560
W_i	122.35 lbs.	-
W_m	65.76 lbs.	65.76 lbs.

OPTFORCE II SOLUTIONS

- INITIAL QUESS - STRESS RATIO METHOD USING MIN. SIZES, W=65.76 LBS.
  ↓
- ENTER LINEAR PROGRAMMING ITER NO. 1 SOLUTION IS FEASIBLE. DESIGN CONVERGED IN PARTIAL NEWTON-RAPHSON
  ↓
- LAGRANGE MULTIPLIER CHECK: ALL λ'S POSITIVE USE DESIGN FROM LINEAR PROGRAMMING.

- INITIAL QUESS - MIN. SIZES W=13.94 LBS.
  ↓
- ENTER LIN[illegible] PROGRAMMING, ITER. NO. 1 SOLUTION IS FEASIBLE. DESIGN CONVERGED IN PARTIAL NEWTON-RAPHSON.
  ↓
- LAGRANGE MULTIPLIER CHECK: NEGATIVE λ'S ENTER FULL N-R.
  ↓
- DESIGN CONVERGED IN FULL N-R.

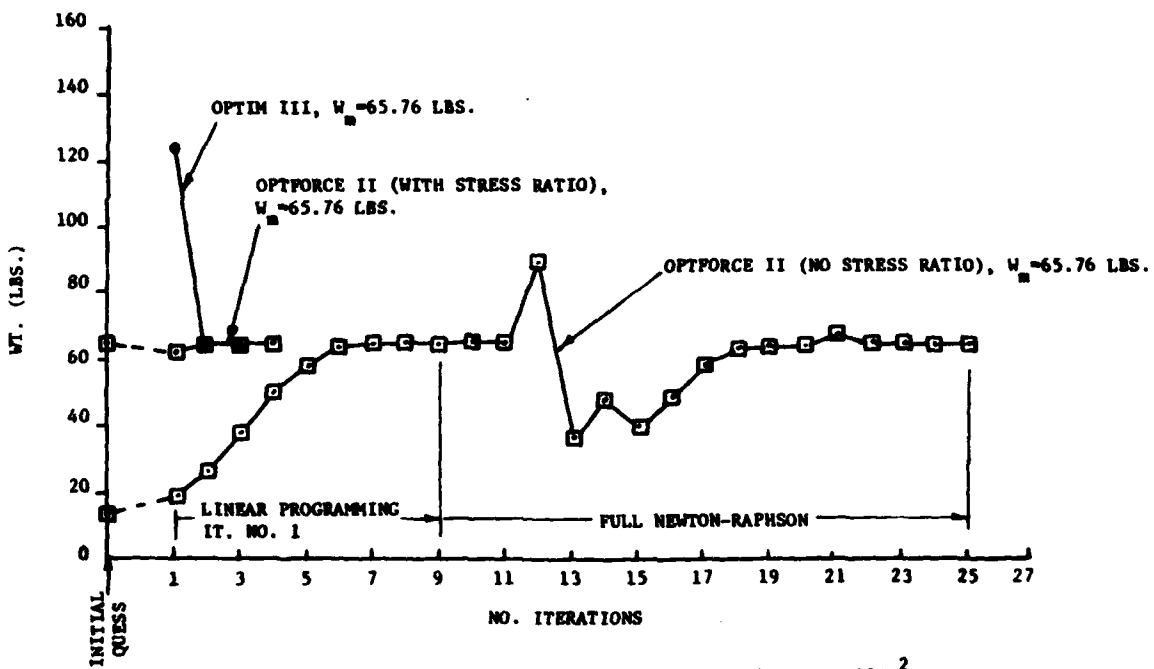

Figure 16 Four Bar Pyramid - Case 1 A_{min}=.10in^2

OPTFORCE II SOLUTIONS

- INITIAL QUESS - STRESS RATIO METHOD USING MIN. SIZES, W=65.76 LBS.
  ↓
- ENTER LINEAR PROGRAMMING, ITER NO. 1. SOLUTION IS FEASIBLE. DESIGNED CONVERGED IN PARTIAL NEWTON-RAPHSON.
  ↓
- LAGRANGE MULTIPLIER CHECK: ALL λ'S POSITIVE. USE DESIGN FROM LINEAR PROGRAMMING.

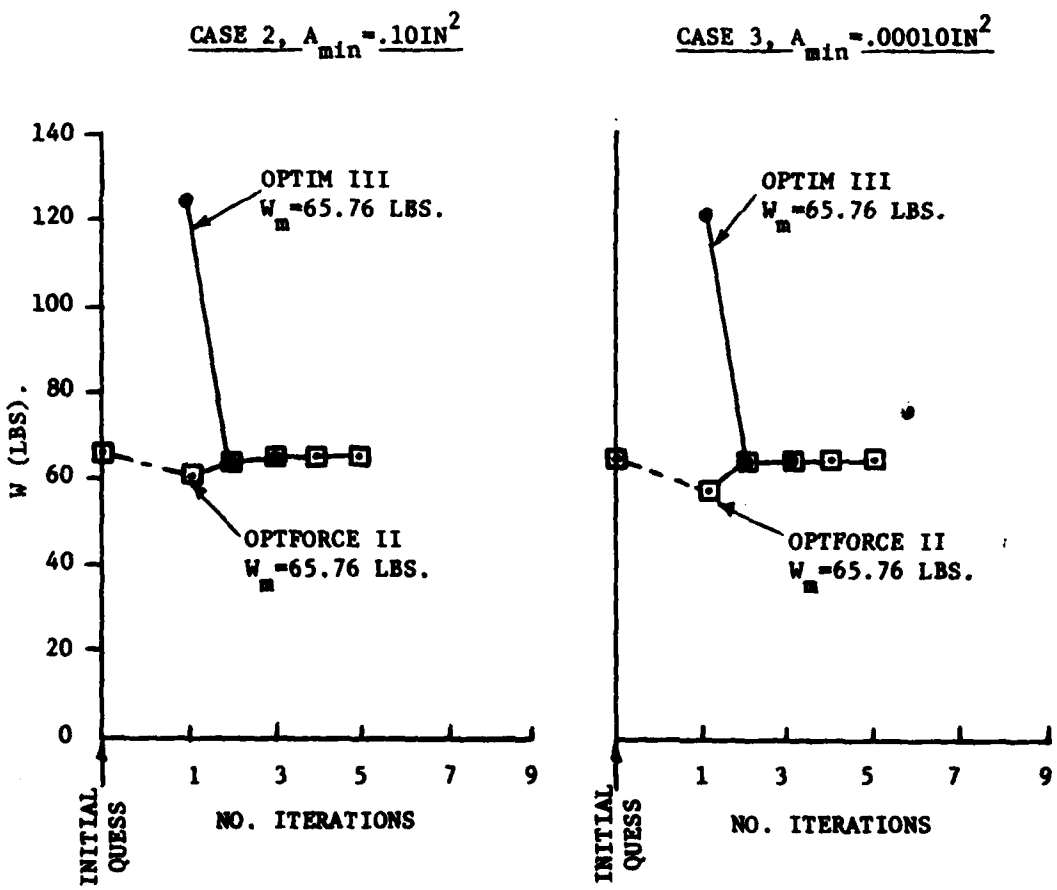

Figure 17 Four Bar Pyramid - Cases 2 & 3

of the minimum area constraint to .10 in^2 gave the results tabulated for Case 2 in Table 6 and Figure 17. In this instance OPTFORCE II computations yielded the vector (.78, 1.47, 1.66, .10) and OPTIM III again yielded the vector (.43, 1.75, 1.26, .55). Further reduction of the area constraint to .0001 in^2 yielded the area vectors listed under Case 2, Table 7 and Figure 17.

Perusal of the above results suggests that multiple sets of design variables satisfy the minimum weight state. Such is the case in this instance as thoroughly discussed by Gellatly and Venkayya. Their results are shown under Case 4, Table 7. Further work done by Venkayya showed that multiple minima exist for the structure under consideration. He states that "the design weight of 65.76 lbs. appears to be the absolute minimum for this structure and there are three designs having the minimum weight. The other two may be considered relative minimums". The design vectors listed in Reference 24, for A_{min} = 0.0 in^2, are (0.0, 2.105, .770, 1.097) (.859, 1.406, 1.746, 0.0) and (.430, 1.755, 1.258, .548) with the latter associated with the absolute minimum weight listed in Table 7 Comparison of these area vectors with those tabulated shows that the OPTIM III solutions, regardless of the minimum size constraint value, agrees with the absolute minimum solutions of Gellatly and Venkayya using A_{min} = 0.0. The OPTFORCE II solution procedure tends to one of the relative minimums as the minimum size constraint vanishes which thoroughly agrees with the results obtained by the above two investigators. Thus, it is concluded that OPTFORCE II yields the correct optimal solution for Case 1; the initial design problem. Note that Harless, Reference 25, obtains yet another solution. This solution listed in Table 7 is very close to one of the relative minimums obtained by Venkayya. Examination of

Tables 6 and 7 shows that OPTFORCE II requires more cpu seconds than that required for OPTIM III for nearly the same number of solution iterations. What is most interesting, as was observed in the seventeen bar truss solutions, is that the initial weight values, W_i, used in the OPTFORCE II code are very close to the optimum weight W_m. This is not the situation with the other reference computer codes. Thus, the initial guess using the optional stress-ratio method is definitely an asset to the User and as demonstrated in Case 1 its use reduces computer cpu time and the number of iteration cycles required.

3.1.3 Wingbox

The configuration of the eighteen element wingbox is given in Figure 18 with the location of the single external load. Material properties and problem constraints are listed in Table 8; only minimum size and stress constraints were considered. Figure 19 displays OPTFORCE II input data. The OPTIM III input data file is essentially the same at that shown in Figure 19.

Results of the analyses conducted are displayed in Table 9 and Figure 20. Examination of these results shows that the minimum weights obtained are relatively close to one another with the OPTFORCE II code yielding a weight nearly 10% less than that calculated using the OPTIM III code. The displacement characteristics obtained from both codes were essentially identical. Viewing the design variable vector shows that two different designs were obtained. The most radical departure between these designs appears in the rod and web finite elements aligned with the applied force (elements 4, 5, 6, 10, 11 and 12). The quadrilateral membrane elements also exhibit the same behavior. This disagreement is attributed to two factors; namely, 1) difference in optimization solution

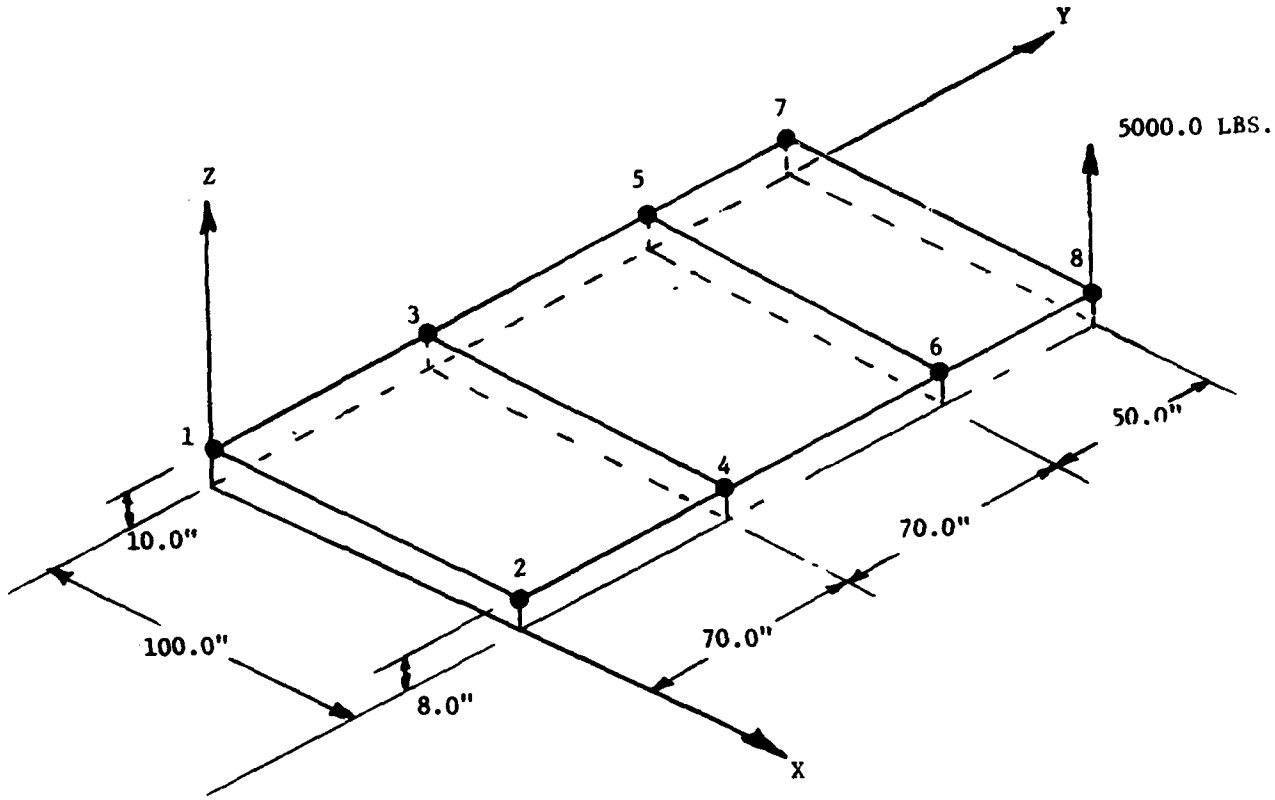

Figure 18 Wingbox Configuration

TABLE 8 MATERIAL PROPERTIES & CONSTRAINTS - WINGBOX

(1) Material Properties

$E = 10.0 \times 10^6$ psi

$\rho = .10$ lbs. per cubic inch

$\nu = .30$

(2) Minimum size (size constraints)

Bar element area = .10 in^2
Web element thickness = .02 in
Membrane element thickness = .02 in

(3) Allowable stresses (stress constraint)

$\sigma_l = -10000.0$ psi, $\sigma_u = 10000.0$ psi

```
 10 TITLE
 20    EIGHTEEN ELEMENT WINGBOX
 30 GRID          1              0.     0.0      10.0
 40 GRID          2             100.    0.0       8.0
 50 GRID          3               0.   70.0      10.0
 60 GRID          4             100.   70.0       8.0
 70 GRID          5               0.  140.0      10.0
 80 GRID          6             100.  140.0       8.0
 90 GRID          7               0.  190.0      10.0
100 GRID          8             100.  190.0       8.0
110 SPC1         1       123       1     THRU       2
120 OPTIM        NO      NO      YES                                  OPT
130 OPLOADS       1                       10
140 FORCE        10       8            5000.0     0.0      0.0      1.0
150 CONROD        1       1       3       28     0.10
160 CONROD        2       3       5       28     0.10
170 CONROD        3       5       7       28     0.10
180 CONROD        4       2       4       28     0.10
190 CONROD        5       4       6       28     0.10
200 CONROD        6       6       8       28     0.10
210 CWEB          7      50       3        4
220 CWEB          8      50       5        6
230 CWEB          9      50       7        8
240 CWEB         10      50       2        4
250 CWEB         11      50       4        6
260 CWEB         12      50       6        8
270 CWEB         13      50       1        3
280 CWEB         14      50       3        5
290 CWEB         15      50       5        7
300 CQDMEM1      16      33       2        4        3        1
310 CQDMEM1      17      33       4        6        5        3
320 CQDMEM1      18      33       6        8        7        5
330 MAT1         28  1.0E7             .30       .1                        FD
340 +CD      -1.0E4  1.0E4
350 PWEB         50      28     .02
360 PQDMEM1      33      28     .02
370 ENDDATA
```

Figure 19 Optforce II Input Data - Wingbox

TABLE 9 WINGBOX RESULTS

El. No.	Element Type	OPTFORCE II A_i*	OPTFORCE II Stress(psi)	OPTIM III A_i*	OPTIM III Stress(psi)
1	Rod	.1000	-9897.0	.2404	-7996.0
2	Rod	.1000	-7684.0	.1010	-6073.0
3	Rod	.1000	-1274.0	.1010	-2172.0
4	Rod	4.5500	-10000.0	.3437	-8927.0
5	Rod	2.1060	-10000.0	.1446	-8349.0
6	Rod	.2527	-10000.0	.1010	-6224.0
7	Web	.0200	-1590.0	.0202	-1446.0
8	Web	.0200	-731.0	.0202	2321.0
9	Web	.0200	5018.0	.0202	8052.0
10	Web	.0966	5774.0	.0449	9896.0
11	Web	.0897	5774.0	.0420	9903.0
12	Web	.0865	5774.0	.0466	9918.0
13	Web	.0200	2157.0	.0202	5714.0
14	Web	.0200	3429.0	.0202	6639.0
15	Web	.0200	4014.0	.0202	5153.0
16	Quad	.0434	9999.0+	.0931	8735.0+
17	Quad	.0326	10000.0+	.0643	8568.0+
18	Quad	.0211	10000.0+	.0303	8496.0+
W_i		136.64 lbs.		234.69 lbs.	
W_m		135.96 lbs.		148.15 lbs.	
Z_s		2.54 in.		2.42 in.	
CPU		19.96 sec.**		.96 sec.**	
I		14		6	

*A_i = Design variable value, rod cross-sectional area (in^2), web thickness (in.), quad. membrane thickness (in.)

** IBM 3033

\+ Mises-Henchy stress criteria shown.

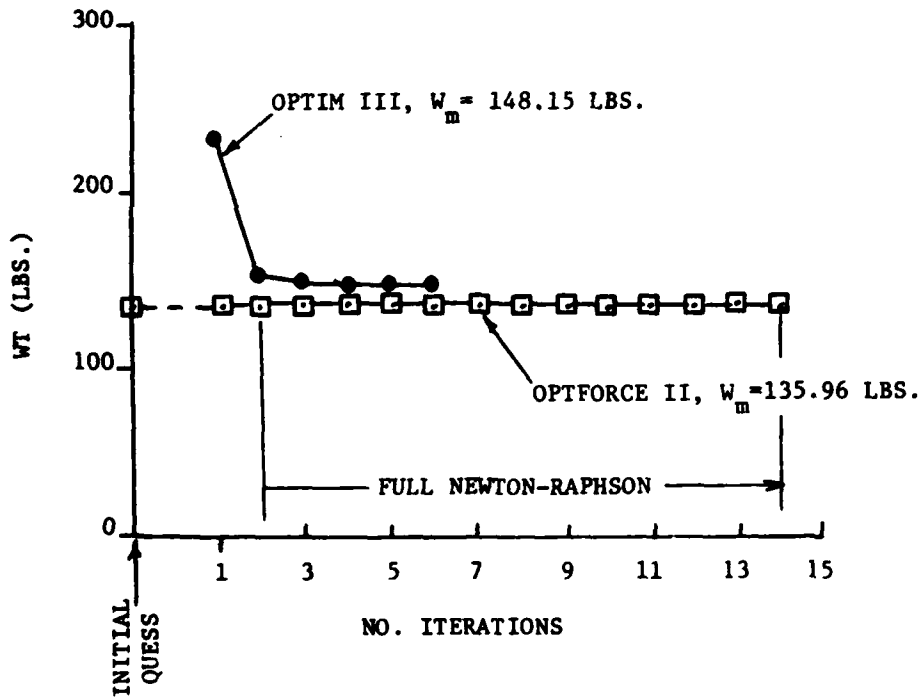

OPTFORCE II SOLUTION

- INITIAL QUESS - STRESS RATIO METHOD USING MIN. SIZES, W=136.64 LBS.
  ↓
- ENTERED LINEAR PROGRAMMING, ITER #1 SOLUTION NOT FEASIBLE - USE FULLY STRESSED DESIGN.
  ↓
- LAGRANGE MULTIPLIER CHECK: NEGATIVE λ'S. ENTER FULL N-R.
  ↓
- DESIGN CONVERGED IN FULL N-R.

Figure 20 Wingbox Results

procedure, e.g. "force" method versus "displacement" method and 2) possible finite element formulations. As noted in the discussions of the seventeen bar truss and four bar pyramid solutions the OPTFORCE II code appears to be the more accurate one when the weight optimization option is exercised. This fact is particularly emphasized when the statics option was used. Results of this exercise demonstrated that both codes yielded nearly identical values of the displacement, stress and reaction vectors. Cpu times recorded for the statics case were .88 sec using OPTFORCE II and .68 sec. for OPTIM III a negligible difference. The stresses displayed in Table 9 are the element stresses themselves with exception of those given for the quadrilateral membrane elements. Three element stresses are calculated (σx, σy, τxy) for these elements and these have been combined using the Mises-Henchy stress failure criteria for the sake of brevity and comparison.

Computer time recorded shows that OPTFORCE II used 19.96 sec. of cpu time versus .96 sec. for OPTIM III solutions on the IBM 3033 computer. The number of iterations required for OPTFORCE II are greater than those shown for OPTIM III. Examination of Figure 20 and the computer output shows that the minimum weight value obtained from OPTFORCE II has converged in less than the number of iterations shown (successive weight values only differing in the second or third decimal place). Additional iterations were required to obtain convergence of the design variable values. This was observed to be case in other applications of the subject computer codes.

3.1.4 Concluding Remarks

The above discussions clearly illustrate the fact that there can be more than one design with the same stress distribution and minimum weight but different design variable values or so-called area vectors. It appears that this fact, the accuracy component of the efficiency study,

is the driving force behind optimization computer code selection rather than computer time and/or the number of iterations required. The OPTFORCE II code not only yields the correct minimum structural weight but the correct design variable population. This conclusion cannot be over-emphasized to the potential structural designer. Computer time is beginning to have less relevance as a measure of computer code efficiency than in the past due to the higher speeds attained with the newer machines. Several of the solutions discussed in this section were re-run using Bell's more recently acquired IBM 3033 computer. Identical minimum weight solutions were obtained using both OPTFORCE II and OPTIM III codes at approximately one-fifth the original cpu times quoted using the IBM 3031 machine. It is concluded from these facts and the discussions of minimum weight solutions that the OPTFORCE II code is more "efficient" than the reference OPTIM III code.

3.2 Applications

The development of the structural optimization technique using the force method, which has been amply described in Section 2.0, is further illustrated below using the swept wing-box idealization shown in Figure 21. Two material cases were chosen; namely, Case 1 an all-aluminum structure and Case 2 a graphite/epoxy-aluminum structure. Vertical loads are applied at grid points 4, 7, and 10 and are considered as a single load case.

Case 1 idealization consists of modeling the upper skins with quadrilateral finite elements whereas the spars and ribs are modeled using the symmetric shear panel elements. Spar and rib caps are idealized using rod finite elements. It is noted that only one-half of the wing-box structure needed to be modeled by virtue of the geometric symmetry of the

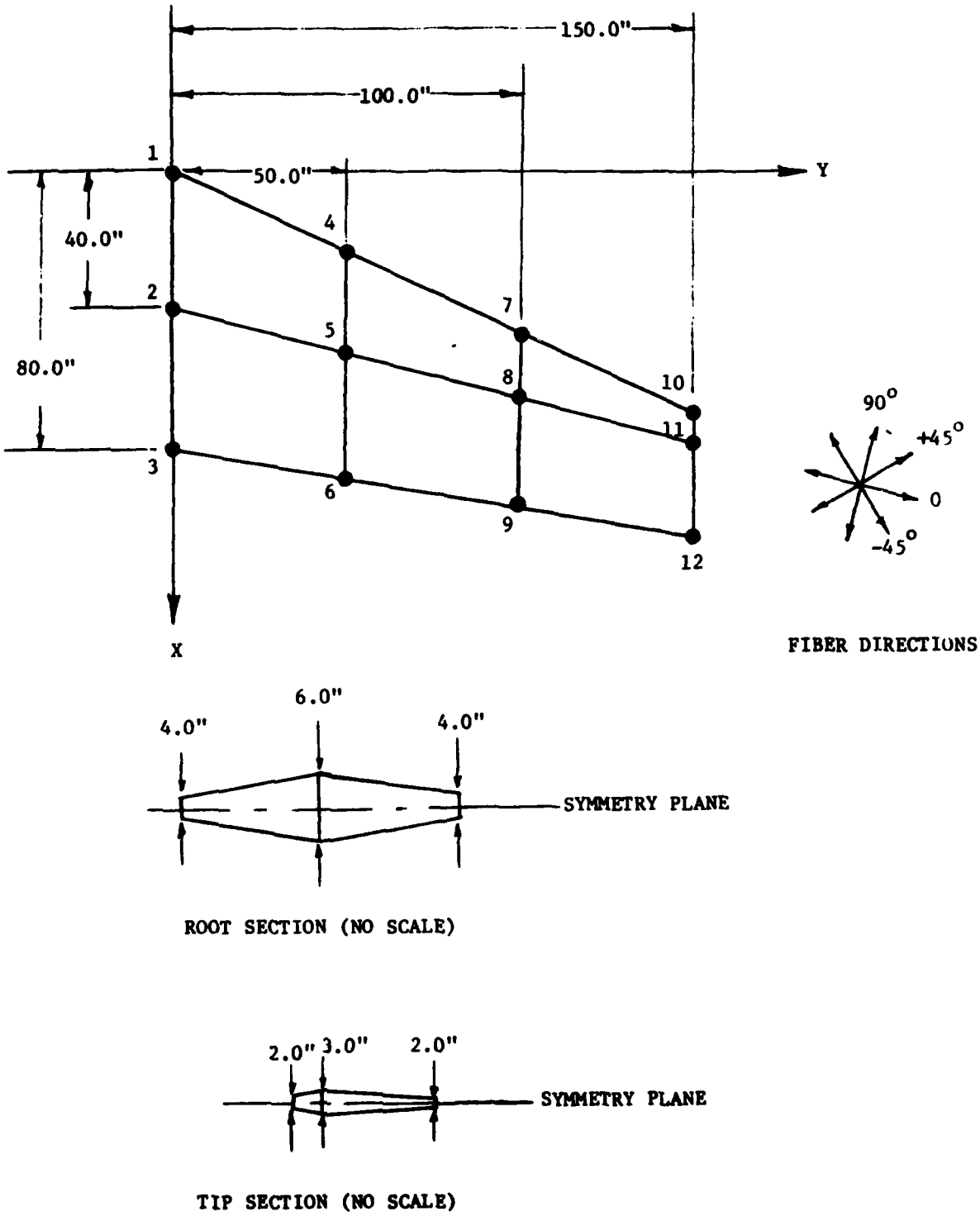

Figure 21 Swept Wingbox Configuration

structure and use of the symmetric shear panel element. As a result, only six quadrilateral membrane, fifteen shear panel and fifteen rod finite elements are used to idealize the entire wing-box yielding a total of thirty-six elements. Twenty-seven degrees-of-freedom describe the structural behavior. The design variables are quadrilateral membrane thickness (t_m), rod cross-sectional area (A) and shear web thickness (t_w); thirty-six in number. Material properties; minimum sizes of design variables and allowable stress levels are given in Table 10. NASTRAN compatible input for this structure is displayed in Figure 22.

Case 2 idealization consisted of again modeling the upper skins using quadrilateral membrane elements. However, in this case, the skins consisted of four layers of elements containing common grid points. Each of the layers contain a different fiber orientation in the graphite/epoxy material. The spars, ribs, and caps were modeled as in the Case 1 structure. A total of fifty-four elements and twenty-seven degrees-of-freedom results from this idealization. The number of design variables increased from thirty-six to sixty-four due to the layered quadrilateral membrane elements. Table 11 lists material properties, minimum sizes constraints and fiber orientation. The NASTRAN compatible input data is displayed in Figure 23.

Results of Case 1 analysis reside in Table 12 and Figure 24. The solution procedure path followed in OPTFORCE II is depicted below:

- Initial guess for design variable vector: Minimum size constraint with the stress ratio option, W_i = 107.40 lbs.
- Program entered the Linear Programming phase: "Solution Not Feasible"; Use fully stressed design (FSD) as minimum weight solution. W_{FSD} = 110.73 lbs.
- Performed check on the Lagrange multiplier (λ_i) calculations which used the design variable vector from FSD. Since all $\lambda_i \geq 0$ the optimization routine terminated with the FSD. Note that in this application there are thirty-six λ's associated with the design variables, thirty-six λ's associated with

TABLE 10 MATERIAL PROPERTIES & CONSTRAINTS - CASE 1 SWEPT WINGBOX

(1) Material Properties:

Aluminum:

$E = 10.6 \times 10^6$ psi

$\rho = .10$ lbs/in^3

$\nu = .25$

(2) Minimum sizes (size constraints)

Quadrilateral membranes	$t_m = .10$ in.
Rods	$A = .05$ in.^{2}
Shear webs	$t_w = .05$ in.

(3) Allowable stresses (stress constraints)

$\sigma_{lower} = -30{,}000.0$ psi, $\sigma_{upper} = 30{,}000$ psi

```
 10 TITLE
 20   TASK V WINGBOXC ALUMINUM MTL.
 30 GRID    1                 0.0      0.0      2.0
 40 GRID    2                 40.0     0.0      3.0
 50 GRID    3                 80.0     0.0      2.0
 60 GRID    4                 23.32    50.0     1.67
 70 GRID    5                 53.40    50.0     2.5
 80 GRID    6                 88.82    50.0     1.67
 90 GRID    7                 46.63    100.0    1.33
100 GRID    8                 66.79    100.0    2.0
110 GRID    9                 97.63    100.0    1.33
120 GRID    10                69.95    150.0    1.0
130 GRID    11                80.19    150.0    1.5
140 GRID    12                106.45   150.0    1.0
150 SPC1    1        123      1        THRU     3
160 OPLOADS 1                           1
170 FORCE   1        4                  6000.0   0.0      0.0      1.0
180 FORCE   1        7                  4000.0   0.0      0.0      1.0
190 FORCE   1        10                 2000.0   0.0      0.0      1.0
200 OPTIM   YES      NO       YES                                              OPT
210 CQDMEM1 1        1        2        5        4        1
220 CQDMEM1 2        1        3        6        5        2
230 CQDMEM1 3        1        5        8        7        4
240 CQDMEM1 4        1        6        9        8        5
250 CQDMEM1 5        1        8        11       10       7
260 CQDMEM1 6        1        9        12       11       8
270 CWEB    7        1        1        4
280 CWEB    8        1        4        7
290 CWEB    9        1        7        10
300 CWEB    10       1        2        5
310 CWEB    11       1        5        8
320 CWEB    12       1        8        11
330 CWEB    13       1        3        6
340 CWEB    14       1        6        9
350 CWEB    15       1        9        12
360 CWEB    16       1        5        4
370 CWEB    17       1        6        5
380 CWEB    18       1        8        7
390 CWEB    19       1        9        8
400 CWEB    20       1        11       10
410 CWEB    21       1        12       11
420 CROD    22       1        1        4
430 CROD    23       1        4        7
440 CROD    24       1        7        10
450 CROD    25       1        2        5
460 CROD    26       1        5        8
470 CROD    27       1        8        11
480 CROD    28       1        3        6
490 CROD    29       1        6        9
500 CROD    30       1        9        12
510 CROD    31       1        5        4
520 CROD    32       1        6        5
530 CROD    33       1        8        7
540 CROD    34       1        9        8
550 CROD    35       1        11       10
560 CROD    36       1        12       11
570 PQDMEM1 1        1        .10
580 PWEB    1        1        .05
590 PROD    1        1        .05
600 MAT1    1        10.5+6            .25      .10                                M
610 +M      -30000.030000.0
```

Figure 22 Optforce II Input Data - Case 1 Swept Wingbox

TABLE 11 MATERIAL PROPERTIES & CONSTRAINTS - CASE 2 SWEPT WINGBOX

(1) Material Properties:

Aluminum: $E = 10.5 \times 10^6$ psi, $\nu = .30$, $\rho = .10$ lbs/in^3

Graphite/Epoxy: $E_{11} = 18.5 \times 10^6$ psi, $E_{22} = 1.6 \times 10^6$ psi
$G = .65 \times 10^6$ psi, $\nu_{12} = .208$, $\nu_{21} = .0203$
$\rho = .055$ lbs/in^3

(2) Minimum sizes (size constraints)

Quadrilateral membranes	$t_m = .025$ in.
Rods	$A = .05$ in^2
Shear webs	$t_w = .050$ in

(3) Allowable stresses (stress constraints)

Aluminum	$\sigma_{lower} = -30000.0$ psi, $\sigma_{upper} = 30000.0$ psi
Graphite/Epoxy	$\sigma_{lower} = -110000.0$ psi, $\sigma_{upper} = 110000$ psi

(4) Fiber orientation

Layer No. 1 (top)	$\Theta = 0^o$
Layer No. 2	$\Theta = 45^o$
Layer No. 3	$\Theta = -45^o$
Layer No. 4 (bottom)	$\Theta = 90$

```
10 TITLE
20   TASK V WINGBOXD GRAPHITE/EPOXY & ALUMINUM
30 GRID    1                 0.0     0.0     2.0
40 GRID    2                 40.0    0.0     3.0
50 GRID    3                 80.0    0.0     2.0
60 GRID    4                 23.32   50.0    1.67
70 GRID    5                 53.40   50.0    2.5
80 GRID    6                 88.82   50.0    1.67
90 GRID    7                 46.63   100.0   1.33
100 GRID   8                 66.79   100.0   2.0
110 GRID   9                 97.63   100.0   1.33
120 GRID   10                69.95   150.0   1.0
130 GRID   11                80.19   150.0   1.5
140 GRID   12                106.45  150.0   1.0
150 SPC1   1       123       1       THRU    3
160 OPLOADS 1                        1
170 FORCE  1       4                 6000.0  0.0     0.0     1.0
180 FORCE  1       7                 4000.0  0.0     0.0     1.0
190 FORCE  1       10                2000.0  0.0     0.0     1.0
200 OPTIM  NO      NO      YES       0       50      .01     .01     OP
210 CQDMEM1 1      2       2       5       4       1       0.0
220 CQDMEM1 37     2       2       5       4       1       45.0
230 CQDMEM1 43     2       2       5       4       1       315.0
240 CQDMEM1 49     2       2       5       4       1       90.0
250 CQDMEM1 2      2       3       6       5       2       355.0
260 CQDMEM1 38     2       3       6       5       2       40.0
270 CQDMEM1 44     2       3       6       5       2       310.0
280 CQDMEM1 50     2       3       6       5       2       85.0
290 CQDMEM1 3      2       5       8       7       4       0.0
300 CQDMEM1 39     2       5       8       7       4       45.0
310 CQDMEM1 45     2       5       8       7       4       315.0
320 CQDMEM1 51     2       5       8       7       4       90.0
330 CQDMEM1 4      2       6       9       8       5       355.0
340 CQDMEM1 40     2       6       9       8       5       40.0
350 CQDMEM1 46     2       6       9       8       5       310.0
360 CQDMEM1 52     2       6       9       8       5       85.0
370 CQDMEM1 5      2       8       11      10      7       0.0
380 CQDMEM1 41     2       8       11      10      7       45.0
390 CQDMEM1 47     2       8       11      10      7       315.0
400 CQDMEM1 53     2       8       11      10      7       90.0
410 CQDMEM1 6      2       9       12      11      8       355.0
420 CQDMEM1 42     2       9       12      11      8       40.0
430 CQDMEM1 48     2       9       12      11      8       310.0
440 CQDMEM1 54     2       9       12      11      8       85.0
450 CWEB   7       1       1       4
460 CWEB   8       1       4       7
470 CWEB   9       1       7       10
480 CWEB   10      1       2       5
490 CWEB   11      1       5       8
500 CWEB   12      1       8       11
510 CWEB   13      1       3       6
520 CWEB   14      1       6       9
530 CWEB   15      1       9       12
540 CWEB   16      1       5       4
550 CWEB   17      1       6       5
560 CWEB   18      1       8       7
570 CWEB   19      1       9       8
580 CWEB   20      1       11      10
590 CWEB   21      1       12      11
600 CROD   22      1       1       4
610 CROD   23      1       4       7
620 CROD   24      1       7       10
630 CROD   25      1       2       5
640 CROD   26      1       5       8
650 CROD   27      1       8       11
660 CROD   28      1       3       6
670 CROD   29      1       6       9
680 CROD   30      1       9       12
690 CROD   31      1       5       4
700 CROD   32      1       6       5
710 CROD   33      1       8       7
720 CROD   34      1       9       8
730 CROD   35      1       11      10
740 CROD   36      1       12      11
750 PQDMEM1 2      2       .025
760 PWEB   1       1       .05
770 PROD   1       1       .05
780 MAT1   1       10.5+6          .25     .10                                 *
790 +M     -30000.030000.0
800 MAT2   2       18.578+6.3342+6 0.0     1.607+6 0.0     .65+6   .055    *
810 +A                                                 -110000.110000.
820 ENDDATA
```

Figure 23 Optforce II Input Data - Case 2 Swept Wingbox

TABLE 12 SWEPT WINGBOX RESULTS - CASE 1, ALUMINUM MATERIAL

El. No.	Element Type	A_i*	$\frac{Y_i}{A_i}$+	El. No.	Element Type	A_i*	$\frac{Y_i}{A_i}$+
1	Quad	.1000	27109.0	22	Rod	.0500	19879.0
2	Quad	.1000	27101.0	23	Rod	.0500	13616.0
3	Quad	.1000	21560.0	24	Rod	.0500	5235.0
4	Quad	.1000	20566.0	25	Rod	2.361	30000.0
5	Quad	.1000	9675.0	26	Rod	.0500	24598.0
6	Quad	.1000	6955.0	27	Rod	.0500	8486.0
7	Web	.0806	29946.0	28	Rod	.0500	22407.0
8	Web	.0804	29946.0	29	Rod	.0500	15907.0
9	Web	.0500	24010.0	30	Rod	.0500	6154.0
10	Web	.1611	30000.0	31	Rod	.0500	7886.0
11	Web	.0587	30000.0	32	Rod	.0500	4767.0
12	Web	.0500	6874.0	33	Rod	.0500	6235.0
13	Web	.0500	17029.0	34	Rod	.0500	3639.0
14	Web	.0500	7287.0	35	Rod	.0500	2792.0
15	Web	.0500	9057.0	36	Rod	.0500	2081.0
16	Web	.1211	30000.0	W_i = 107.40 lbs.			
17	Web	.0500	17783.0	W_m = 110.73 lbs.			
18	Web	.0742	30000.0	Z_{10} = 12.63 in.			
19	Web	.0500	1684.0	CPU = 24.08 sec.**			
20	Web	.0500	27382.0	I = 1			
21	Web	.0500	8031.0				

*A_i = Design variable value, rod cross-sectional area (in^2) web thickness (in), quad membrane thickness (in)

** IBM 3033

+ Stress constraint quantity: $g_\sigma^i = \frac{Y_i}{A_i \sigma_i *} - 1 \leq 0$

where σ_i* is the yield stress or some other failure stress for the ith finite element.

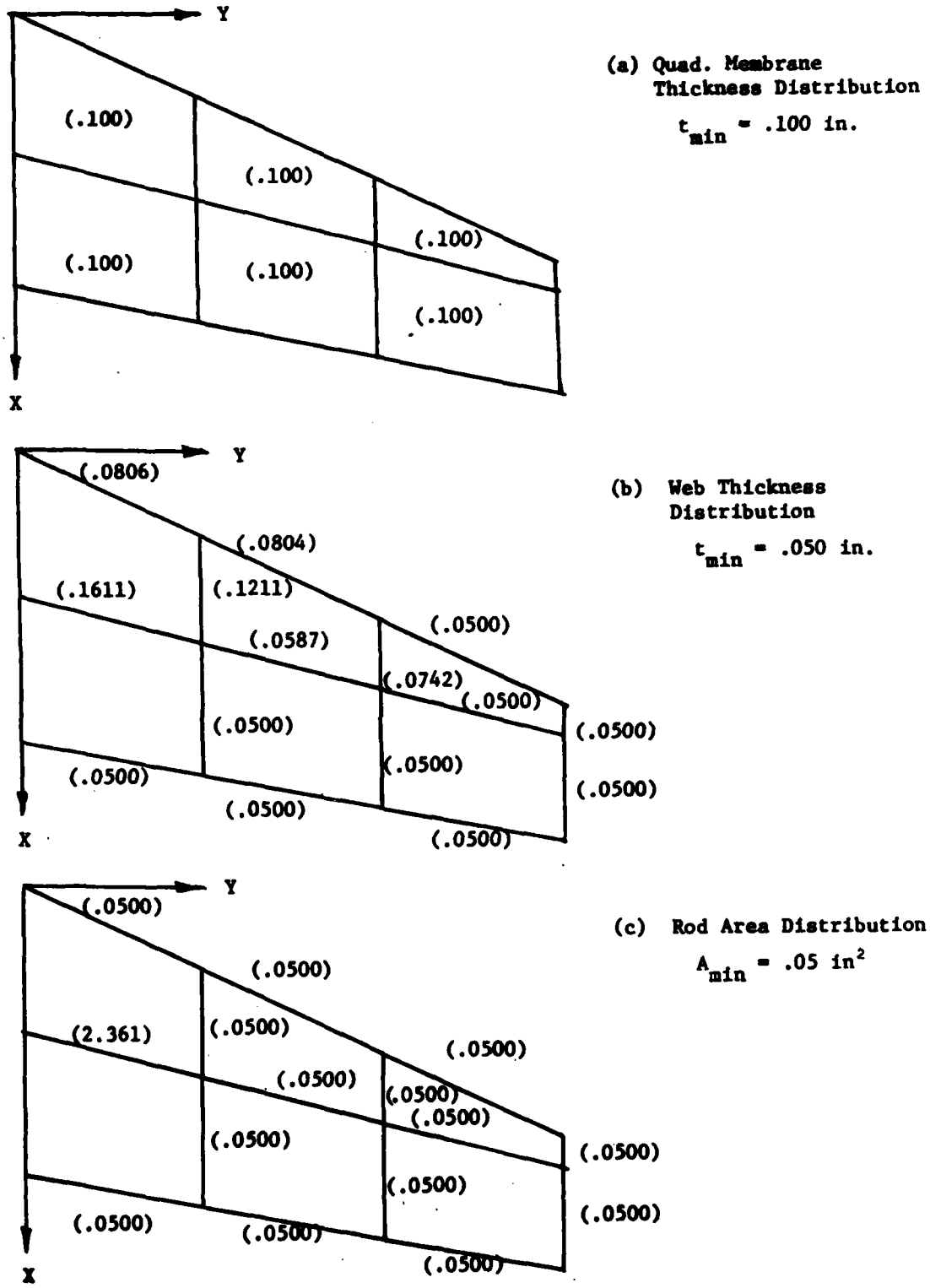

Figure 24 Design Variable Distribution - Swept Wingbox - Case 1, Aluminum Material W_m = 110.73 lbs.

thirty-six λ's associated with internal stress fields and thirty-three λ's associated with the redundants for a total of 105. The design variable and stress λ's sum to the minimum weight value of W_m=110.73 lbs. This is a verification of the theoretical development given in Section 2.0.

- The final design variable, displacement, element stress and reaction vectors are calculated and presented to the User for review. Minimum weight value is W_m = 110.73 lbs.

Examination of Table 12 and Figure 24 shows the design variable vector and element stress constraint quantity Y_i/A_i. The initial and final weight of the structure is also depicted with a maximum vertical displacement of 12.63 inches. IBM 3033 computer time was recorded to be 24.08 seconds. The number of iterations, I=1, is tabulated to indicate the Linear Programming phase operation. Figure 24 displays the design variable vector in pictorial form.

The solution procedure for Case 2 was as follows:

- Initial guess vector: Minimum size constraint with stress ratio option, W_i = 60.05 lbs.
- Program entered the Linear Programming phase: "Solution Not Feasible"; Use fully stressed design as minimum weight solution, W_m = 83.32 lbs.
- Performed check on Lagrange Multiplier (λ_i) calculation. Since certain λ's associated with the design variables were negative the full Newton-Raphson routine was entered. This particular application of OPTFORCE II required fifty-four λ's associated with the design variable vector, fifty-four λ's associated with internal stress distribution and one-hundred twenty-three λ's associated with the redundants for a total of 231.
- Solution procedure terminated after four iterations in the full N-R routine due to an excessive numerical increment associated with the first redundant causing structural weight divergence. User may use the FSD solution.

Table 13 shows pertinent data obtained from the above solution procedure. Note the drop in minimum weight through use of the graphite/epoxy wingbox skins as compared to the all aluminum wingbox structural

TABLE 13 SWEPT WINGBOX RESULTS - CASE 2, GRAPHITE/EPOXY & ALUMINUM MATERIALS

El. No.	Element Type	A_i*	$\frac{Y_i}{A_i}$ +	El. No.	Element Type	A_i*	$\frac{Y_i}{A_i}$ +
1	Quad	.0250	41417.0	31	Rod	.0500	6560.0
2	Quad	.0250	48073.0	32	Rod	.0500	3308.0
3	Quad	.0250	41611.0	33	Rod	.0500	8279.0
4	Quad	.0250	41496.0	34	Rod	.0500	4512.0
5	Quad	.0250	11889.0	35	Rod	.0500	1219.0
6	Quad	.0250	18946.0	36	Rod	.0500	5853.0
7	Web	.0655	30000.0	37	Quad	.0250	62091.0
8	Web	.0875	30000.0	38	Quad	.0250	67220.0
9	Web	.0520	29968.0	39	Quad	.0250	51672.0
10	Web	.1654	30000.0	40	Quad	.0250	33913.0
11	Web	.0500	27775.0	41	Quad	.0250	26318.0
12	Web	.0500	3625.0	42	Quad	.0250	11784.0
13	Web	.0500	13716.0	43	Quad	.0250	3079.0
14	Web	.0500	5412.0	44	Quad	.0250	10121.0
15	Web	.0500	12279.0	45	Quad	.0250	4762.0
16	Web	.1368	30000.0	46	Quad	.0250	18134.0
17	Web	.0500	14070.0	47	Quad	.0250	23628.0
18	Web	.0784	30000.0	48	Quad	.0250	2260.0
19	Web	.0500	1374.0	49	Quad	.0250	6327.0
20	Web	.0500	21784.0	50	Quad	.0250	4139.0
21	Web	.0500	10887.0	51	Quad	.0250	14479.0
22	Rod	.0500	17595.0	52	Quad	.0250	10712.0
23	Rod	.0500	18751.0	53	Quad	.0250	10238.0
24	Rod	.0500	6953.0	54	Quad	.0250	10683.0
25	Rod	3.9950	30000.0				
26	Rod	.7203	30000.0				
27	Rod	.0500	12794.0				
28	Rod	.0500	24769.0				
29	Rod	.0500	16438.0				
30	Rod	.0500	10148.0				

W_i = 60.05 lbs.
W_m = 83.32 lbs.
Z_{10} = 13.94 in.
CPU = 249.54 sec**
I = 5

*A_i = Design variable value, rod cross-sectional area (in^2), web thickness (in), quad membrane thickness (in)

** IBM 3033

+ Stress constraint quantity

weight. Computer time was registered to be 249.54 cpu seconds almost a ten-fold increase over the all-metallic wing solution time. This is a significant amount that the User should note for future applications of OPTFORCE II. The increase in cpu time can be attributed to the increased number of design variables and Lagrange multipliers. One hundred and five λ's were needed for the aluminum wing box solution. This number increased to two hundred and thirty-one for the composite wing solution. The number of iterations I=5 is tabulated to indicate the Linear Programming and full Newton-Raphson phase computations.

It is of interest to note that two additional analyses were conducted to show the effect of convergence criteria (OPTIM input card) and minimum size constraint imposed on the graphite/epoxy quadrilateral membrane elements (PQDMEM1 input card). The initial convergence criteria of .010 was changed to .0010. Results obtained were essentially those shown in Table 13 except that the full N-R iteration routine was terminated due to an excessive delta thickness experienced on element number 18. Thus, in this particular application the change in convergence criteria had very little effect upon determining the minimum weight design with the exception of increasing cpu time from 249.54 sec to 287.41 sec. The second additional analysis completed reduced the minimum thickness constraint of the membrane elements from .0250 inch to .0100 inches. The solution procedure again followed those steps initially shown. The minimum weight value dropped to 73.47 lbs. as would be expected and the deflection of the wingbox decreased slightly to 13.49 inches. Cpu time increased about 45 seconds to a value of 290.06. The distribution of the design variables for this case is shown in Figure 25.

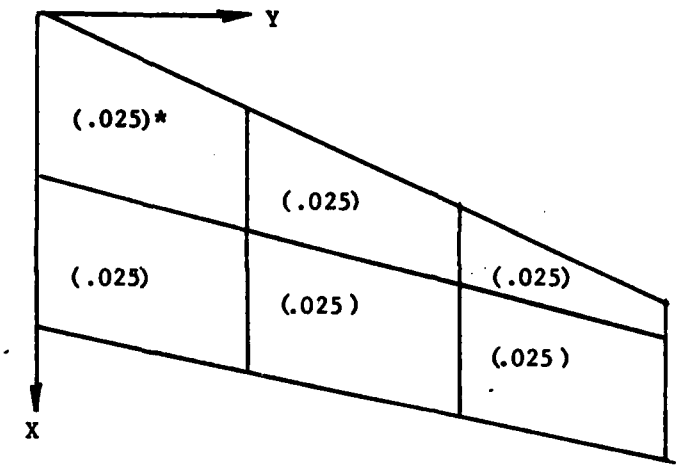

(a) Quad, Membrane Thickness Distribution

t_{min} = .025 in.

* all layers have equal thickness

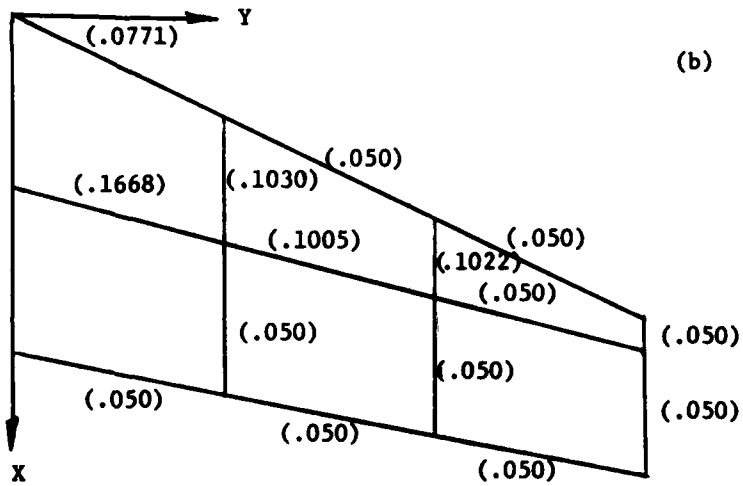

(b) Web thickness Distribution

t_{min} = .050 in.

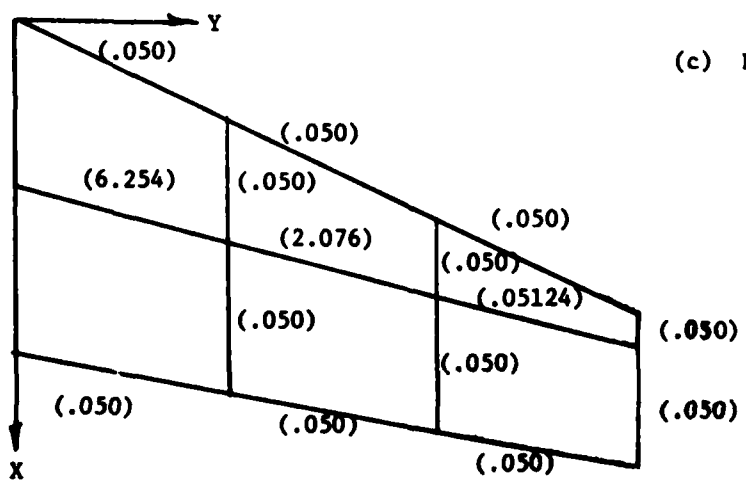

(c) Rod Area Distribution

A_{min} = .050 $in.^2$

Figure 25 Design Variable Distribution - Swept Wingbox - Case 2, Graphite-Epoxy & Aluminum Materials, W_m=73.47 lbs.

4.0 CONCLUSIONS & RECOMMENDATIONS

The pilot optimization program, OPTFORCE I (Ref. 4), has been successfully extended to include new finite elements, optimization constraints and analysis type capabilities. Additionally, it has been expanded into a general purpose type optimization code featuring NASTRAN compatible input data formats and engineering User output features. As a result, it is concluded that the technical requirements stated in Section C of the subject contract F33615-80-C-3214 documents have been met. This has resulted in a new optimization code labeled OPTFORCE II, the mathematical basis of which has been amply described in this volume. The use of this code has also been illustrated herein and its input/output features and programming aspects are given in Volume Two of this publication, Ref. 11.

Specific tasks which came to a successful conclusion were the formulation of finite element matrices based upon the force method approach. Membrane triangle, membrane quadrilateral, shear panel and bar (axial force) elements were developed. The resultant formulations proved to be accurate for use in the prediction of both static and dynamic behavior of structural components. Their use in optimization analyses also proved to be successful. Formulation of optimization constraint equations were straightforward and provided for the first time the opportunity to optimize structures including variable stress, multiple displacement, maximum and minimum size and dynamic stiffness (natural frequency) constraints all within the context of the force method. Multiple load conditions are also included in the formulation.

The force method formulation of a rapid re-analysis technique concluded in a highly efficient means for evaluating the effect of damage

on the static and dynamic response of optimized structures. The general theory developed in Section 2.4 included the use of the aforementioned finite elements, however, resources only permitted the coding of a rapid re-analysis program using bar elements. This code is described and illustrated in Appendix B of Volume II and is successfully demonstrated in Section 2.4 of this volume. Its potential is proven therein by the applications shown and provides a means for determining the residual strength and response of damaged structures. The method is a direct one and eliminates the iterative nature of other methods presently available in the literature.

Executions of OPTFORCE II were ample enough to conclude that the initial capabilities of the force method code OPTFORCE I could be successfully extended to optimize three-dimensional truss-like and aerospace type structures. The applications of OPTFORCE II further proved that the force method yields more accurate optimization solutions than the displacement based OPTIM III reference computer code. The efficiency studies conducted and profusely described in Section 3.1 showed this fact to be true. These studies further demonstrated that computer time (cpu seconds) is a less relevant measure of computer code "efficiency" than originally thought. It is concluded from these studies that the OPTFORCE II code is preferred over the reference displacement based OPTIM III code.

No difficulties were experienced with the use of OPTFORCE II whenever structures were optimized subject to minimum size and stress constraints. Minimum weight solutions including displacement and/or dynamic constraints in addition to size and stress constraints proved troublesome. No satisfactory solutions could be found for the numerical difficulties encountered. Obviously additional resources are needed to obviate this problem. It is

concluded at this time that the difficulty lies not in the force method formulation of those type of constraints but in the numerical application of attendant governing equations. It is recommended that further studies of this perplexity be pursued.

Finally, it is concluded that the research conducted and reported herein has shown that the force method of structural optimization has provided the solution to the technical problems discussed in the introduction to this report. The force method approach gives the means to express constraints, in particular the stress constraint, in such a manner as to provide the needed mathematical expressions for use in the Lagrangan formulation of the weight optimization solution procedure. This enhances the definition of the optimality criteria and attendant first and second derivatives used in the nonlinear solution procedure. Thus, it is further recommended that the force method optimization procedure resident in OPTFORCE II be seriously considered as the future general purpose structural optimization code.

REFERENCES

1. Michell, A.G.M., "The Limits of Economy of Material in Frame Structures," Phil. Mag, Series 6, Volume 8, 1904.

2. Maxwell, C., "Scientific Papers II," 1869 - Reprinted by Dover Publications, New York, 1952.

3. Moses, F., "Optimization of Sturctures with Reliability Constraints," AGARD-CP-36-70, Symposium on Structural Optimization, October 1969.

4. Gellatly, R.A., et al, "Force Method Optimization - An Approach to Satisfying Multiple Mixed Equality and Inequality Constraints in Structural Design," AFWAL-TR-80-3006, February 1980.

5. Berke, L. and Khot, N.S., "Use of Optimality Criteria Methods for Large Scale Systems," AGARD Lecture Series No. 70, Structural Optimization, 1974.

6. Venkayya, V.B., Khot, N.S., Tischler, V.A. and Taylor, R.F., "Design of Optimum Structures for Dynamic Loads," Third Conference on Matrix Methods in Structural Mechanics, WPAFB, Ohio, October 1971.

7. Melosh, R.J. and Luik, R,Proc. Paper 6644, Journal of the Structural Division, ASCE, Volume 95, No. ST7, July 1969, pp. 1586-1589.

8. Venkayya, V.B., Khot, N.S. and Estep, F.E., "Vulnerability Analysis of Optimized Structures," 18th AIAA/ASME/SAE SDM Conference, March 24-25, 1977, San Diego, CA.

9. Venkayya, V.Khot, N.S. and Estep, F.E., "Vulnerability Analysis of Optimized Structures," AIAA Journal, Volume 16, No. 11, November 1978.

10. Dale, B.J., Padlog, J., and Thom, R.D., "OPTIM III: A NASTRAN Compatible Large Scale Automatic Minimum Wright Design Program - Users and Programmers Manual" AFWAL-TR-80-3007, February 1980.

11. Batt, J.R., Dale, B.J., Skalski, S.C., Witkop, D.L., and Gellin, S., "Force Method Optimization II", Volume II User's Manual, AFWAL-TR December 1982.

12. Gallagher, R.H., "Finite Element Analysis Fundamentals", Prentice Hall 1975.

13. Gellin, S., and Batt, J.R., "Force Method Dynamics" Proceedings of 6th Invitational Symposium on the Unification of Finite Elements, Finite Differences and Calculus of Variations, Pg. 123-152, The University of Connecticut, May 7, 1982.

14. Kuhn, H.W. and Tucker, A.W., Nonlinear Programming Proc. 2nd Berkley Symposium Math Statistics Probabilities, J. Neyman (ed.) University of California Press, Berkley 1951.

15. Arora, J.S., Haskell, D.F. and Gavil, A.K., "Optimal Design of Large Structures for Damage Tolerances", AIAA Journal Volume 18, No. 5. Article No. 80-4038, May 1980.

16. Scott, D.S., Westkaemper, J.C., Sejal, A. and Stearman, R.O., "The Influence of Ballistic Damage on the Aeroelastic Characteristics of Lifting Surfaces", AFSOR TR 80-0220, May 1979.

17. Hemming, F.G. and Venkayya, V.B., "Efficiency Considerations in Flutter Optimization with Effects of Damage Included", AIAA Paper No. 80-0788-CP Presented at 21st AIAA/ASME/ASCE/AHS Conference, Seattle, Washington May 1980.

18. Hemming, F.G., Venkayya, V.B. and Eastep, F.E. "Flutter Speed Degradation of Damaged Optimized Flight Vehicles" Proceedings of 20th AIAA/ASME/ ASCE/AHS Conference St. Louis, Mo., April 1979.

19. Venkayya, V.B., "A Perturbation Method for the Analysis of Damaged Structures", Presented at Symposium on Applications of Computer Methods in Engineering Los Angeles, CA., August 1977.

20. Venkayya, V.B. and Khot, N.S., "Vulnerability Analysis of Optimized Structures", AIAA Journal Volume 16, No. II, November 1978.

21. U.S. Air Force Contract No. F33615-79-C-3209, entitled "Optimization and Damage Assessment of Aerospace Structures".

22. Khot, N.S. and Berke, L., "Structural Optimization Using Optimality Methods", Paper presented at the International Symposium on Optimal Structural Design", Tucson, AR, October 19-22, 1981.

23. Gellatly, R. A. "Proposal for A Novel Approach to the Definition and Selection of Optimal Structures" Bell Aerospace Textron Report No. D2398-953001A, July 1969.

24. Venkayya, V.B. "Design of Optimum Structures", Computers and Structures, Volume 1, pg. 265-309, 1971, Paper presented at the Conference on Computer Oriented Analysis of Shell Structures, 10-14 August 1970, Palo Alto, CA.

25. Harless, R.I. "A Method for Synthesis of Optimal Weight Structures", An International Journal of Computers and Structures Volume 12, No. 6, December 1980.

DATE
FILMED

5-8